SKB

TECHNICAL REPORT

97-04

ÄSPÖ HRL – Geoscientific evaluation 1997/3

Results from pre-investigations and detailed site characterization

Comparison of predictions and observations

Geology and mechanical stability

Roy Stanfors[1], Pär Olsson[2], Håkan Stille[3]

1   RS Consulting, Lund
2   Skanska, Stockholm
3   KTH, Stockholm

May 1997

ÄSPÖ HRL - GEOSCIENTIFIC EVALUATION 1997/3

RESULTS FROM PRE-INVESTIGATIONS AND DETAILED SITE CHARACTERIZATION

COMPARISON OF PREDICTIONS AND OBSERVATIONS

GEOLOGY AND MECHANICAL STABILITY

Roy Stanfors[1], Pär Olsson[2], Håkan Stille[3]

1   RS Consulting, Lund
2   Skanska, Stockholm
3   KTH, Stockholm

May 1997

ÄSPÖ HRL

GEOSCIENTIFIC EVALUATION 1997/3

RESULTS FROM PRE-INVESTIGATIONS AND DETAILED SITE CHARACTERIZATION

COMPARISON OF PREDICTIONS AND OBSERVATIONS

GEOLOGY AND MECHANICAL STABILITY

Roy Stanfors, RS Consulting, Lund
Pär Olsson, Skanska, Stockholm
Håkan Stille, KTH, Stockholm

Maj 1997

FOREWORD

The booklet *Äspö Hard Rock Laboratory - 10 years of research*, available from SKB, provides the reader with a popular review of the achievements. This report is No 3 of six Technical Reports summarizing the pre-investigation and construction phase of the Äspö Hard Rock Laboratory.

The reports are:

1   Stanfors R, Erlström M, Markström I.
     Äspö HRL - Geoscientific evaluation 1997/1.
     Overview of site characterization 1986-1995
     SKB TR 97-02.

2   Rhén I (ed), Bäckblom (ed), Gustafson G, Stanfors R, Wikberg P.
     Äspö HRL - Geoscientific evaluation 1997/2.
     Results from pre-investigations and detailed site characterization.
     Summary report.
     SKB TR 97-03.

3   Stanfors R, Olsson P, Stille H .
     Äspö HRL - Geoscientific evaluation 1997/3.
     Results from pre-investigations and detailed site characterization.
     Comparison of predictions and observations.
     Geology and Mechanical stability.
     SKB TR 97-04.

4   Rhén I, Gustafson G, Wikberg P.
     Äspö HRL - Geoscientific evaluation 1997/4.
     Results from pre-investigations and detailed site characterization.
     Comparison of predictions and observations.
     Geohydrology, Groundwater chemistry and Transport of solutes.
     SKB TR 97-05.

5   Rhén I (ed), Gustafson G, Stanfors R, Wikberg P.
     Äspö HRL - Geoscientific evaluation 1997/5.
     Models based on site characterization 1986-1995.
     SKB TR 97-06.

6   Almén K-E (ed), Olsson P, Rhén I, Stanfors R, Wikberg P
     Äspö Hard Rock Laboratory
     Feasibility and usefulness of site investigation methods.
     Experiences from pre-investigation phase.
     SKB TR 94-24.

The background and objectives of the project are presented in a background report to SKB R&D Programme 1989 (Hard Rock Laboratory), which contains a detailed description of the HRL project.

The purpose of this report, No. 3, is to present the evaluation of the geology and mechanical stability of the pre-investigation for the Äspö HRL. An overview of all the investigations performed is summarized in *Report 1*. The evaluation of the pre-investigation is presented in *Reports 2-4*. *Report 5* presents the 1996 models of the Äspö HRL, the concepts and some comments on how the models have developed, based on data from the pre-investigation and construction phases of the Äspö HRL. Finally, *Report 6* outlines the usefulness and feasibility of pre-investigation methods.

April 1997

Roy Stanfors   Pär Olsson   Håkan Stille

ABSTRACT

The pre-investigations for the Äspö Hard Rock Laboratory were started in 1986 and involved extensive field measurements aimed at characterizing the rock formations with regard to geology, geohydrology, groundwater chemistry and rock mechanics.

Prior to excavation of the laboratory which started in the autumn of 1990 predictions for the excavation phase were made. The predictions concern five key issues: geology, groundwater flow, groundwater chemistry, transport of solutes and mechanical stability.

Comparisons between predictions and observations were made during excavation in order to verify the reliability of the pre-investigations. This report presents a comparison between the geological and mechanical stability predictions and observations and an evaluation of data and investigation methods used for the 700 - 2874 m section of the tunnel.

The report is specially highlighting on the following conclusions:

- It is possible to localize major fracture zones during the pre-investigation phase at shallow (<200 m) depths. However, the prediction accuracy regarding position, width and character decreases with increasing depth.

- A number of minor fracture zones striking NNW-NNE were predicted to be hydraulically important and penetrate the southern Äspö area. A number of narrow fracture zone indications - decimetre to metre wide - striking WNW-NE were mapped in the tunnel and pre-grouted sections confirm hydraulic conductors.

- It has not been possible to confirm the gently dipping zone EW-5, which was predicted as 'possible', with data from the tunnel.

- Predictions of the amount of different rock types were generally reliable as regards the major rocks but the prediction of the distribution in space were poor as regards the minor rock types (dikes and veins of fine-grained granite and greenstone).

- The prediction of rock stress orientation corresponds well to the outcome. The relation between the maximum horizontal stress and the theoretical vertical stress, K_o, was predicted to be in the range of 1.7 while the outcome proved to be 2.9.

- The prediction of rock quality for the tunnel, while applying the RMR-system, shows good correspondence to the observations made in the tunnel.

ABSTRACT (in Swedish)

Förundersökningarna för Äspölaboratoriet startade 1986 med syfte att karakterisera berget geologiskt, hydrogeologiskt, grundvattenkemiskt och bergmekaniskt.

Innan byggandet av Äspölaboratoriet startade hösten 1990 gjordes prediktioner för byggfasen av laboratoriet avseende fem huvudfrågor: geologi, grundvatten-flöde, grundvattenkemi, transport av lösta ämnen och mekanisk stabilitet.

Jämförelser mellan prediktioner och observationer har gjorts under byggfasen med syfte att verifiera förundersökningarnas tillförlitlighet. Denna rapport redovisar resultat av den jämförelse som gjorts mellan geologiska och bergmekaniska prediktioner och utfall för delsträckan 700 - 2874 m av tunneln.

Följande huvudslutsatser i rapporten kan framhållas:

• Resultaten visar att det i allmänhet är möjligt att under förundersöknings-skedet lokalisera större sprickzoner, men att precisionen i prediktionerna avseende zonernas position, bredd och karaktär blir sämre på större djup.

• Ett antal strukturer predikterades som smala hydrauliskt betydelsefulla sprickzoner med orientering NNV-NNO. I tunneln har flera dm-meterbreda sprickzoner med strykning VNV-NO påträffats. Den exakta positionen för denna typ av mindre sprickzoner är mycket svår att prediktera.

• Den flackt stupande sprickzonen EW-5, vilken predikterats som "möjlig", har inte påträffats i tunneln.

• Fördelning och relativa mängder av huvudbergarterna är möjliga att prediktera medan exakta läget av finkornig granit och grönsten i form av gångar och linser är mycket svårt att förutse i en komplex bergmassa.

• Bergspänningsmätningarna visar god överensstämmelse mellan prediktion och observationer i tunneln avseende huvudspänningarnas orientering. Förhållandet mellan maximal horisontell huvudspänning och teoretiskt beräknad vertikalspänning, K_o, predikterades till storleksord-ningen 1,7 men visade sig vid mätningar i tunneln vara 2,9.

• Prediktionen för bergkvalitet i tunneln enligt RMR-systemet visar genomgående god överensstämmelse med observationer i tunneln.

CONTENTS

SUMMARY

The report concerns the comparison between geological and mechanical stability predictions and observations in the 700 - 2874 m section of the Äspö tunnel.

The evaluation of predictions and the observations - based on documentation data - are presented on three different scales: The site scale (500 - 1000 m) the block scale (50 - 100 m) and the detailed scale (5-10 m). A brief analysis of the accuracy of the predictions is also presented for the different scales.

A simplified overview of subjects, predictions and observed outcome are shown in *Tables 1 to 4*. The ability to predict a certain subject (parameter) is shown by the amount of outcome results which are inside the predicted range. Results outside the predicted range are discussed from the aspect of the reason for the deviation. The '+' sign represents the most common parameter result (>50%).

LITHOLOGY

A lithological description comprise an overall distribution of the main rock units on a regional scale, while *'Rock composition'*, *'Rock boundaries'*, and *'Rock type characteristics'* refer to a more detailed description of small-scale petrographic variation on the block and detailed scales. *'Rock type characteristics'* refers to the mineralogical composition and petrophysics of the four most frequent rock types in the Äspö area: Småland (Ävrö) granite, Äspö diorite, fine-grained granite and greenstone.

Airborne geophysics (magnetic and electromagnetic) gave valuable information on the distribution of the major rock types on the regional site scale, especially with respect to extensive basic intrusions and diapirs of younger granite. Gravity data provided estimates of the depth extent of diapiric granites and bodies of basic rock. Data from surface mapping contributed to a good understanding of the two-dimensional extent of the main rock types. In order to obtain a three-dimensional lithological model borehole investigations were performed, comprising core mapping and geophysical logging.

The reliability of the predictions of the relative amount of the main rock units is rather good, mostly due to well exposed bedrock and borehole data (core and geophysical logging).

Table 1. Comparison between prediction and outcome.

Subject	Site scale Within predicted	Site scale Outside range	Block scale Within predicted	Block scale Outside range	Detailed scale Within predicted	Detailed scale Outside range	Comments
Lithology							
Rock types	+						
Position of different rock types				+			Very difficult to predict in a complex lithology.
Rock boundaries (No/100 m)	+		+				
Rock composition (%)	+			+			
Major fracture zones							
Geometry							
Position in tunnel	+						Prediction of the more exact orientation and width uncertain due to the winding extent and variation in thickness along most fracture zones.
Strike	+ *						
Dip	+						
Width	+						
Properties							
Character		+					
Minor fracture zones							
Geometry							
Position in tunnel		+					The more exact location and width at depth of the minor fracture zones were not predicted.
Strike	+						
Dip	+	+ **					
Width	+	+ **					

*   Verification based only on tunnel observations.
**   Subhorizontal fracture zones.

The predictions generally comprise both point estimates and a confidence interval at a certain confidence level. These point estimates and confidence intervals are obtained both from sample properties and expert judgement. Rather than obtaining a very wide interval for a confidence level, the level of confidence is in these cases lowered to 60% for most geological parameters, which indicates an estimated low level of certainty.

Table 2. Comparison between prediction and outcome.

Subject	Site scale		Block scale		Detailed scale		Comments
	Within predicted	Outside range	Within predicted	Outside range	Within predicted	Outside range	
Rock type characteristics							
Mineralogical composition			+		+		Mean values of a great number of core samples normally give reliable predictions for most of these parameters.
Alteration			+		+		
Density			+		+		
Porosity				+		+	
Small scale fracturing							
Number of fracture sets			+		+		Surface and borehole data mostly give reliable predictions of the number of fracture sets and fracture infilling. Changes in orientation at depth, spacing and fracture length are more difficult to predict based solely on borehole data.
Orientation			+		+		
Spacing				+		+	
Length				+		+	
Fracture infilling minerals			+		+		

The predictions generally comprise both point estimates and a confidence interval at a certain confidence level. These point estimates and confidence intervals are obtained both from sample properties and expert judgement. Rather than obtaining a very wide interval for a confidence level. The level of confidence is in these cases lowered to 60% for most geological parameters, which indicates an estimated low level of certainty.

The very irregular distribution of rock types like the fine-grained granite and the greenstone makes it almost impossible to deterministically describe the position and extent of the minor rock units.

On the detailed scale the prediction of the mineralogical composition of the four main rock types was based on numerous microscopical analyses of core samples from the Äspö area. The petrophysical parameters density and porosity were based on geophysical logging data. **There is a rather good agreement between prediction and outcome regarding alteration and the major minerals.** The outcome data are normally based on 2-3 microscopical analyses and the density and porosity on 10-12 analyses per 50 m rock block along the tunnel.

DISCONTINUITIES

On the site scale it is possible to localize sub-vertical major fracture zones (>5 metres wide) during the pre-investigation phase at shallow (<200 m) depths. However, the prediction accuracy regarding position, width and character at increasing depth. The error in predicting the position of a major fracture zone at depth is mainly due to dip uncertainty.

There is generally good agreement between the prediction and observations concerning the main orientation of sub-vertical fracture zones and their importance for construction. An exception, however, was fracture zone NE-2 which was predicted to be major and dip to the NW, outwards from the tunnel spiral, but underground the zone was demonstrated to be a minor fracture zone dipping to the SE. The predicted dip was estimated mainly based on one cored borehole. Underground, the undulating character of NE-2 was confirmed by various measurements in the tunnel. A summarized comparison between prediction and outcome is presented in *Table 3* and *Figures 1 and 2*.

There is not always a clear correlation between distinct geophysical indications and the hydraulic importance of a fracture zone. For example, the topographically and geophysically very distinct regional zone EW-1 - which divides Äspö into two blocks - is of fairly low transmissivity and mostly of rather good mechanical strength for construction purposes. The zone NE-1, however, which was crossed by the tunnel, proved to be very difficult to excavate due to very high transmissivity and low mechanical strength. This zone was rather faintly indicated geophysically during the regional stage of pre-investigations, partly because it is located under the sea.

A number of minor, mostly steeply dipping, fracture zones were predicted to intersect the tunnel volume trending NNW-NNE. On the 500-m site scale, however, no exact position and extent of a particular zone was predicted - only the frequency and main orientation of the minor zones. The different zones in the 'NNW' system were predicted to be 'possible-probable' and their predicted

Table 3. Summarized comparison between prediction and outcome. Major fracture zones.

Prediction (based on pre-investigation data)					Outcome (mainly based on tunnel observations)			
Fracture zone	Position along main tunnel (centre of zone)	Strike	Dip	Width (m)	Position along main tunnel (centre of zone)	Strike	Dip	Width (m)
EW-7	773 m($\pm$20)*	N70°E	65°S($\pm$10)*	10($\pm$5)*	787 m	N75°E	75°S	10
NE-4	830 m($\pm$20)*	N45°E	65°S($\pm$5)*	50($\pm$10)**	828 m	N50°E	60°S	41
NE-3	988 m($\pm$20)*	N45°E	70°N($\pm$5)**	60($\pm$10)**	992 m	N60°E	75°N	49
NE-1	1285 m($\pm$20)*	N45°E	65°N($\pm$5)**	45($\pm$5)**	1284 m	N50-55°E	70-75°N	61
EW-3	1427 m($\pm$20)*	N70°E	85°S($\pm$5)**	10($\pm$5)**	1414 m	N80°E	75-80°	14
NE-2***	1740 m($\pm$30)*	N45°E	75°N($\pm$5)**	15($\pm$5)*	1602 m 1844 m 2480 m	N15-36°E	70-80°S	1-6
EW-5	see *Figure 3-9*				see *Figure 3-9*			

*   Confidence level 60 %
**   Confidence level 75 %
***   NE-2 was not predicted to cross the tunnel spiral - only touch the tunnel at approx. 1740 m.
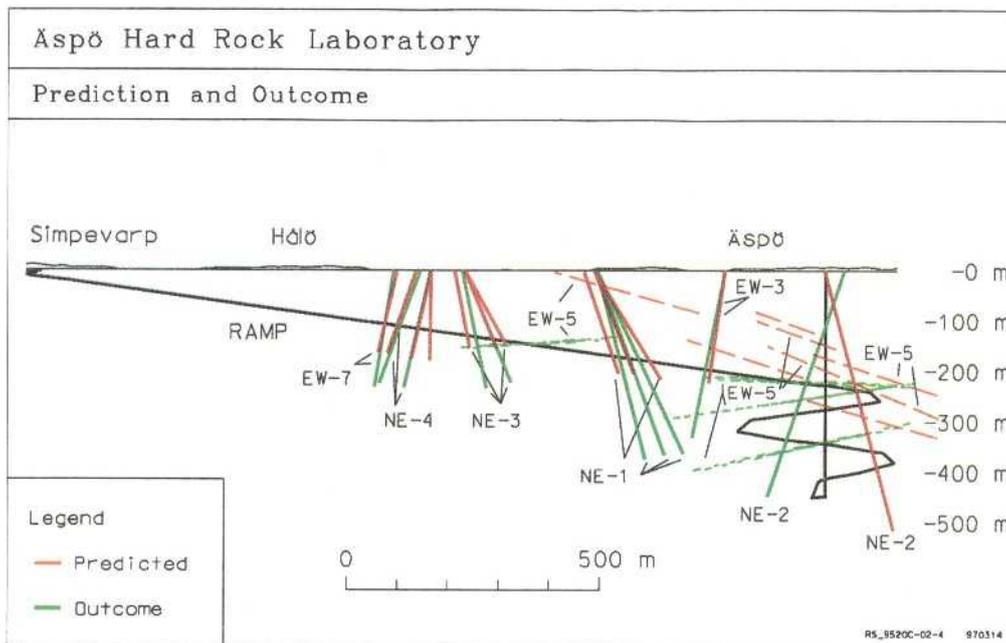
Figure 1. *Prediction and outcome for major fracture zones. The picture illustrates predicted (red) and observed (green) positions and dips in the tunnel.*

position in the tunnel very approximate. The widths were expected to be 0.1-5 m. The characters of the zones were not predicted due to the lack of relevant data.

Only structures that display indicators, such as slickensides, mylonitic fabrics or faults, were mapped in the tunnel as minor fracture zones. Most of them are generally not wider than 1 m. Most consist of a single or up to a handful of faults that generally contain gouge. The host rock is generally mylonitized shear faults. The nature of fracturing in sheets of fine-grained granite make such structures difficult to differentiate from fracture zones. However, fracture zones are here defined as broken volumes of rock that also display kinematic/tectonic indicators which discriminate most sheets of fine-grained granite.

The predicted water-bearing zone NNW-4W is an example of a minor fracture zone which is indicated in the tunnel by two intersections, at 2018 m and 2116 m. Except for NNW-4W it is not possible to find persistent 'minor fracture zones' in the tunnel according to the definition given in the prediction based on surface indications. One reason for this may be the tendency of most fracture zones to be narrower at depth than what could be expected from surface indications in the form of fractured and weathered rock.

Combined results from tunnel mapping and drilling show the characteristic pattern of the 'NNW-structures'. They mostly occur in a complex pattern of steeply dipping fractures (fracture swarms) and some decimetre-wide 'fracture zones' trending WNW to NE. Many of the narrow fracture zones are connected to veins or dikes of fine-grained granite. It seems possible to correlate in the tunnel to observations in boreholes crossing the central part of the spiral and forming a hydraulically active pattern trending WNW-NNW. The character of
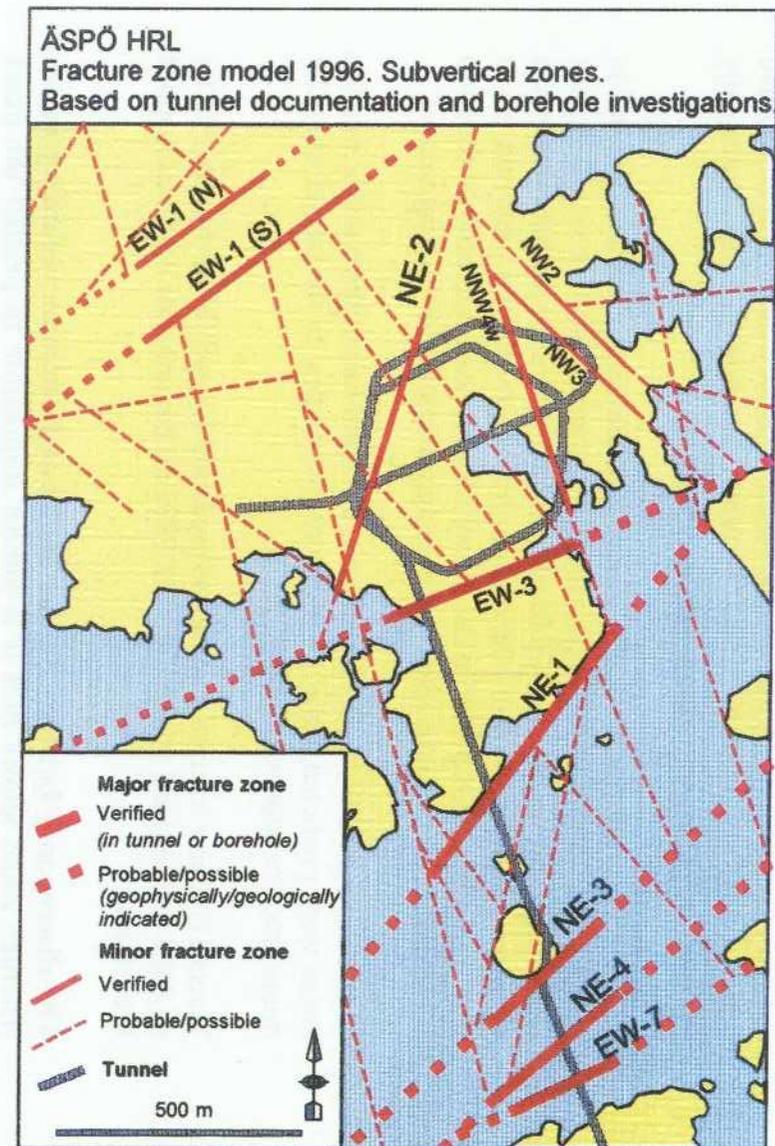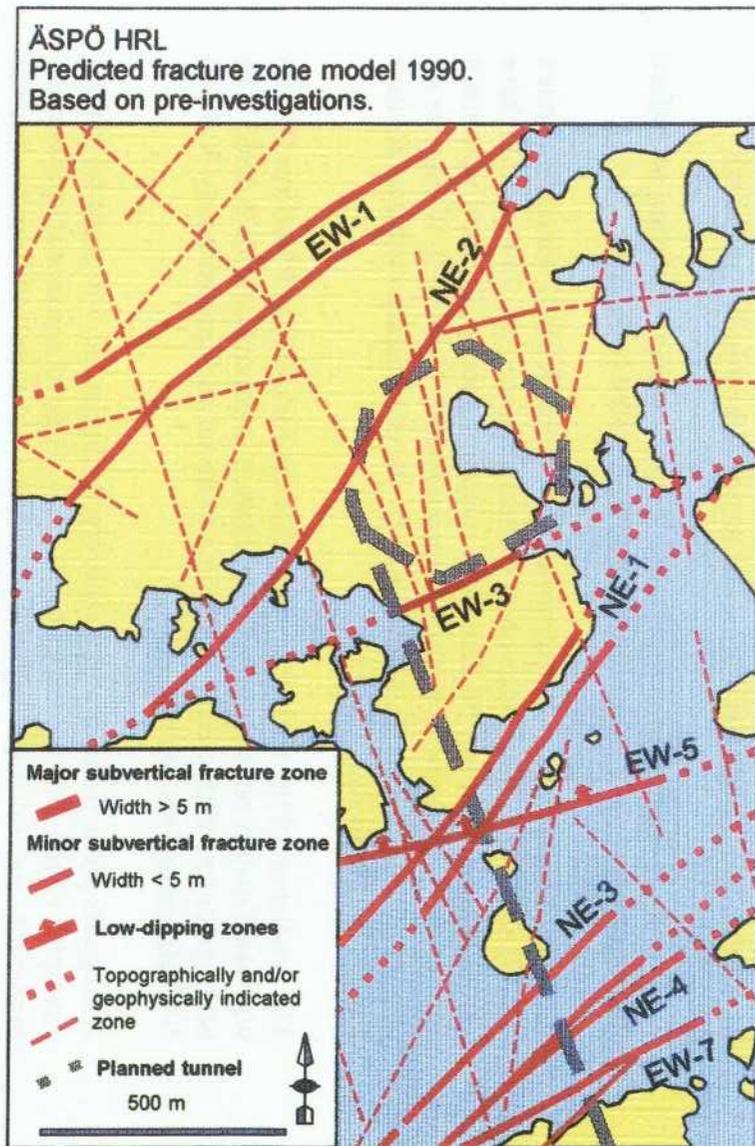
Figure 2. Structural model of the Äspö area, with predicted main structures at ground level, prior to construction (left) and after construction (right).

many of these structures as 'fracture zones' is not very evident. They should rather be described as a 10-30 m wide swarm of mostly subvertical conductive fractures trending WNW-N, where the WNW trending fractures are normally the most frequent and hydraulically important.

On the 50-m scale minor fracture zones are penetrated by the access tunnel in rock blocks P50-01 and P50-02. (Predictions were made for six 50 m rock blocks along the tunnel.) In rock block P50-01 – where the prediction/outcome discrepancy is most evident – three minor fracture zones were predicted, based on cored borehole KBH02. In the tunnel the increased fracturing is found to occur more or less continuously over an approximately 40-m long section.

In rock block P50-04, at 1570-1620 m in the spiral tunnel three minor fracture zones were predicted, based on the cored boreholes. In the tunnel only one minor fracture zone was found.

Three(±1) minor fracture zones were predicted for each of the blocks P50-05 (at 2422-2472 m) and P50-06 (at 2752-2802 m) but only one zone was mapped in each block.

The discrepancy between the prediction and outcome regarding minor fracture zones shows that it is almost impossible to predict the exact position and extent of a specific minor fracture zone based solely on surface data and information from a single borehole in or close to an actual rock block. This is mainly due to the mostly irregular and short extent of the minor zones. The main orientation, however, of the 'NNW zones' and its water-bearing character was in fair accordance with the prediction.

Predictions, in the 50-m blocks, of small scale fracturing were based on surface fracture mapping and analysis of fracturing in cored boreholes.

As no core orientation was determined in borehole KBH02 which penetrated P50-01 to P50-03, the prediction of the main fracture set orientation in these blocks was based solely on data from surface mapping. The best agreement with predictions seems to be for the approximately N-S and E-W fracture set orientations, which could be explained by the dominating character of these fracture sets in the whole area.

The prediction of the main fracture set for the rock blocks P50-04 to P50-06 was based mainly on data from TV orientation in cored borehole KAS05. The best agreement with predictions seems to be for the approximately N-S and NW-SE fracture set orientations.

As regards predictions of small scale fracturing on the 5-m scale for typical examples of the four main rock types, there is good agreement between the prediction and outcome regarding 'fracture minerals' and 'main fracture orientation' especially concerning the two dominant fracture sets striking approximately E-W and N-S – but less good regarding fracture spacing and fracture length.

MECHANICAL STABILITY

The difference between results from laboratory testing of rock type parameters in the pre-investigation phase and the excavation phase is significant. The outcome for several parameters were wider than the predicted range. Further, the number of samples is small, both from the pre-investigation phase and the excavation phase, thereby providing a low level of confidence for mean and variance values.

The prediction of rock stress orientation corresponds well to the outcome. The relation between the maximum horizontal stress and the theoretical vertical stress, K_o, was predicted to be in the range of 1.7 while the outcome was 2.9. Average values for individual boreholes vary between 1.7 and 4.0. Single measurements in individual boreholes vary between 1.5 and 4.0.

The difference between the predicted rock stress levels and the outcome can possibly be explained by geometric factors and geological variations. It is also probable that a large portion of the differences is due to the different methods used to make the measurements. Hydraulic fracturing shows lower maximum horizontal stress levels than the results of measurements made using the overcoring method.

The prediction of rock quality for the tunnel, utilizing the RMR system, shows acceptable correspondence to the observations made in the tunnel. The rock quality is very dependent on the rock type. Fine-grained granite exhibits both larger variations and significantly lower mean RMR values than greenstone, Småland (Ävrö) granite and Äspö diorite.

It proved to be difficult to predict in detail the mechanical characteristics, especially of greenstone. The compressive strength and elastic moduli were underestimated in the prediction while the Poisson's ratio and brittleness ratio corresponded well to the outcome. It seems as if the mechanical characteristics of greenstone vary over a rather wide range. The deviations observed here are, however, of such a magnitude that the overall stability conditions not will be influenced in practice.

The predictions of fracture surface properties corresponded rather poorly to the outcome. The evaluation of fracture surface properties involves major difficulties both in predicting and documenting the selected parameters. Fracture surface properties are, however, an important factor for the stability conditions in a underground construction. The evaluation proved that further improvements are required in the recommendations for applying JRC and JCS.

It seems possible to make rather good fracture frequency and fracture density predictions on the assumption that a general model of the structural geology is established.

It seems very difficult to make a good rock stress prediction on the 5 m detailed scale. Further knowledge is required on the variations of rock stresses in a rock mass and also on local variations in geological conditions.

At Äspö experts judged that only a few possible rock burst problems would occur and that greenstone was the most likely rock type for rock burst. No indications of rock burst were collected and thus the overall expert judgement of mechanical stability at Äspö proved to be correct. However, relevant data to make these judgements are normally sparse and scattered due to large natural variability and model and parameter uncertainty. Models for excavation stability have not been thoroughly tested due to the limited stress levels at Äspö.

Table 4. Overview of subjects, predictions and observed outcomes of relevance for the key issue of mechanical stability.

Subject	Site scale		Block scale		Detailed scale		Comments
	Within predicted range	Outside	Within predicted range	Outside	Within predicted range	Outside	
Rock quality (RMR)	+		+			+	
Primary stress		+		+		+	In order to make precise predictions of the rock stresses on the block and detailed scales further investigations of geological variations and measuring methods are needed .
Rock burst	+						
Mechanical characteristics (laboratory measurements)							
Rock strength					+		Predictions for greenstone and Småland (Ävrö granite) outside the range.
Elastic moduli						+	
Poisson's ratio					+		
Brittleness					+		
Fracture properties (laboratory measurements)							
JRC						+	Only a few measurements were made prior to construction and during the construction phase. Further improvements are required in the recommendations for applying JRC and JCS.
JCS						+	
Spacing						+	
RQD					+		

1 INTRODUCTION

1.1 ÄSPÖ HARD ROCK LABORATORY (Äspö HRL)

The Äspö Hard Rock Laboratory (HRL) constitutes an important part of the work of developing a deep repository and developing and testing methods for investigating and licensing a suitable site. The plan to build an underground rock laboratory was presented in *R&D Programme 86 /1986/* and was received very positively by the reviewing bodies. In the autumn of 1986, SKB initiated the field work for the siting of the underground laboratory in the Simpevarp area of the municipality of Oskarshamn. At the end of 1988, SKB arrived at a decision in principle to site the laboratory on southern Äspö, about 2 km north of the Oskarshamn Nuclear Power Station (see *Figure 1-1*). After regulatory review and approval, construction work on the facility was commenced in the autumn of 1990.

The Äspö HRL has been designed to meet the projected needs of the planned research, development and demonstration activities. The underground part takes the form of a tunnel from the Simpevarp peninsula to the southern part of the island of Äspö (see *Figure 1-2*). Below Äspö, the tunnel runs in two turns down to a depth of 450 m (see *Figure 1-3*). The total length of the tunnel is 3600 m. The first part of the tunnel was excavated using the drill-and-blast technique. The last 400 metres were excavated by a tunnel boring machine (TBM) with a diameter of 5 metres. The underground excavations are connected to the surface facilities by a hoist shaft and two ventilation shafts. The Äspö Research Village with offices, stores and hoist and ventilation building is located at the surface, (see *Figure 1-4*).

The work at the Äspö HRL was divided into three phases: the pre-investigation phase, the construction phase and the operating phase. The **pre-investigation phase**, 1986–1990, involved siting the Äspö HRL. The natural conditions in the bedrock were described and predictions made with respect to the geohydrological and other conditions that would be observed during the construction phase /Gustafson et al, 1991/. Planning for the construction and operating phases was also carried out.

During the **construction phase**, 1990–1995, extensive investigations, tests and experiments were carried out in parallel with the civil engineering activities, mainly to check the reliability of the pre-investigations. The tunnel was excavated to a depth of 450 m and construction of the Äspö Research Village was completed. The Äspö Research Village was taken into service during the summer of 1994. The underground civil engineering works were mostly completed in the summer of 1995.

The **operating phase** began in 1995. A programme for these studies is presented in *RD&D Programme 95 /1995/*.
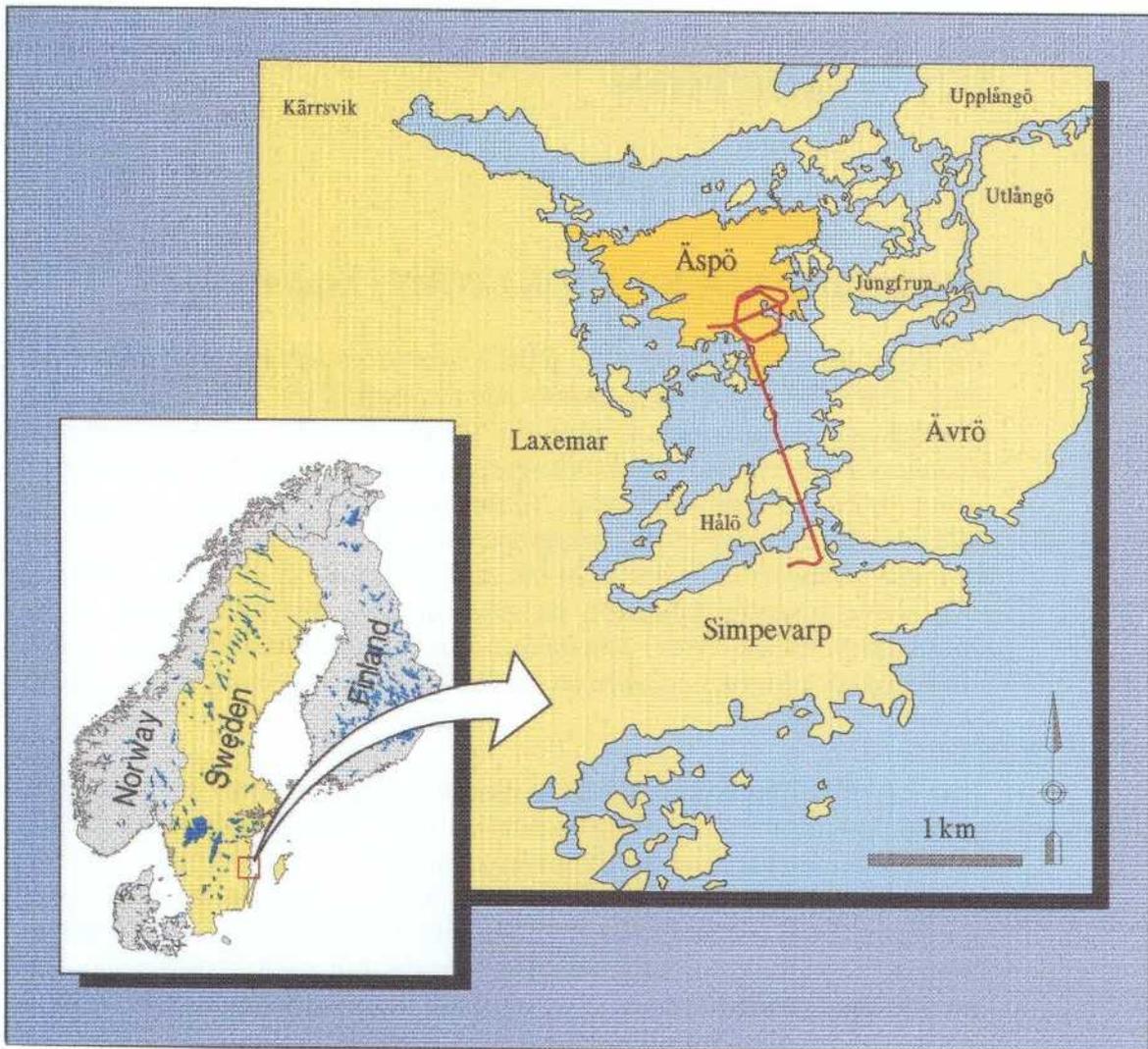
Figure 1-1. Location of the Äspö Hard Rock Laboratory.

Figure 1-2. Overview of the area around the Äspö HRL.
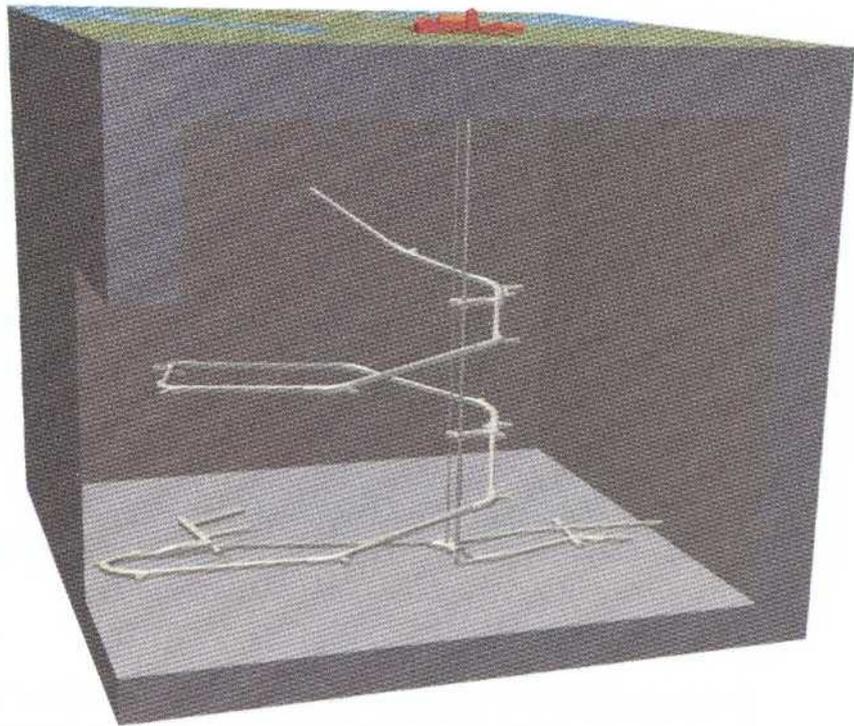
Figure 1-3. *General layout of the Äspö HRL. The total length of the tunnel is 3600 m. The first part of the tunnel was excavated using the drill-and-blast technique. The last 400 metres were excavated by a Tunnel Boring Machine (TBM) with a diameter of 5 metres. The underground excavations are connected to the Äspö Research Village, containing offices, stores, hoist and ventilation building, by a hoist shaft and two ventilation shafts.*

Figure 1-4. *Bird's-eye view of the Äspö Research Village.*

1.2 OVERALL GOALS OF THE ÄSPÖ PROJECT

One of the basic motives for SKB's decision to build the Äspö HRL was to provide an opportunity for research, development and demonstration in a realistic and undisturbed rock environment down to the depth planned for a future deep repository.

To meet the overall schedule for SKB's RD&D work, the following (here abbreviated) stage goals were set up in *R&D-Programme 89 /1989/* for the activities at the Äspö HRL.

1   Verify pre-investigation methods.
2   Finalize detailed characterization methodology.
3   Test models for groundwater flow and radionuclide migration.
4   Demonstrate construction and handling methods.
5   Test important parts of the repository system.

In the planning and design of activities to be performed at the Äspö HRL during the operating phase, priority is being given to projects which aim to:

*   increase scientific understanding of the deep repository's safety margins,
*   develop and test technology which reduces costs and simplifies the repository concept without sacrificing high quality and safety, and
*   demonstrate technology that will be used for the deposition of spent nuclear fuel and other long-lived waste.

The start of the operating phase has motivated a revision and focusing of the goals of the Äspö HRL, based on the experience gained to date. For the operating phase, the stage goals have been worded as follows, */R&D-Programme 95 /1995/*:

1   Verify pre-investigation methods
Demonstrate that investigations at the ground surface and in boreholes provide sufficient data on essential safety-related properties of the rock at repository level.

2   Finalize detailed characterization methodology
Refine and verify the methods and the technology needed for characterization of the rock in the detailed characterization of a site.

3   Test models for description of the barrier function of the rock
Refine and at repository depth test methods and models for describing groundwater flow, radionuclide migration and chemical conditions during the repository's operating period and after closure.

4   Demonstrate the technology for and function of important parts of the repository system
Test, investigate and demonstrate on a full scale different components of importance for the long-term safety of a deep repository system and show

that high quality can be achieved in the design, construction and operation of system components.

The four reports mentioned in the foreword mainly address the first and, to some extent, the second of the above stage goals.

The Äspö HRL comprises an important part of the work being pursued within SKB's RD&D-Programme.

1.3 AIM OF THIS REPORT

The purpose of this report, No. 3, is to present the evaluation of geology and mechanical stability predictions made during the pre-investigation phase.

Part 1 presents the evaluation of the geology.

Part 2 presents evaluation of the mechanical stability.

1.4 COORDINATE SYSTEM

For various reasons a number of coordinate systems have been used during the pre-investigation and construction phases.

At Äspö four different coordinate systems are used. The systems are rotated relative to one another and have different North directions. Within the Äspö Project all geological information on the orientation of structures is given relative to magnetic North. This reference direction is generally used in this report. Geographic North is also used occasionally as a reference direction, but for practical purposes this is the same as magnetic North, considering the accuracy in orientation that can be obtained for geological features.

Location of drifts and boreholes are always given in the local Äspö coordinate system.

The relative orientation between the four coordinate systems are:

- RAK-38 North is 11.819 degrees East of Äspö local North map system.
- Geographic North is 11.119 degrees East of Äspö local North.
- Magnetic North is approximately 12 degrees East of Äspö local North (1985-1990).

The coordinate transformation between the RAK-38 and local Äspö systems is according to the equations below:

$$X_{RAK-38} = 6367978.295 + 0.978799 \, (X_{Äspö} - 7484.309) + 0.204822 \, (Y_{Äspö} - 1956.68)$$

$$Y_{RAK-38} = 1551210.173 - 0.204822 \, (X_{Äspö} - 7484.309) + 0.978799 \, (Y_{Äspö} - 1956.68)$$

$$(6360251.890, \ 1550827.928)_{RAK-38} = (0,0)_{Äspö}$$

The length correction between the systems is as follows:

$$L_{RAK-38} = 0.999999852 \cdot L_{Äspö}$$

1.5 CHAINAGE DIFFERENCES DUE TO MODIFIED LAYOUT OF THE TUNNEL

There are chainage differences in the tunnel between the planned layout and the actual excavated layout. The reason is that the layout was modified during construction.

In September 1991 the layout of the tunnel was changed because core borehole KBH02 was hit by the tunnel. It was decided to move the tunnel about 35 m to the east and then go back to the original position of the tunnel close to the position of the shafts at about chainage 1 650 m (see *Figure 1-5*).

During excavation of the tunnel SKB decided to test full-face boring using a Tunnel Boring Machine (TBM). Because of this the tunnel layout was changed from about tunnel section 2600 m, As a result of this it was decided that the comparison of predictions and measured entities should only be made up to tunnel section 2875 m (excavated length) as from there the difference between planned an excavated layout was considered to be too large for a relevant comparison (see *Figure 1-6*).

The layout modification during construction affected the evaluation of the concepts and models to a minor degree. Where this is considered relevant for the evaluation it is discussed in the report.

Figure 1-5. *The planned and excavated tunnel layouts.*

Planned	Excavated
0/900	0/900
1/000	1/006
1/500	1/506
1/700	1/720
1/800	1/822
2/200	2/222
2/243	2/265

▨▨▨ Planned tunnel

▬▬ Excavated tunnel

RS_TUNDR-02-2 940303

Differences in chaining between planned and excavated tunnel due to modified design
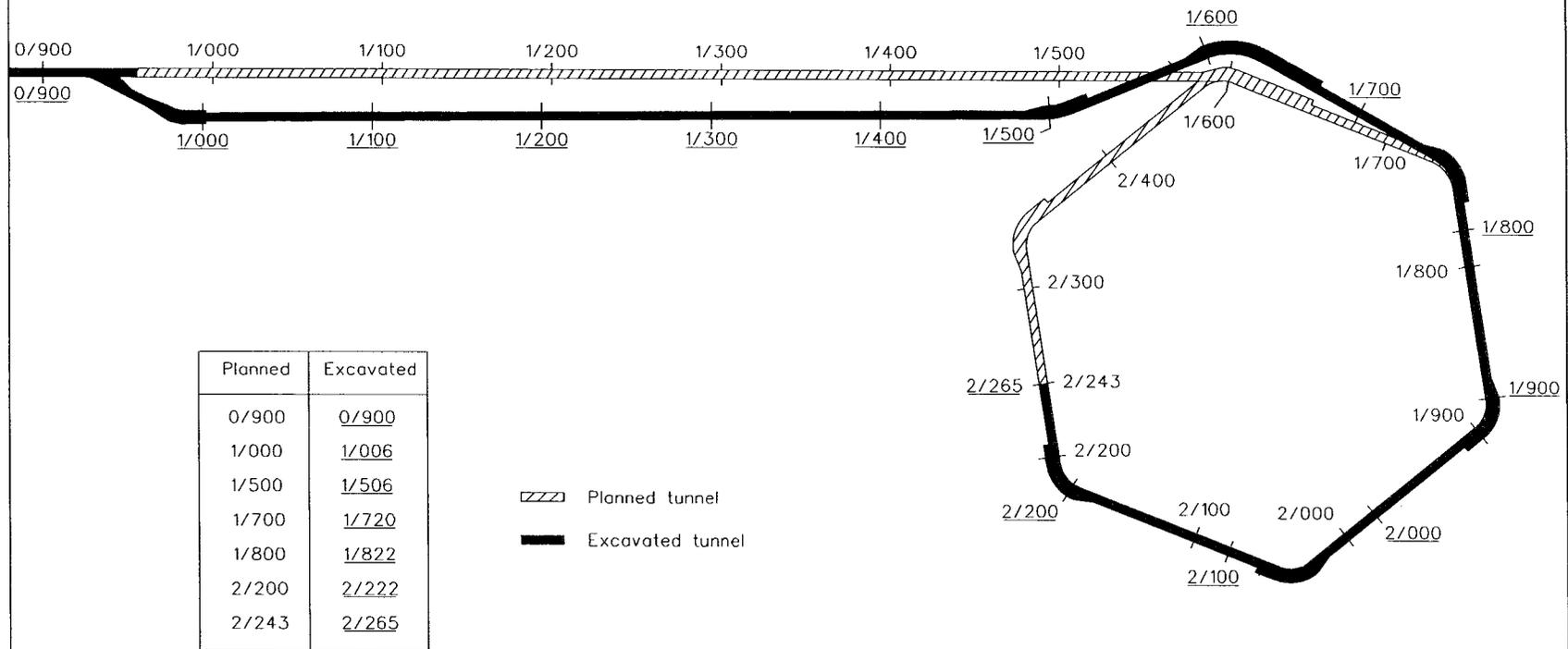
Figure 1-6. *The planned and excavated tunnel layouts.*

Planned	Excavated
2/100	2/122
2/200	2/222
2/243	2/265
2/300	2/322
2/400	2/436
2/500	2/560
2/600	2/661
2/700	2/774
2/793	2/900
2/800	2/907

▨▨ Planned tunnel

▬▬ Excavated tunnel

8

ACKNOWLEDGEMENTS

PART 1

GEOLOGY

1   SUBJECT: MAJOR FRACTURE ZONES

1.1   SCOPE AND CONCEPTS

The nomenclature and classification according to *Wikberg et al /1991/* treats aspects of the use of nomenclature for site investigations and addresses the way in which geological, geophysical, geohydrological results should be named. A special section is devoted to the uniqueness and completeness of investigations.

According to *Bäckblom /1989/* a fracture zone is a fracture zone if - and only if - geological field evidence support zones **with the characteristic that the intensity of natural fractures is at least twice as high as that of the surrounding rock.** Completely disintegrated and/or chemically altered rock is included in the definition of fracture zone.

The term 'major fracture zone' was used for a feature more than about 5 m wide and extending several hundred metres. Features less than about 5 m and more than 0.1 m wide and of lesser extent were called 'minor fracture zones'.

To define a 'level of reliability' three separate definitions were used.

'Possible' is the lowest level of confidence. By additional studies the level of reliability can be raised to 'Probable'. For minor fracture zones this is more seldom possible.

Its extent and direction is 'Certain' after confirmation by investigations or measurements at several points.

Mapping in the tunnel, according to that definition would, however, designate most fine-grained granite as fracture zones. For this reason it was found necessary to add a tectonic/kinematic constraint to the definition of 'fracture zone' such as shearing, faulting and clay alteration. Sections in the tunnel with more than 5 fractures/m with no obvious tectonic/kinematic influence were mapped as zones with 'increased fracturing', which are not necessarily two-dimensional features.

1.2   METHODOLOGY FOR TESTS OF CONCEPTS AND MODELS

1.2.1   Prediction methodology

The different methods used for characterization and localization of major fracture zones are presented in */Figure 1-1/.*

Surface methods

Airborne geophysics

Geophysical data - especially magnetic and electric - obtained by aerial survey were used to interpret the location and character of presumed major fracture zones /Nisca, 1987; Wikberg et al, 1991 and Almén et al 1994/.

Interpretation of lineaments

Lineaments in the Simpevarp area were interpreted from four different digital terrain models using image processing and analysis techniques. The aero-geo-physical results - which were also processed using this system - were compared with the results from the digital terrain models based on processed elevation data /Tirén et al, 1987; Wikberg et al 1991 and Almén et al 1994/.

Ground geophysical profiling

Ground geophysical profiling was used to confirm the aero-geophysical and topographical indications of major fracture zones. Low magnetic intensity due to oxidation, VLF anomalies (water-bearing zones) and low seismic refraction velocities contributed to the characterization of fracture zones as regards width and extent of fracturing/alteration / Stenberg and Sehlstedt, 1989/.

Structural-geological mapping

Fracture mapping and a structural characterization study of the main fracture zones were performed based on analyses of terrain features, geophysical data and topographical contour maps /Ericsson, 1987; Talbot et al, 1988; Talbot and Munier, 1989; Wikberg et al 1991 and Almén et al 1994/.

Seismic reflection

Two seismic reflection profiles were recorded across Äspö island for the main purpose of testing the ability of this method to map especially low-dipping and horizontal fracture zones in crystalline bedrock /Plough and Klitten, 1989/.

Ground radar investigation

Three ground radar profiles running N-S were measured in the southern part of Äspö to test the ability of this method to locate shallow low-dipping fracture zones.

Borehole methods

Geological structural analysis contributed to a rather good understanding of the two-dimensional extent of major fracture zones in the Äspö area. In order to get a three-dimensional model of the major fracture zones and to characterize it, a core drilling programme was carried out in three different campaigns.

Core mapping

Core mapping gave information on fracturing and rock quality of the fracture zones /Sehlstedt and Triumf, 1988/. In percussion boreholes it was often possible to identify intersections between the borehole and a fracture zone. Inflow rates, increased fracturing and to some extent also rock type were assessed during drilling.

Geophysical logging

The complete geophysical logging programme carried out comprised the following methods:

- gamma-gamma
- neutron (cored boreholes only)
- borehole deviation
- caliper (cored boreholes only)
- sonic
- natural gamma
- single-point resistance
- self-potential (SP)
- magnetic susceptibility
- normal resistivity (1.6 m)
- lateral resistivity (1.6 - 0.1 m)
- temperature
- borehole fluid resistivity

The aim of the 'major fracture zone' interpretation was to describe the geophysical logging data in terms of fracturing and hydrogeology. The sonic logging, single-point resistance, normal resistivity, caliper and self-potential methods were mainly used for delineation and classification of fracturing in cored borehole walls.

Borehole radar measurements

Borehole radar measurements were made in all cored boreholes to obtain information on the orientation of the fracture zones. The radar measurements were made as single-hole measurements using omni-directional dipole antennas with a 22 MHz frequency using 60 Mhz frequency /Niva and Gabriel, 1988/

or in some of the last boreholes a directional radar antenna /Carlsten, 1989, 1990/.

Vertical seismic profiling (VSP)

As a complement to the borehole radar investigation, a VSP survey - aimed at obtaining information on the orientation of fracture zones - was made in a borehole, KAS07, on southern Äspö down to a depth of 410 m /Cosma et al, 1990/.

1.2.2 Methodology for determining outcome

Geological documentation in the tunnel

All fracture zones were mapped in connection with the general geological mapping performed after each new round. The mapping comprised position, strike, dip, width, rock type and fracture data, such as trace length, fracture filling and fracture orientation.

Core drilling

Core drilling - often related to experiments concerning major fracture zones - provided supplementary information regarding fracture zones EW-7, NE-3 and, especially, NE-1.

During drilling of the percussion boreholes the drilling rate and colour of the drilling water were recorded continuously. From these data it was possible to identify possible fracture zones and roughly estimate the rock type.

Borehole radar and Vertical Seismic Profiling (VSP) investigations

Borehole radar and VSP investigations were made to obtain information on the orientation of fracture zones, especially NE-1.

1.3 COMPARISON OF PREDICTED AND MEASURED ENTITIES

The prediction to be compared with tunnel data comprised the major fracture zones EW-7, NE-4, NE-3, NE-1, EW-3 and NE-2 /Gustafson et al, 1991/.

The conceptual geological-structural model also included the low-dipping 'possible' fracture zones EW-5 and EW-X and the certain Äspö shear-zone EW-1 north of the tunnel area.

The prediction of the major fracture zones was based on geological-geophysical data, presented in the following *Tables 1-1, 1-3, 1-6, 1-8, 1-9 and 1-11 and Figures 1-2, 1-4, 1-7, 1-10 and 1-12.*

The outcome is mainly based on tunnel mapping data and borehole observations, presented in the following *Tables 1-2, 1-4, 1-5, 1-7, 1-10 and 1-12 and Figures 1-3, 1-5, 1-6, 1-8, 1-9, 1-11 and 1-13.*
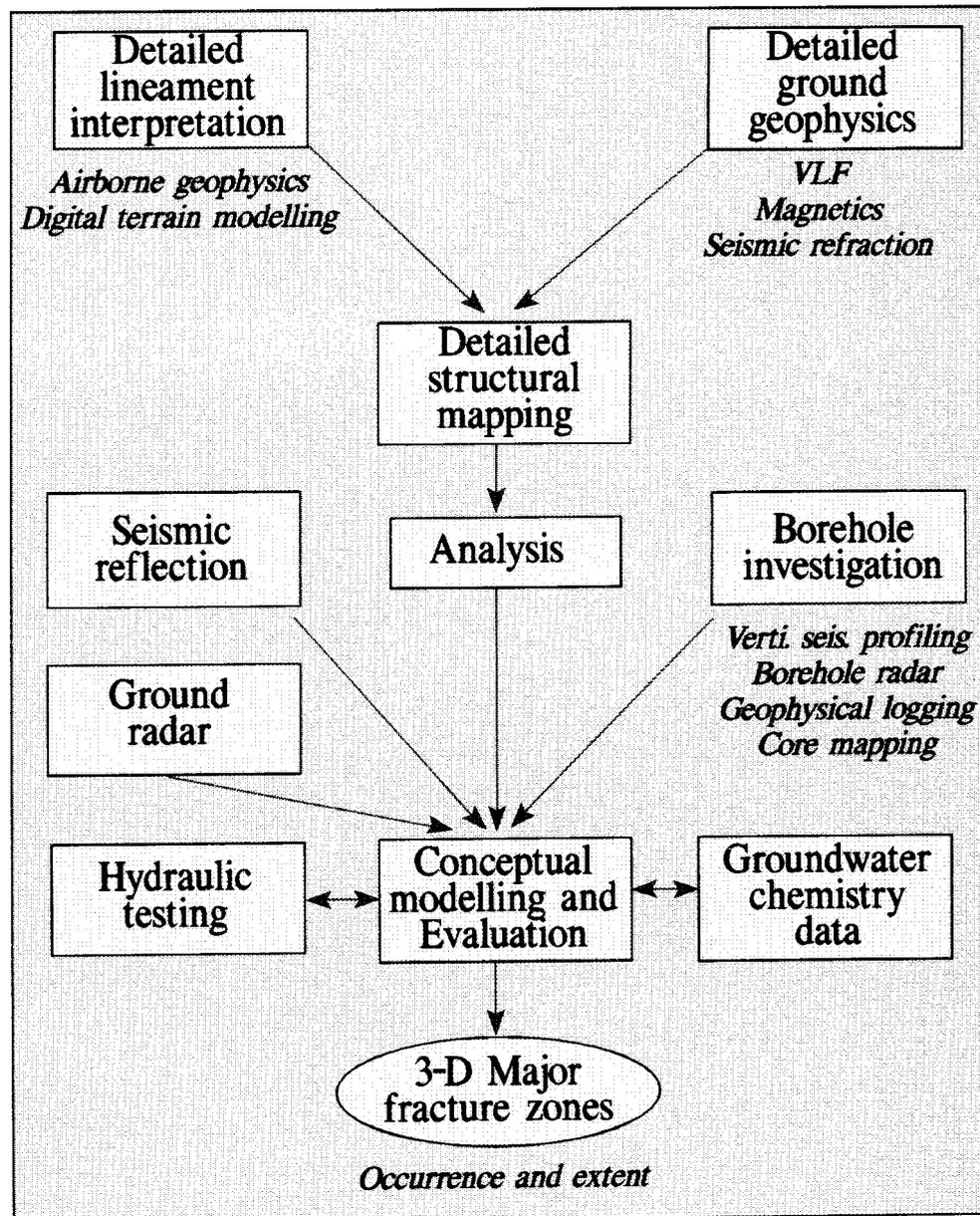
Figure 1-1. Pre-investigation methodology. Structural-geological characterization. Major fracture zones.

Fracture zone EW-7

Table 1-1. Geological-geophysical data. Fracture zone EW-7.

Fracture zone	Orientation (O) Estimated width (W) *Length at surface (L)	Topographical identification (T) Geophysical identification (G)	Geological identification Borehole section	Reliability
EW-7	O: ENE/70-78°S W: 10-20 m (sub-zones 1-5 m) L: 300-800 m	T: Assumed to surface in the sea north of Hålö G: Evident (magnetic, and seismic)	KBH01: 55-70 m KBH01: 50-75 m	'Probable'

* Based solely on geophysical data
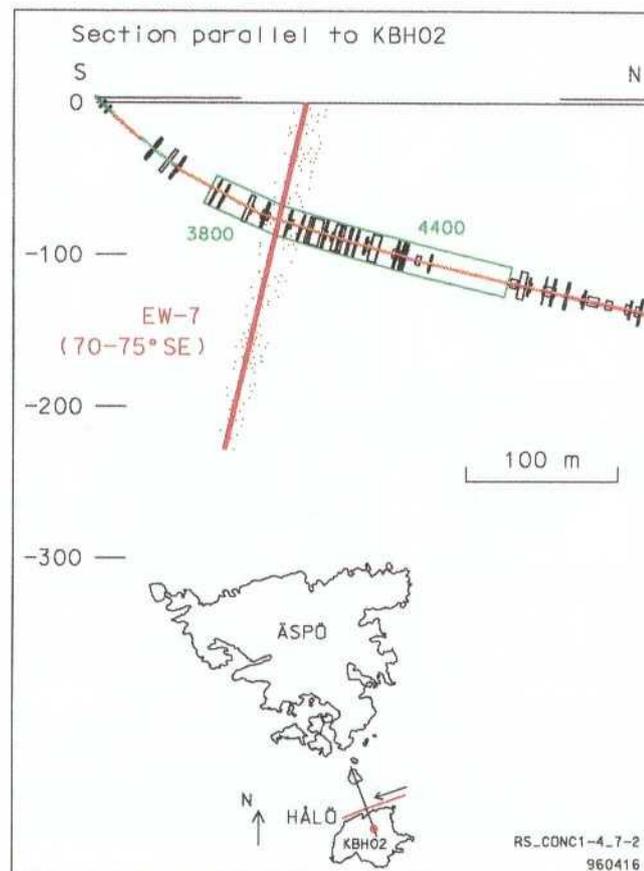
Figure 1-2. *Fracture zone EW-7. Prediction. /According to Gustafson et al, 1991/.*

Table 1-2. Prediction-outcome. Fracture zone EW-7.

Data concerning 'Position', 'Width' and 'RQD' refer to tunnel observations. Data concerning 'Strike', 'Dip' and 'Length' are estimated values based on pre-investigation and tunnel observations.

	Position (centre of zone)	Strike	Dip	Length (m)	Width (m)	RQD
Prediction	773 m(±20)**	ENE	65°S(±10)**	<1000	10(±5)**	0-25 (25%)* 25-50 (50%) 50-100 (25%)
Outcome	787 m	N75°E	75°S	<1000	10	0-25 (0%) 25-50 (30%) 50-100 (70%)

* 25 % of the total zone width in tunnel.
** Confidence level 60 %.
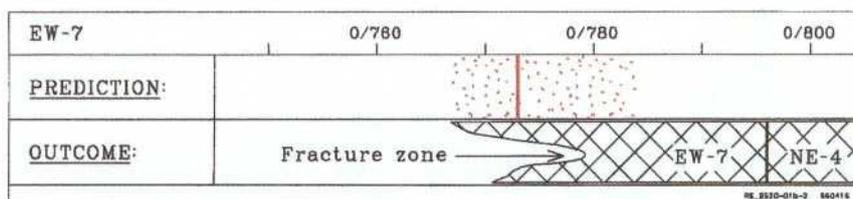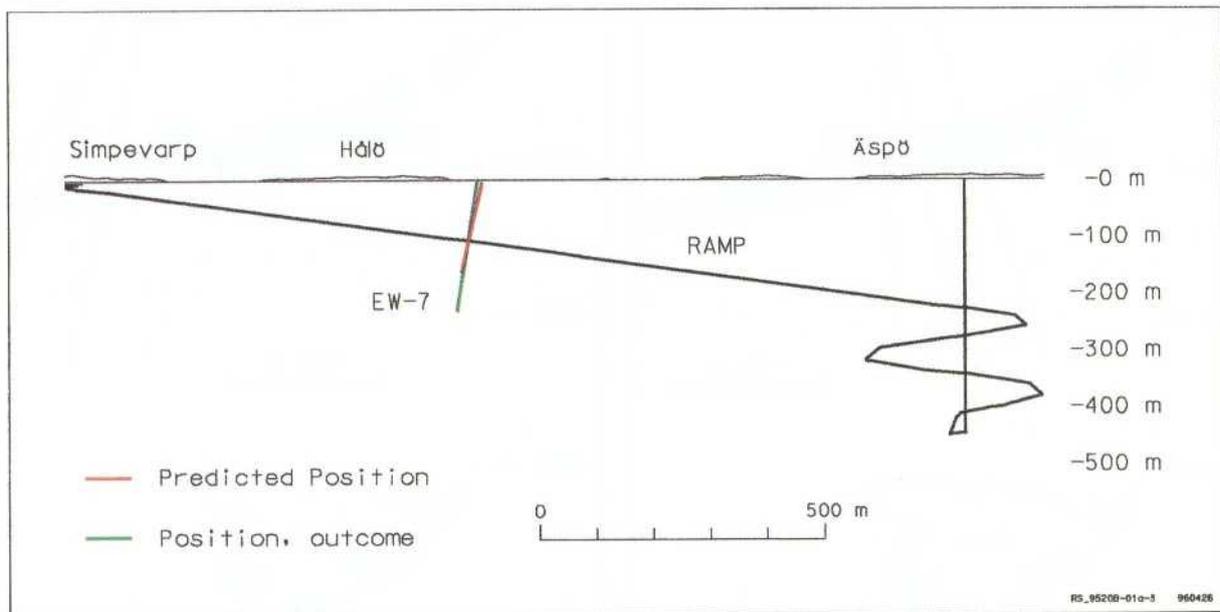
Figure 1-3. Fracture zone EW-7. Prediction - outcome.

Fracture zones NE-3 and NE-4

Table 1-3. Geological-geophysical data. Fracture zones NE-3 and NE-4.

Fracture zone	Orientation (O) Estimated width (W) *Length at surface (L)	Topographical identification (T) Geophysical identification (G)	Geological identification Borehole section	Reliability
NE-3 NE-4	O: NE/60-75°N (NE-3) O: NE/60-75°S (NE-4)	T: Assumed to surface in the sea north of Hålö	KBH02: 310-400 m KBH02: 120-250 m	'Certain'
NE-3 NE-4	W: 50 m (sub-zones 1-5 m) 5-10 m L:>1000 m	G: Evident (magnetic, and seismic)		

*   Based solely on geophysical data
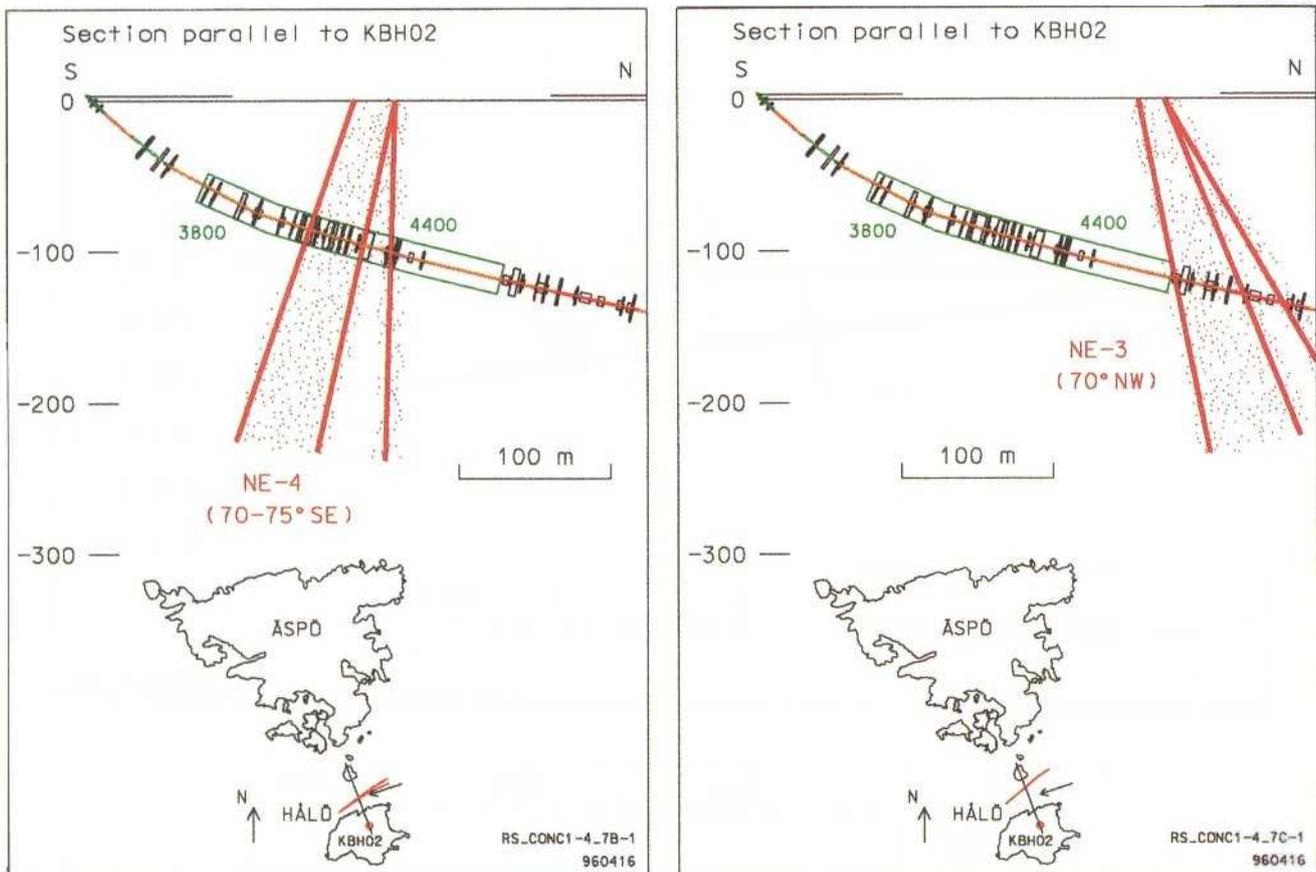
Figure 1-4.   *Fracture zones NE-3 and NE-4. Prediction. /According to Gustafson et al, 1991/.*

Table 1-4. Prediction-outcome. Fracture zone NE-4.

Data concerning 'Position', 'Width' and 'RQD' refer to tunnel observations. Data concerning 'Strike', 'Dip' and 'Length' are estimated values based on pre-investigation and tunnel observations.

	Position (centre of branch)	Strike	Dip	Length (m)	Width (m)	RQD
Prediction (three branches)	797 m(±20)[**] 839 m(±20)[**] 863 m(±20)[**]	NE	65°S(±5)[**]	>1000	50(±10)[***]	0-25 (50%)[*] 25-50 (25%) 50-100 (25%)
Outcome	802 m	N50°E	60°S	>1000	41[****]	0-25 (29 %) 25-50 (62%)
	855 m	N50°E	43°S	>1000		50-100 (9%)

[*]   50 % of the total zone width in tunnel.
[**]   Confidence level 60 %.
[***] Confidence level 75 %.
[****] Total zone width in tunnel.
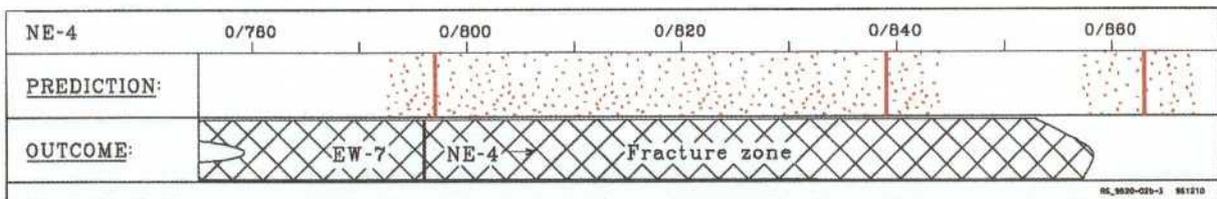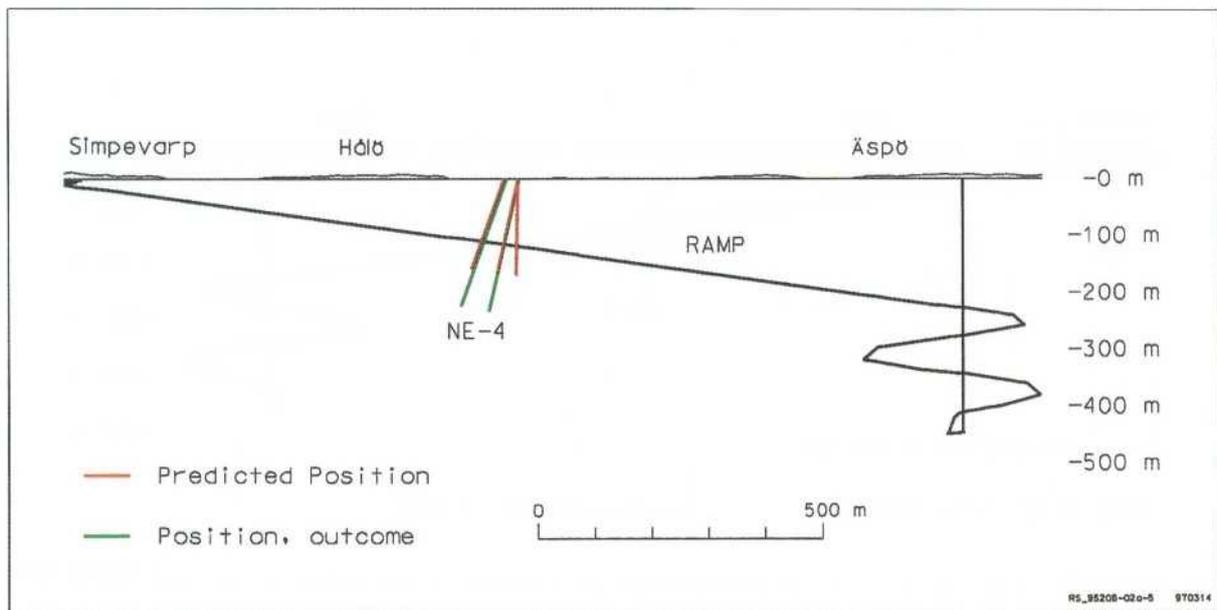
Figure 1-5. Fracture zone NE-4. Prediction - outcome.

Table 1-5. Prediction-outcome. Fracture zone NE-3.

Data concerning 'Position', 'Width' and 'RQD' refer to tunnel observations. Data concerning 'Strike', 'Dip' and 'Length' are estimated values based on pre-investigation and tunnel observations.

	Position (centre of branch)	Strike	Dip	Length (m)	Width (m)	RQD
Prediction (three branches)	945 m(±20)[**] 1005 m(±20) 1031 m(±20)	NE	70°N(±5)[****]	>1000	10(±5)[****] 50(±10)[****]	0-25 (25%)[*] 25-50 (50%) 50-100 (25%)
Outcome	975 m 1009 m	N50°E N70°E	80°N 70°N	>1000 >1000	49 [***]	0-25 (38 %) 25-50 (48%) 50-100 (14%)

*	25 % of the total zone width in tunnel.
**	Confidence level 60 %
***	Total zone width in tunnel.
****	Confidence level 75 %.
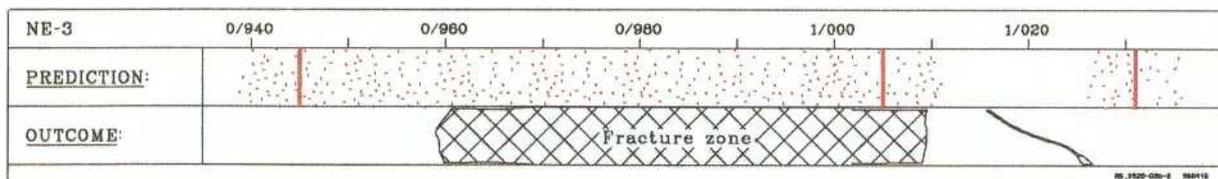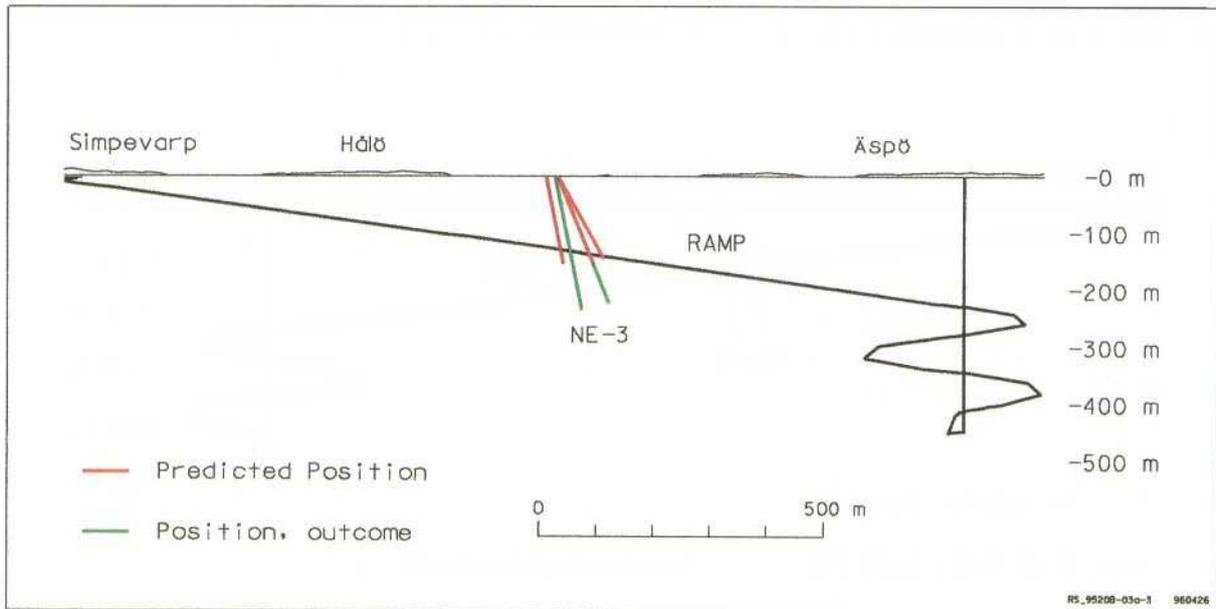
Figure 1-6. *Fracture zone NE-3. Prediction - outcome.*

Fracture zone NE-1

Table 1-6. Geological-geophysical data. Fracture zones NE-1.

Fracture zone	Orientation (O) Estimated width (W) *Length at surface (L)	Topographical identification (T) Geophysical identification (G)	Geological identification Borehole section	Reliability
NE-1	O: NE/50-60°NW W: 50 m L: 400-600 m	T: The fracture zone NE-1 is assumed to surface in the sea app. 50-100 m south of Äspö G: Evident (seismic and magnetic)	KAS09: 100-150 m KAS14: 100-125 m KAS11: 310-400 m KBH02: 310-400 m KAS08: 570-600 m KAS07: 520-550 m	'Certain'

* Based solely on geophysical data
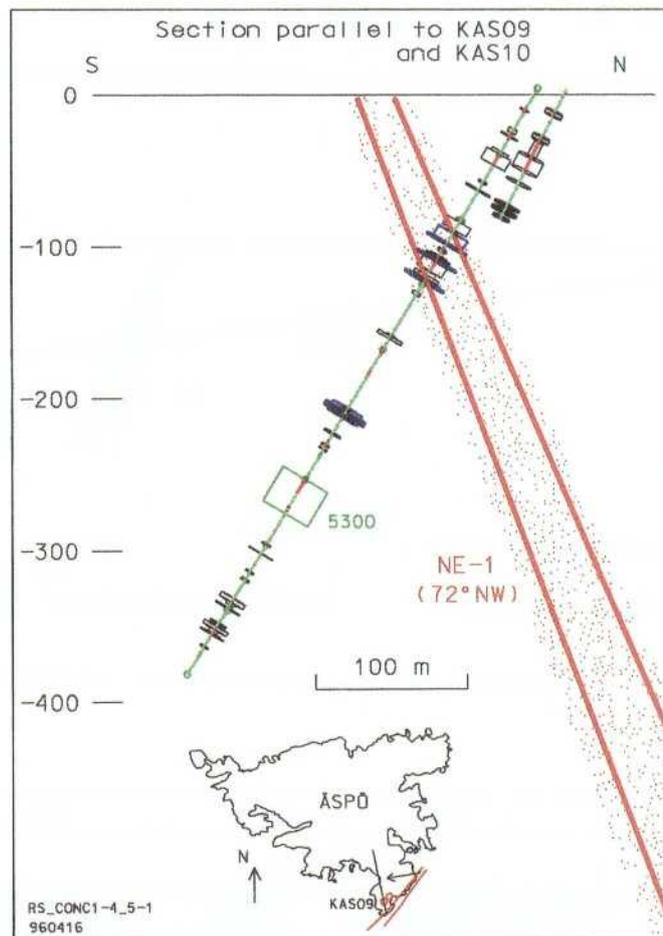
Figure 1-7. *Fracture zone NE-1. Prediction. /According to Gustafson et al, 1991/.*

Table 1-7. Prediction-outcome. Fracture zone NE-1.

Data concerning 'Position', 'Width' and 'RQD' refer to tunnel observations. Data concerning 'Strike', 'Dip' and 'Length' are estimated values based on pre-investigation and tunnel observations.

	Position (centre of branch)	Strike	Dip	Length (m)	Width (m)	RQD
Prediction (three branches)	1244 m(±20)[**] 1275 m(±20)[**] 1326 m(±20)[**]	NE	65°N(±5)[***]	>1000	30(±5)[***] 15(±5)[***]	0-25 (25%)[*] 25-50 (50%) 50-100 (25%)
Outcome	1263 m 1280 m 1305 m	N50°E N50°E N60°E	75°N 75°N 70°N	>500	25 8 28	0-25 (39 %) 25-50 (34%) 50-100 (27%)

*   25 % or the total zone width in tunnel
**   Confidence level 60 %
***   Confidence level 75 %
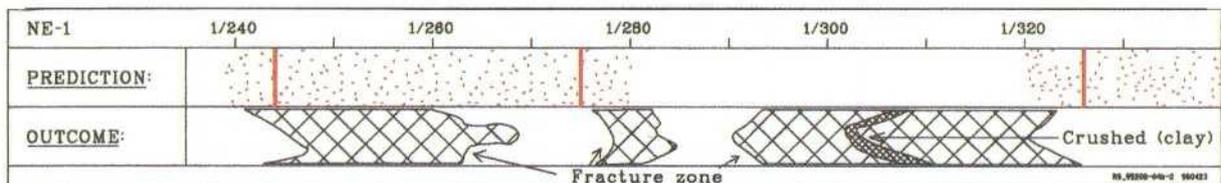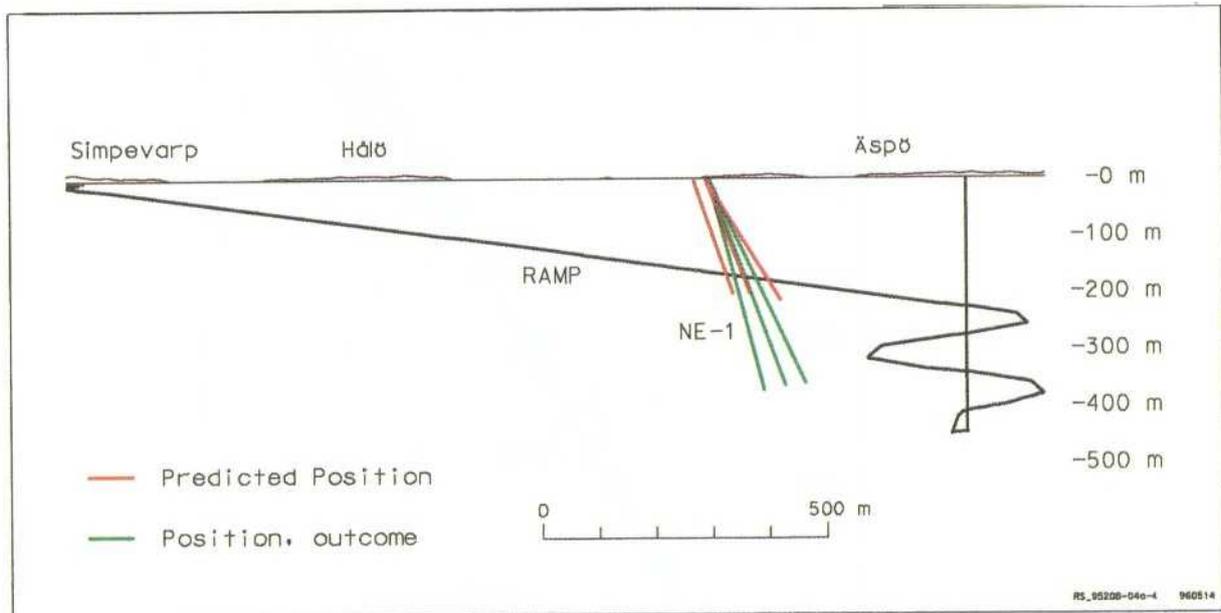
Figure 1-8.   Fracture zone NE-1. Prediction - outcome.

Fracture zone EW-5

Table 1-8. Geological-geophysical data. Fracture zone EW-5.

Fracture zone	Orientation (O) Estimated width (W) *Length at surface (L)	Topographical identification (T) Geophysical identification (G)	Geological identification Borehole section	Reliability
EW-5	O: ENE/20-30°NNW W:approx. 100 m? L:400-600 m?	T: EW-5 is assumed to surface in the sea 50-100 m south of Äspö G: Seismic reflection	KAS09,11,14: 10-60 m KAS04: 330 m KAS11: 120-130 m 275 m KAS05: 100-115 m 210-220 m KAS06: 60-70 m HAS13,14: 50-60 m	'Possible'
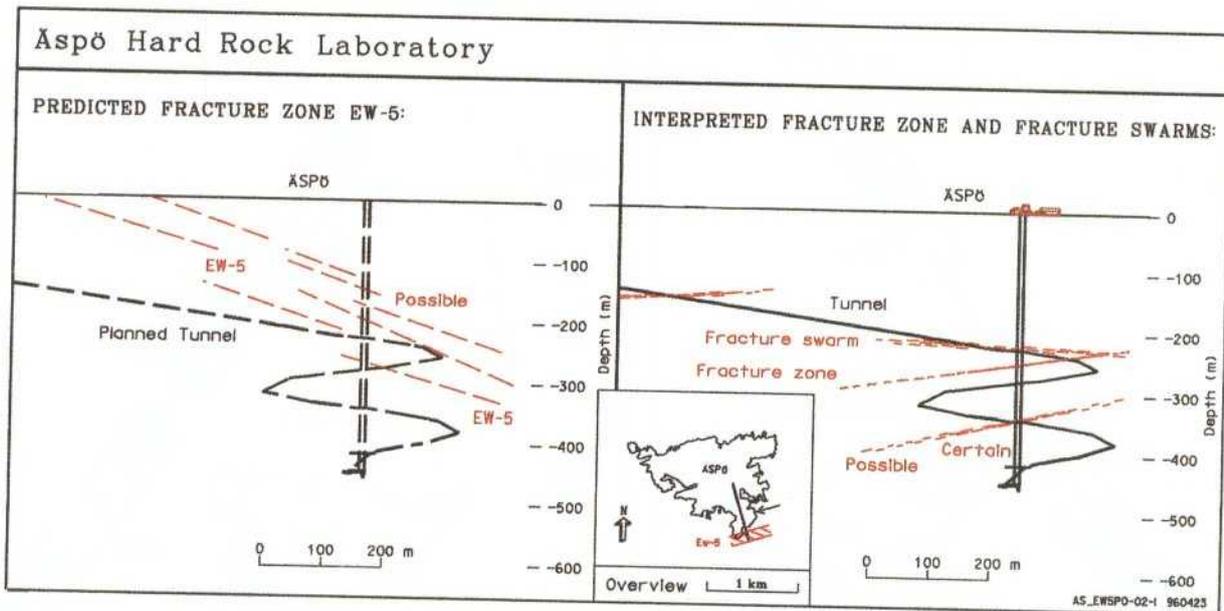
Figure 1-9. Fracture zone EW-5. Prediction - outcome.

Fracture zone EW-3

Table 1-9. Geological-geophysical data. Fracture zones EW-3.

Fracture zone	Orientation (O) Estimated width (W) *Length at surface (L)	Topographical identification (T) Geophysical identification (G)	Geological identification Borehole section	Reliability
EW-3	O: ENE/85°S	T: distinct	KAS06: 60-70 m	'Certain'
	W: 10-15 m	G: Evident (magnetic, electric and seismic)	KAS07: 420 m	
	L: 200 m			

*   Based solely on geophysical data.
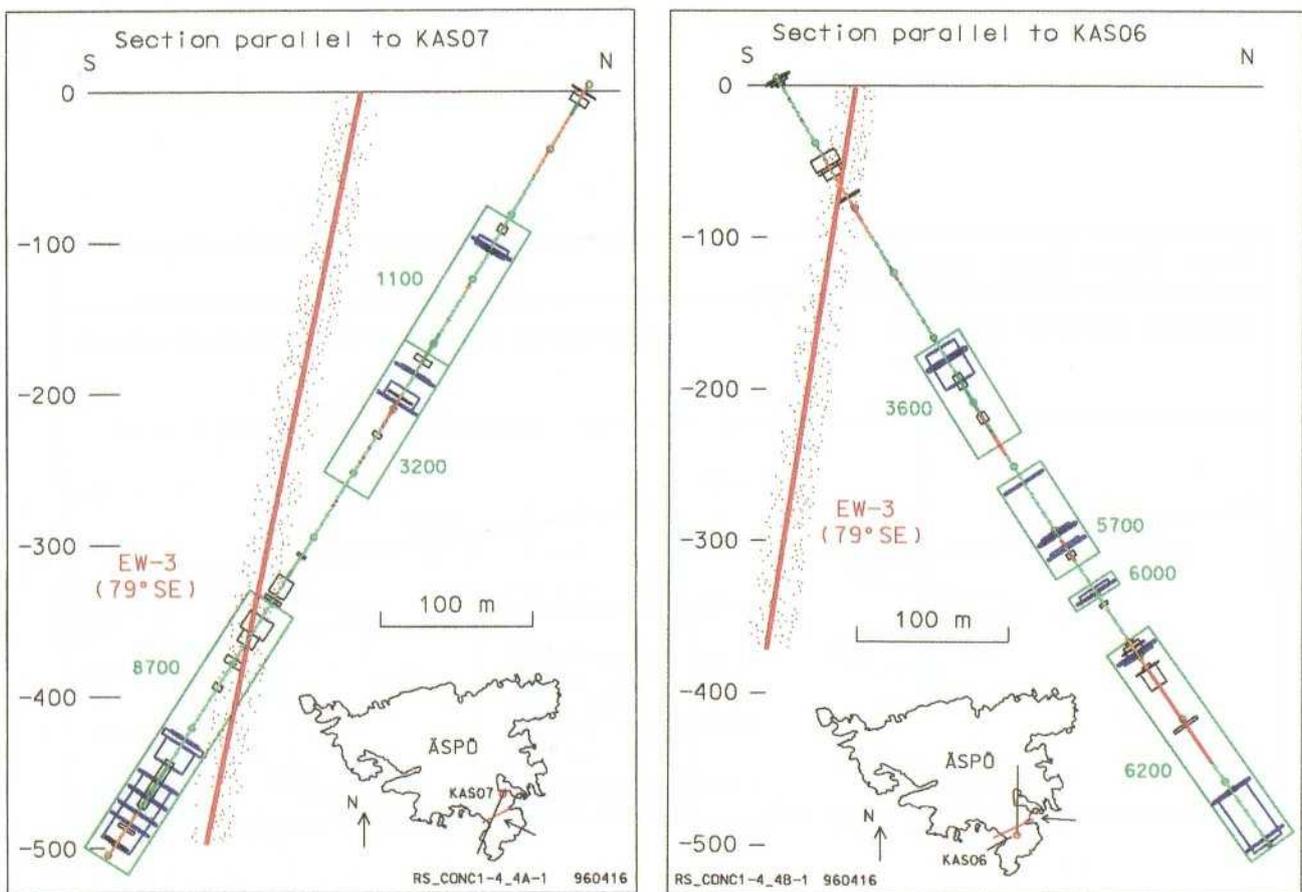
Figure 1-10. *Fracture zone EW-3. Prediction. /According to Gustafson et al, 1991/.*

Table 1-10. Prediction-outcome. Fracture zone EW-3.

Data concerning 'Position', 'Width' and 'RQD' refer to tunnel observations. Data concerning 'Strike', 'Dip' and 'Length' are estimated values based on pre-investigation and tunnel observations.

	Position (centre of zone)	Strike	Dip	Length (m)	Width (m)	RQD
Prediction	1427 m(±20)[**]	ENE	85°S(±5)[***]	<1000	10(±5)[***]	0-25 (50%)[*] 25-50 (50%)
Outcome	1414 m	N80°E	75-80°S	<1000	14	0-25 (28 %) 25-50 (31%) 50-100 (41%)

[*]   50 % of total zone width in tunnel
[**]   Confidence level 60 %
[***] Confidence level 75 %
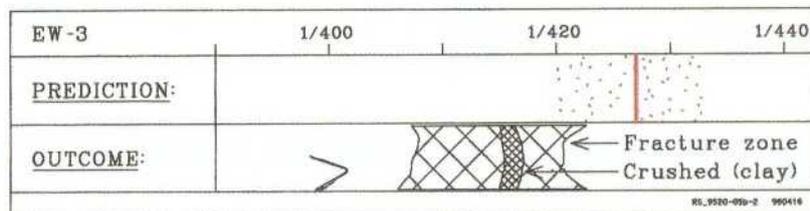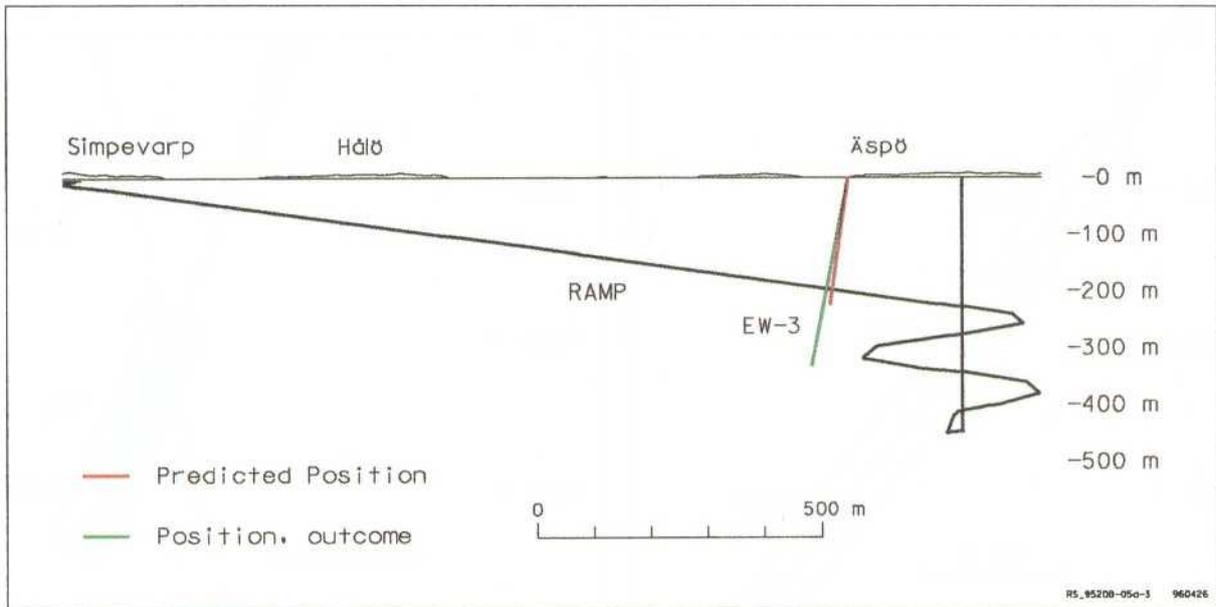
Figure 1-11. Fracture zone EW-3. Prediction - outcome.

Fracture zone NE-2

Table 1-11. Geological-geophysical data. Fracture zones NE-2.

Fracture zone	Orientation (O) Estimated width (W) *Length at surface (L)	Topographical identification (T) Geophysical identification (G)	Geological identification Borehole section	Reliability
NE-1	O: NE/75°NW	T: Faint	KAS04: 430 m	'Certain'
			KAS08: 40-60 m	
	W: 5-10 m	G: Evident (magnetic and electric)	KAS12: 270-300 m	
			KAS13: 370-410 m	
	E: 500-600 m		HAS16: 20-80 m	

*   On the target area (Äspö) above sea level
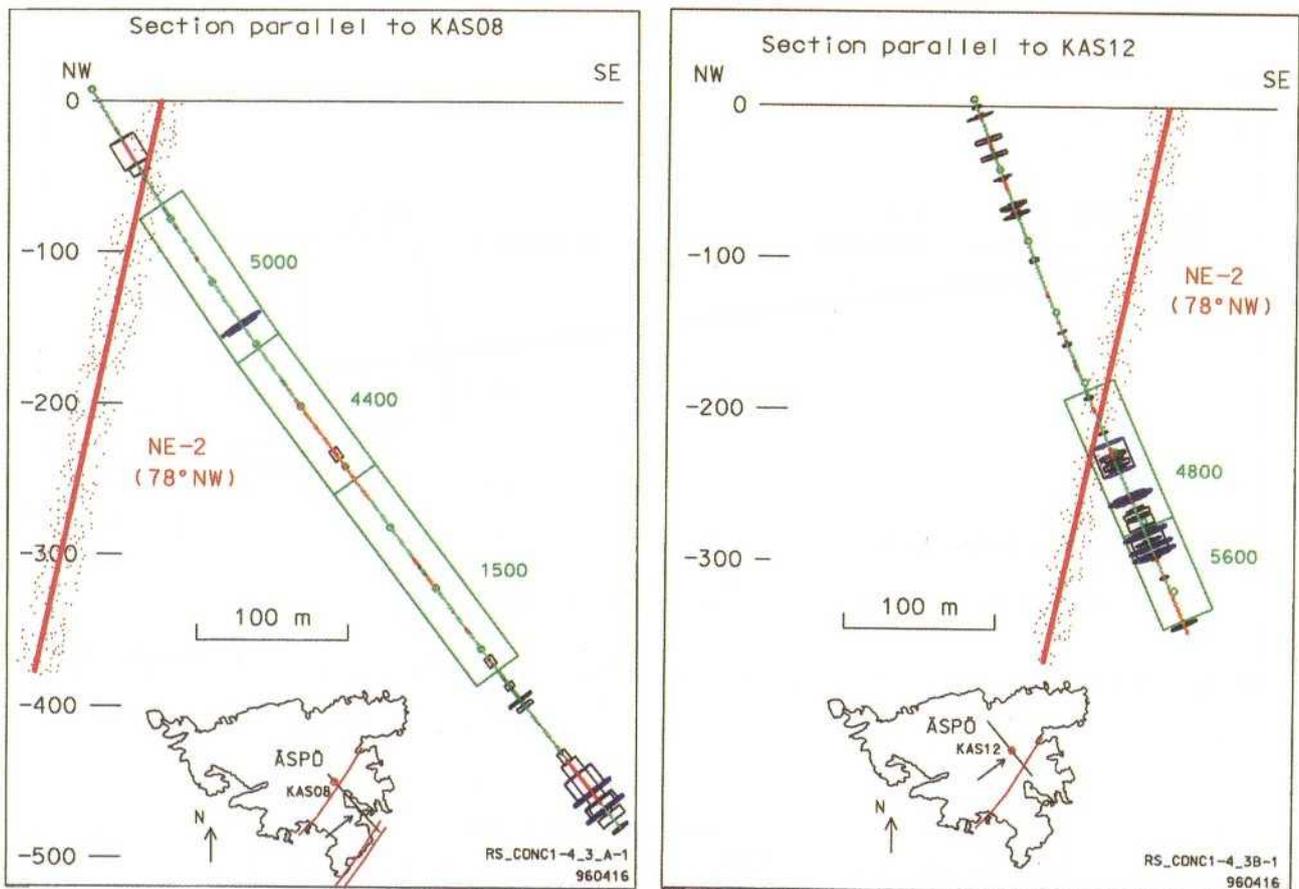
Figure 1-12. *Fracture zone NE-2. Prediction. /According to Gustafson et al, 1991/.*

Table 1-12. Prediction-outcome. Fracture zone NE-2.

Data concerning 'Position', 'Width' and 'RQD' refer to tunnel observations. Data concerning 'Strike', 'Dip' and 'Length' are estimated values based on pre-investigation and tunnel observations.

	Position (centre of zone)	Strike	Dip	Length (m)	Width (m)	RQD
Prediction	1740(±30)**	NE	75°N(±5)***	500-600	15(±5)**	0-25(50%)* 25-50(50%)
Outcome	1602 m 1844 m 2480 m	N36°E N15°E N32°E	82°S 70°S 65°S	500-600 500-600 500-600	1 1 5	0-25(25%) 25-50(75%)

*   50 % of the total zone width in tunnel.
**   Confidence level 60 %
***   Confidence level 75 %.
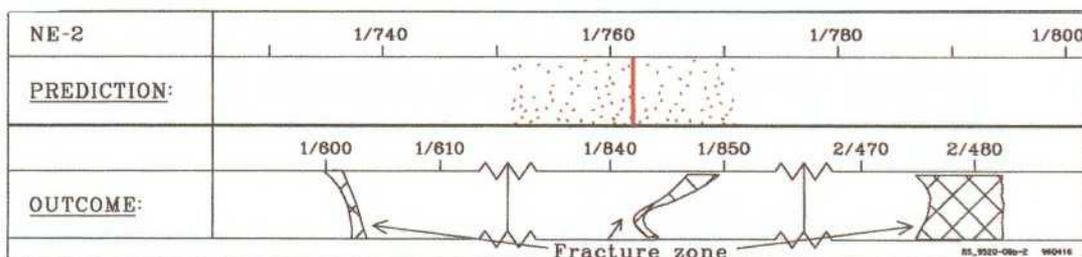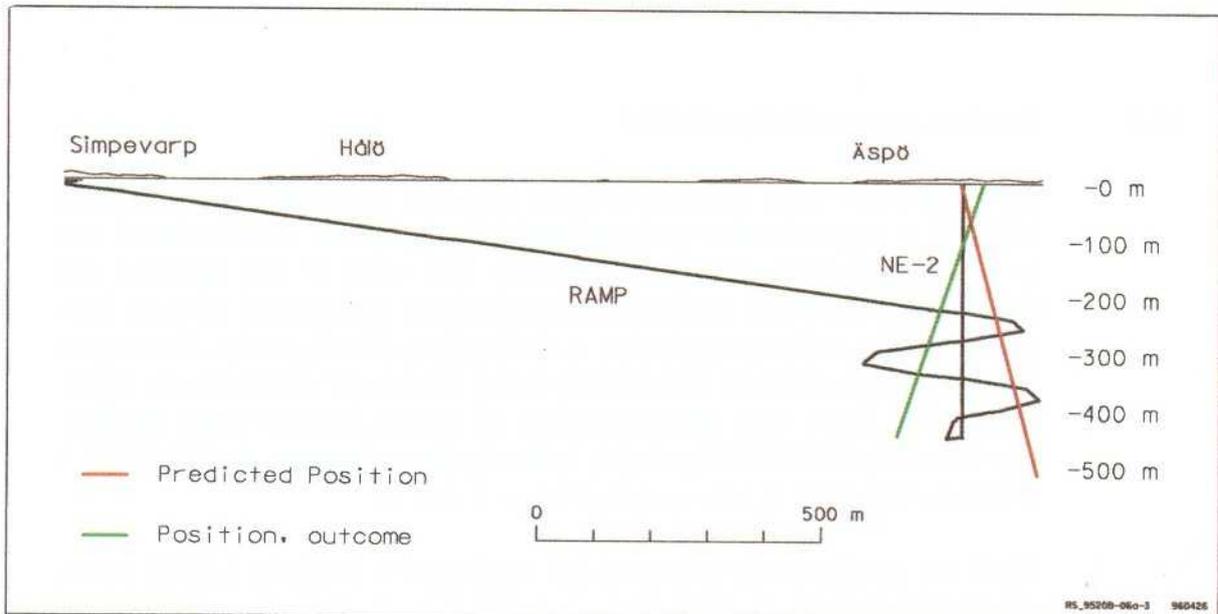
Figure 1-13. Fracture zone NE-2. Prediction - outcome.

1.4   SCRUTINY AND EVALUATION

1.4.1   Fracture zone EW-7

Fracture zone EW-7 was estimated to be a part of a zone system, which occurs in the ENE-NE and is regarded as being of regional extent. It was geophysically significant in the strait immediately north of Hålö and the northern branch of the zone was also indicated in core borehole KBH02. In the tunnel EW-7 consists of one set of fractures trending NNE - which are the most conductive structures - and one fracture set trending WNW. The dominating rock type in the zone is Småland (Ävrö) granite /Wikberg et al, 1991/ /Figures 1-2 and 1-3/.

According to /Gustafson et al, 1991, page A12/ only the northern branch of EW-7 was estimated to occur within the part of the tunnel (north of chainage 700 m) for which predictions were made on the basis of detailed pre-investigations.

Concerning the prediction of two southern branches of EW-7 only one narrow branch was found at 685 m in the tunnel /Stanfors et al, 1992/. However, the investigations for the first 700 m of the access tunnel were not performed to the same extent.

1.4.2   Fracture zones NE-3 and NE-4

NE-3 and NE-4 were regarded as being branches of a zone system trending ENE-NE of regional extent and predicted to be composed of a number of one to a few-metre-wide subzones alternating with slabs of less fractured and altered rock. NE-3 was predicted to be associated with several dikes of fine-grained granite and some mylonites in the Småland (Ävrö) granite. Some open fractures (narrow fracture zones) in NE-3 and NE-4 were assumed to be highly conductive. There were also indications of narrow fracture zones trending approximately NNW-NNE probably hydraulically connecting the NE-1/EW-5 system to NE-3/NE-4 zone system /Figure 1-4--1-6/.

NE-3 was geophysically indicated and confirmed in borehole KBH02 in the pre-investigation phase. After excavation, NE-3 was found to be approximately 49 m wide in the tunnel. Two parallel branches (splays) were identified in the tunnel. Fine-grained granite is the dominating rock type with some intersections of Småland (Ävrö) granite and greenstone. Fracture spacing is mostly 5-20 cm but crushed parts are found locally. Clay filling in fractures and clay altered rock were observed, especially in the middle part of the zone. It was not possible to decide on the different trends of the branches from only one borehole.

NE-4 was also indicated during pre-investigations by geophysics and borehole data (KBH02) and estimated to consist of three branches trending NE. After excavation of the zone - the dominating rock was found to be Småland (Ävrö) granite with inclusions of mylonite and greenstone. Two more or less

continuous branches were identified in the tunnel. The northernmost branch is clearly connected to the mylonite, which is partly crushed.

1.4.3 Fracture zones NE-1 and EW-5

Fracture zones NE-1 and EW-5 were assumed to surface in the sea approx. 50-100 metres south of Äspö /Wikberg et al, 1991/ /Figure 1-7--1-9/.

Zone NE-1, trending approximately NE and dipping approximately 60-70° to the north - according to borehole investigations - was estimated to be complex, with both steeply dipping and gently dipping elements.

NE-1 was well documented in several core boreholes as a series of several-metre-wide, highly fractured and in part mineralogically altered branches (splays). Some of the branches were estimated to be connected with the minor fracture zones trending NNW-NNE and perhaps also EW-5 and estimated to be very important as hydraulic conductors.

NE-1 was predicted to be composed of three branches. In the tunnel all three branches are connected to a rather complex rock mass of Äspö diorite, fine-grained granite and greenstone. The two southernmost branches, trending NE and dipping to NE, can be described as highly fractured and more or less water-bearing. The northern branch, which is approximately 28 m wide in the tunnel, is the most intense part of NE-1 and highly water-bearing. The central - approximately 5-m wide - part of this branch, trending N60°E and dipping 70°N with open, centimetre-wide fractures and cavities and partly clay-altered rock, is surrounded by 10-15 m wide sections of more or less fractured rock.

Fracture zone NE-1 was considered to be 'certain'.

Zone EW-5 was assumed to dip gently (20-30° to NNW and appears to be associated with a thrust trending approximately ENE, observed on land approximately 300 m east of southern Äspö. EW-5 was predicted to comprise a series of more or less parallel fractures, partly open with stepped offsets in the dip direction, with the most significant hydraulic pathways running parallel to the strike of the zone. The different steps of EW-5 - which seem to be poorly hydraulically connected for the most part - were predicted to be intersected by narrow fracture zones trending NNW-NNE and judged to be highly permeable. Talbot /1989/ discussed the possibility of several gently dipping fracture zones parallel to EW-5 with a vertical spacing of about 90-133 m. Fracture zone EW-5 was judged to be 'possible'.

According to Hermanson /1995/ two well defined gently dipping fracture zones were found in the tunnel. The first one intersects the tunnel at chainage 220 m. It consists of fractures with a strike NW and dip 25° with a spacing of less than 10 cm. The width of the zone is 0.5 m. Parts of the zone consist of calcite-impregnated breccia. Epidote and chlorite fillings are also present. The second and most prominent gently dipping fracture zone appears at chainage 1744 m down to 1850 m /Figure 3-23/. Intense fracturing, trending NE with a dip 32°E,

runs subparallel to the tunnel for almost a hundred metres. The width is less than a metre with mineral fillings of epidote, chlorite and Fe-oxide. Parts of the zone contain fault breccia which gradually decreases in intensity to anastomosing fractures with a spacing of 10 cm or more. A minor amount of water inflow (drips) were noticed in the brecciated part of the zone. This particular zone is denoted Z6 in *Stanfors et al /1993/*. It was not possible to determine whether any of these zones have any ductile precursors.

Except for the two gently dipping fracture zones described above, all other subhorizontal fractures occur in 'swarms' rather than 'zones', in much the same way as the NNW hydraulic conductors appear in swarms. The swarms are visible in straight parts of the tunnel, but best detectable in the larger niche corners. */Hermanson, 1995/* defined a 'fracture swarm' as a zone with relatively high fracture frequency, but not so high as a proper 'fracture zone', with fracture orientation essentially parallel to the orientation of the swarm boundary.

Altogether, seven subhorizontal fracture swarms were identified in the HRL. Three of them intersect the spiral part of the tunnel at the levels approximately -220 and -330 m in the two elevator rooms and four swarms in two groups intersect the access ramp at around chainage 450 m and 1050 m. Three of the swarms and one gently dipping fracture zone are illustrated in *Figure 3-23*.

If the four swarms along the straight access ramp are combined into two groups they can be treated as two large swarms. It is notable that the swarms, together with the two identified gently dipping fracture zones, intersect the whole tunnel system within a distance of just under 100 m, which is, in fact, very close to what was predicted by *Talbot and Munier /1989/*. However, all observed swarms dip SW to S (apart from one dipping NE) contrary to *Talbot and Munier's /1989/* gently dipping zones.

1.4.4 Fracture zone EW-3

Fracture zone EW-3 is very well documented topographically (an about ten-metre-wide depression extending approximately E-W across the island with distinct scarps), geophysically (low-magnetic and low-resistivity zone), geologically (outcrop in trench with intense fracturing) and in boreholes (highly fractured and altered sections in drilling cores and VSP indications) */Wikberg et al, 1991/ /Figures 1-10 and 1-11/*.

Zone EW-3 was estimated to dip about 85° to the south.

According to drill-core observations the zone has developed in a heterogeneous bedrock comprising rather thin sheets of Småland (Ävrö) granite/greenstone, and fine-grained granite.

In the tunnel EW-3 was found to be approximately 14 m wide and consists of a 2-3 m wide crushed central section connected to a contact between Äspö diorite and fine-grained granite. The crushed section is surrounded by 5-10 m

of highly fractured Äspö diorite. Clay altered rock is common, especially in the crushed part of the zone.

1.4.5 Fracture zone NE-2

According to the prediction /*Wikberg et al, 1991*/ fracture zone NE-2 trending NE/ENE, should be regarded as the southern part of the main Äspö shear zone and was expected to follow a somewhat winding course. The brittle deformation of this zone is probably greatly influenced by earlier ductile shearing and mylonitization. The dip of NE-2 was estimated to change from steep to the northeast in the NE part to steep to the southeast in the SW part of the zone and to be only moderately hydraulically conductive. The southwestern part of the zone NE-2 was judged to be 'probable' /*Figure 1-12 and 1-13*/.

NE-2 was indicated geophysically, to some extent (low-magnetism and decreased resistivity along almost the entire zone). Geological indications were found in the SW part of zone NE-2 (intense fracturing and alteration of outcrops in the trench). Borehole indications in the form of mylonite and crushed and highly altered sections, as well as VSP and borehole radar data confirm the extent of the zone at depth. Hence, fracture zone NE-2 is only locally developed and rather faintly topographically indicated.

A probable interpretation is that tunnel intersections of fracture zones at 1602 m, 1844 m and 2480 m represent different branches of NE-2. Measured strikes vary between 015° and 036° and measured dips cluster around 75±5°. However, the width of the most intensely foliated portion of the mylonite varies between 1 m and 5 m. An estimated southeastern dip of NE-2 is supported by the fact that there are no indications of fractured mylonites in cored boreholes KA1754A or KA1751A /*Munier, 1995*/.

The most prominent structure in the vertical shaft /*Munier and Hermanson, 1993*/ is an approximately 10-m wide mylonite that strikes locally N to NNE and dips 75° towards the E. The inferred outcropping of this significant mylonite coincides with the location of NE-2 on the surface. What could be interpreted as a branch of NE-2, dips 80° towards the SE as inferred from surface outcrops. It is possible that this mylonite, or any splay of NE-2, rotates or curls with depth towards parallelism with the mylonite intersected in the shaft.

Surface, shaft and tunnel intersections were modelled in three dimensions. The observations cannot be uniquely fitted to a single planar structure. However, the undulating nature of the mylonite obvious on surface, confirmed by various measurements in the tunnel down to approximately 2475 m chainage are well aligned to a sub-planar structure that strikes 025° and dips 75° towards the S on average. The natural variability in mylonite orientation makes accurate predictions of any future intersections uncertain. However, reasonable estimates can be obtained from the derived orientation presented here.

Fracture zone NE-2 – which was predicted to be 'major' – was demonstrated underground in the form of three 1-5 m wide mylonitic 'minor' zones. The error in predicting the orientation of NE-2 can be explained by the fact that borehole information was only available for the northeastern part of the zone (outside the spiral). The reason for the lack of boreholes in the southwest was that NE-2 was estimated to be of minor hydraulic importance.

1.4.6   Assessment of the usefulness of investigation methods

The aero-magnetic method was very useful on the regional scale for mapping possible major fracture zones in which oxidation of magnetite to non-magnetic minerals can cause magnetic minima. Aero-magnetic and Very Low Frequency (VLF) measurements seem to be far superior to the EM measurements for interpreting possible fracture zones. It is important, however, to check the aero-geophysical data with ground investigation methods before final interpretation.

Lineament interpretation of relief maps and structural analysis based on different digital models on a regional scale seem to be a very good basis for further site investigation work, especially when this interpretation has been compared with the topographical expressions of aero-magnetic lineaments.

The reflectors indicated using the seismic reflection method could only in part be correlated with zones with increased frequency of low-dipping fractures in drill cores. The correlation seems to be greatest for reflectors at great depths, judging from borehole indications.

The two gently dipping fracture zones mapped in the tunnel are probably too narrow to be indicated by use of seismic reflection.

Ground geophysical methods were useful for more detailed investigations of major fracture zones in some areas. The VLF method may indicate water-bearing fracture zones under favourable circumstances (though it is greatly disturbed by the salt water). As a complement to the VLF method, resistivity and magnetic measurements, which were partly severely disturbed by man-made installations and saline water, seismic refraction have been very useful in locating and characterizing fracture zones.

Ground radar measurement data gave some interesting correlations with borehole radar reflections from structures/rock contacts, but further development is needed before this method can be regarded as a useful complement to seismic reflection. Vertical seismic profiling and borehole radar are useful for identifying low-dipping fracture zones.

Single-hole radar reflection gave valuable information on the orientation of fracture zones - especially those intersecting the borehole at rather low angles. A number of prominent features were indicated in the boreholes using the directional antenna and dipole antenna radar measurements, which corroborated the presumed orientation of most of the major fracture zones and some of the minor zones interpreted.

Vertical seismic profiling was found to be important as a complement to the borehole radar data, especially after three-dimensional processing using a new technique with image space filtering, which has been developed for seismic reflection studies in crystalline rock.

The results form the caliper log, and the electric logs were of the greatest interest in detecting fractures and fracture zones. It seems, however, to be rather unnecessary to use three different electric logs which give largely identical results, so in most of the geophysical logging surveys, only the single-point resistance log was used. Analysis of structural mapping, combined with lineament data and geophysical data, is very important in final location and characterization of major fracture zones.

1.5 BRIEF ANALYSIS OF ACCURACY AND CONFIDENCE

1.5.1 Measures of accuracy

A general explanation of the word accuracy is the 'goodness of fit', which refers to how well the forecasting model and forecaster can reproduce the information sought.

The accuracy is defined through the error E. The error E may be defined as the difference between the predicted value and what was (later) observed. A positive error then implies a overestimation of the real property. One measure of accuracy that also can be calculated is the absolute error (AE).

We are also interested in the relative error and to compare the errors between different variables. A measure that allows comparison of errors is the absolute percentage error (APE). The APE, which is the absolute error divided by the observed value, transforms the error into a relative error. This APE can be used to compare the accuracy in prediction for the different variables.

1.5.2 Brief analysis of accuracy and confidence

On the site scale, a number of geological variables were predicted and observed. These geological variables are discussed in this chapter:

- Position of major fracture zones
- Dip and strike of major fracture zones
- Widths of major fracture zones
- RQD of major fracture zones

Regarding the major fracture zones, the *positioning* absolute error of nine prediction/outcome pairs is between 5 metres and 30 metres (excluding NE-2). The average absolute error is 15 metres. It is possible to localize major fracture zones (>5 metres wide) during the pre-investigation phase at shallow depths. However, it is more difficult to predict position, width and character at increasing depth.

The error in predicting the position of a major fracture is partly due to dip uncertainty. As expected, the positioning error weakly increases with increasing forecasting range, but there is no clear relationship connecting positioning error, depth and dip error. Subsequently, the positioning error is more correlated to the depth than to the error in dip prediction. The error term in predicting the position of zones is probably a complex composition of several factors.

The absolute error in *dip* prediction ranges from 5 to 50°, with an average absolute error of 20°. The absolute error in predicting the *strike* ranges from 5 to 30°, with an average absolute error of 15°.

The error in predicting the *width* ranges from -16 metres to 11 metres (excluding NE-2). The average error is -0 metres, which suggests that the widths on the whole are fairly predicted.

As regards the RQD of the major zones, the RQD is both over- and underestimated. There exists a tendency of the rock quality of RQD = 0-25% to be predicted more abundantly than it really exists. As for the RQD of 50-100%, it is on average more common than predicted.

The 'good' rock is more common than we predicted, and the 'bad' rock is not as common as we predicted.

2 SUBJECT: MINOR FRACTURE ZONES AND SMALL SCALE FRACTURING IN THE ROCK MASS

2.1 SCOPE AND CONCEPTS

According to *Bäckblom /1989/* a fracture zone is a fracture zone only if geological field evidence supports the zones **with the characteristics that the intensity of natural fractures is at least twice as high as that in the surrounding rock**. Completely disintegrated and/or chemically altered rock is included in the definition of fracture zones.

The term 'major fracture zone' was used for a feature more than about 5 m wide and extending several hundred metres. **Features less than about 5 m and more than 0.1 m wide were called 'minor fracture zones'.**

For the 'level of reliability' three separate definitions were used; possible, probable and certain.

A fracture zone is a more or less two-dimensional feature. Its extent and direction are considered to be 'certain' only after confirmation by investigations or measurements in several points.

Possible is the lowest level of confidence. The level of reliability can be raised to probable or certain by additional studies */Wikberg et al, 1991/.*

Persistent, several-metre-long fractures, mostly steep and estimated to be significant hydraulic conductors were called 'single open fractures' */Gustafson et al, 1991/.*

A detailed description of a rock volume also includes data on the small scale fracturing in the rock mass such as fracture geometry, fracture densities and fracture lengths.

2.2 METHODOLOGY FOR TESTS OF CONCEPTS AND MODELS

The different methods used to characterize and localize minor fracture zones and characterize the small-scale fracturing are presented briefly below and summarized in */Figure 2-1/.*
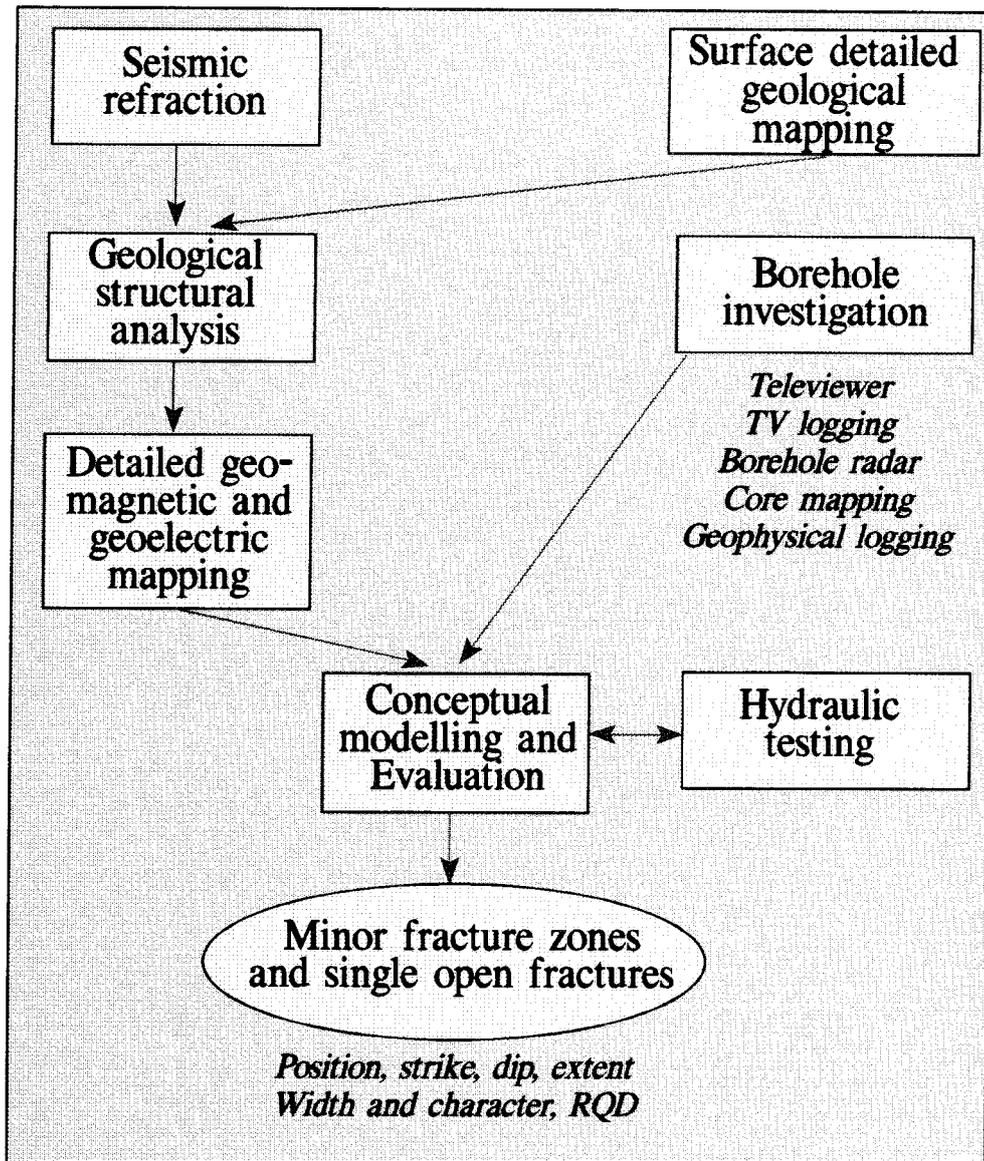
Figure 2-1. *Pre-investigation methodology. Structural-geological characterization. Minor fracture zones, single open fractures and small-scale fracturing.*

2.2.1   Prediction methodology

Detailed geological mapping

Very detailed mapping was performed along cleaned trenches across the island. A geological map to a scale of 1:2000 was prepared, and a classification of the rocks based on chemical and mineralogical analyses presented /Wikberg et al, 1991/.

As a supplement to the structural/geological mapping on outcrops and road cuts, a study of structural elements, including a fracture mapping programme, was performed along the trenches to obtain results for use in geohydrological

and rock mechanics model studies. Data concerning 4500 mapped fractures - such as orientation, length, aperture and fracture filling - were presented /Ericsson, 1988; Wikberg et al, 1991; Almén et al, 1994/.

Borehole investigations

A number of geophysical borehole logs were used to detect and characterize minor fracture zones and single open fractures. To obtain their absolute orientation, TV logging and televiewer measurements were performed /Fridh and Stråhle, 1989; Wikberg et al, 1991; Almén et al, 1994/.

Cored borehole KAS13 was drilled in a direction which was specially intended to locate minor fracture zones trending NNW indicated on southern Äspö. Core mapping data and borehole radar measurements in KAS13 were used to complement the results from a vertical seismic profiling survey (KAS07) and the geological and geophysical indications from surface investigations /Sehlstedt et al, 1990/.

Detailed geomagnetic and geo-electric mapping

As a part of the investigation of the structural pattern of Äspö, detailed ground magnetic and electric mapping were carried out. Magnetic measurements were made every fifth metre along profiles in an east-west direction, with profiles at 10-metre centres in the geomagnetic survey and at 40-metre centres in the geo-electric survey. Different geometrical arrangements of currents and potential electrodes can be used in geo-electrical mapping. In order to effectively map relatively narrow zones (a few metres thick), and low-resistivity zones near the surface, a 5-10-5 metre dipole-dipole configuration was used. These measurements were severely disturbed by industrial installations and saline groundwater.

A combined analysis of geomagnetic and geo-electric data was made, especially with respect to fracture zone delineation /Nisca and Triumf, 1989/.

Seismic refraction

As a complement to the geo-electric and geomagnetic measurements seismic refraction was used to locate minor fracture zones on Äspö /Sundin, 1988, and Rydström et al, 1989; Wikberg et al, 1991; Almén et al, 1994/.

A 22-channel seismic instrument of SEMAB type was used. The signals were generated by explosives. The investigations were performed on southern Äspö with geophones at 2.5-m centres and shot points at about 12.5-m centres, especially to detect minor, narrow fracture zones.

2.2.2 Methodology for determining outcome

Geological documentation in the tunnel

All minor fracture zone indications in the tunnel were mapped in conjunction with the general geological mapping performed after each blasting round. The mapping comprised position, width, orientation and character. The extent of a particular minor zone was estimated first after analysis of all available geological and hydrogeological data. Fracture data were collected and analysed in connection with geological mapping and normally comprised fracture orientation (all fractures longer than 1 m), fracture minerals, fracture trace lengths and degree of fracturing.

Drilling

Borehole investigations (core mapping, geophysical logging, inflow observations and TV data) provided information, especially regarding water-bearing minor fracture zones, single open fractures and fracture density in the rock mass.

Borehole radar and seismic investigations

Borehole radar and seismic investigations gave supplementary information on the orientation and extent of some minor fracture zones.

2.3 COMPARISON OF PREDICTED AND MEASURED ENTITIES

Minor fracture zones

A great number of fractures and narrow (decimetre to a few metres wide) fracture zones striking approximately north were mapped on outcrops or/and were indicated by ground geophysics of Äspö. More or less extensive, they seem to occur in the Äspö area trending NNW to NNE /Figure 2-2/.

Only a few of them are topographically significant but normally too narrow to be geophysically unambiguously indicated by geophysics. Vertical seismic profiling, borehole information and hydraulic investigation data support the notion of steep, mostly easterly dips. All these minor fracture zones were described under the designation 'NNW' /Figure 2-3/.

The position of the different zones in the system NNW were judged to be 'possible' and the existence 'probable'.

A comparison between minor fracture zones, indicated in Figure 2-2 and projected vertically (according to the prediction) down to tunnel level, and minor zones mapped in the tunnel is presented in Figures 2-4 to 2-6. Notice

that these figures only show zones which according to definition are mapped as 'minor fracture zones' (more than 10 cm but less than 5 m wide) in the tunnel. Many hydraulic important fractures, however, are less than 10 cm wide and have for this reason been mapped as 'water-bearing fractures'. They are presented and discussed in more detail in *Report 4*.
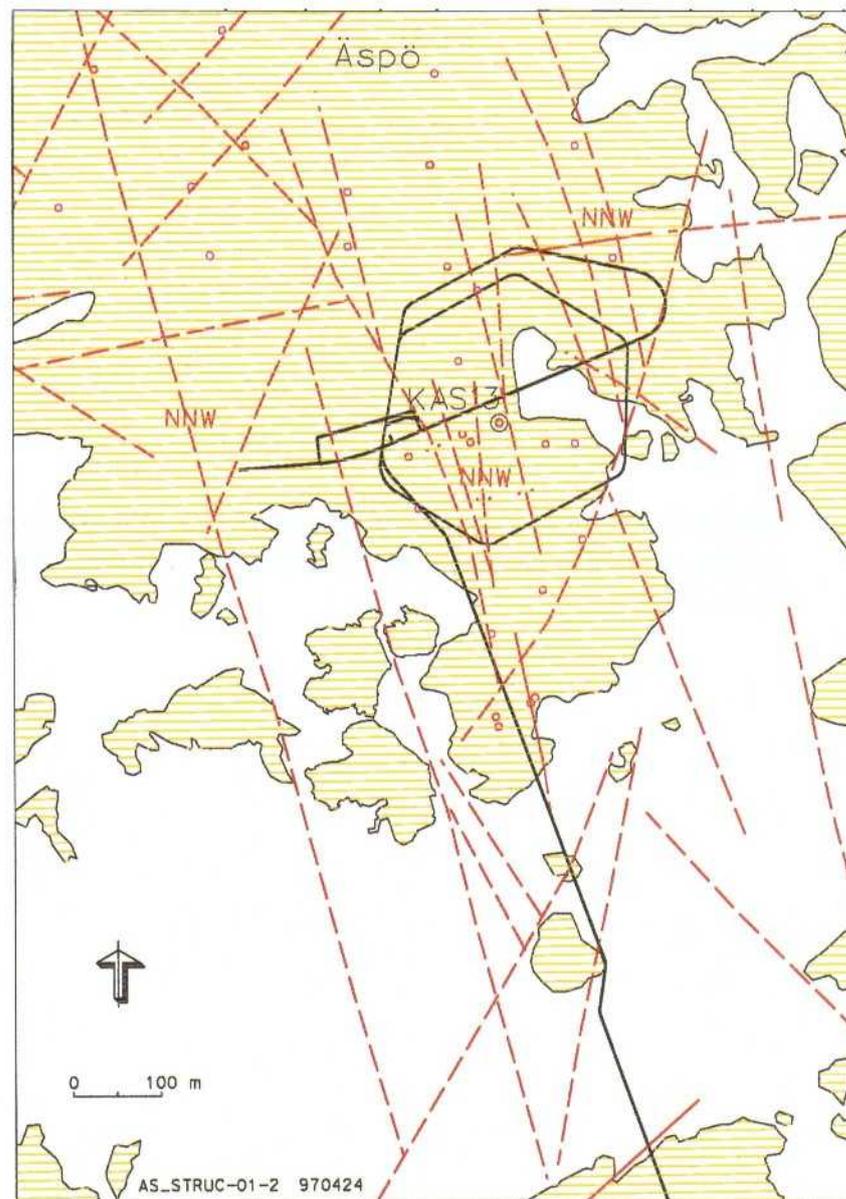
Figure 2-2. *Minor fracture zone interpretation in the Äspö area based on pre-investigation data. Surface map. /Gustafson et al, 1991/.*
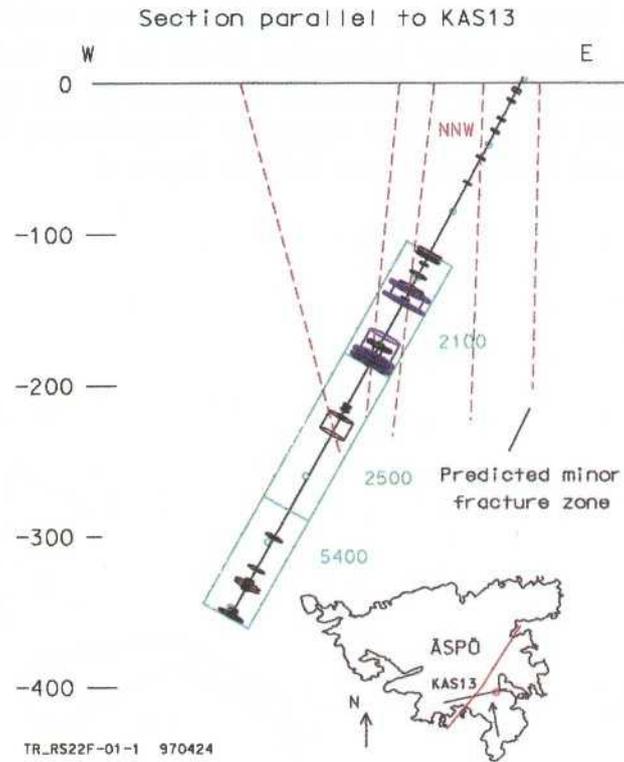
Figure 2-3. *Interpretation of the minor fracture zone system 'NNW' in a section parallel to borehole KAS13 based on pre-investigation data /Wikberg et al, 1991/.*
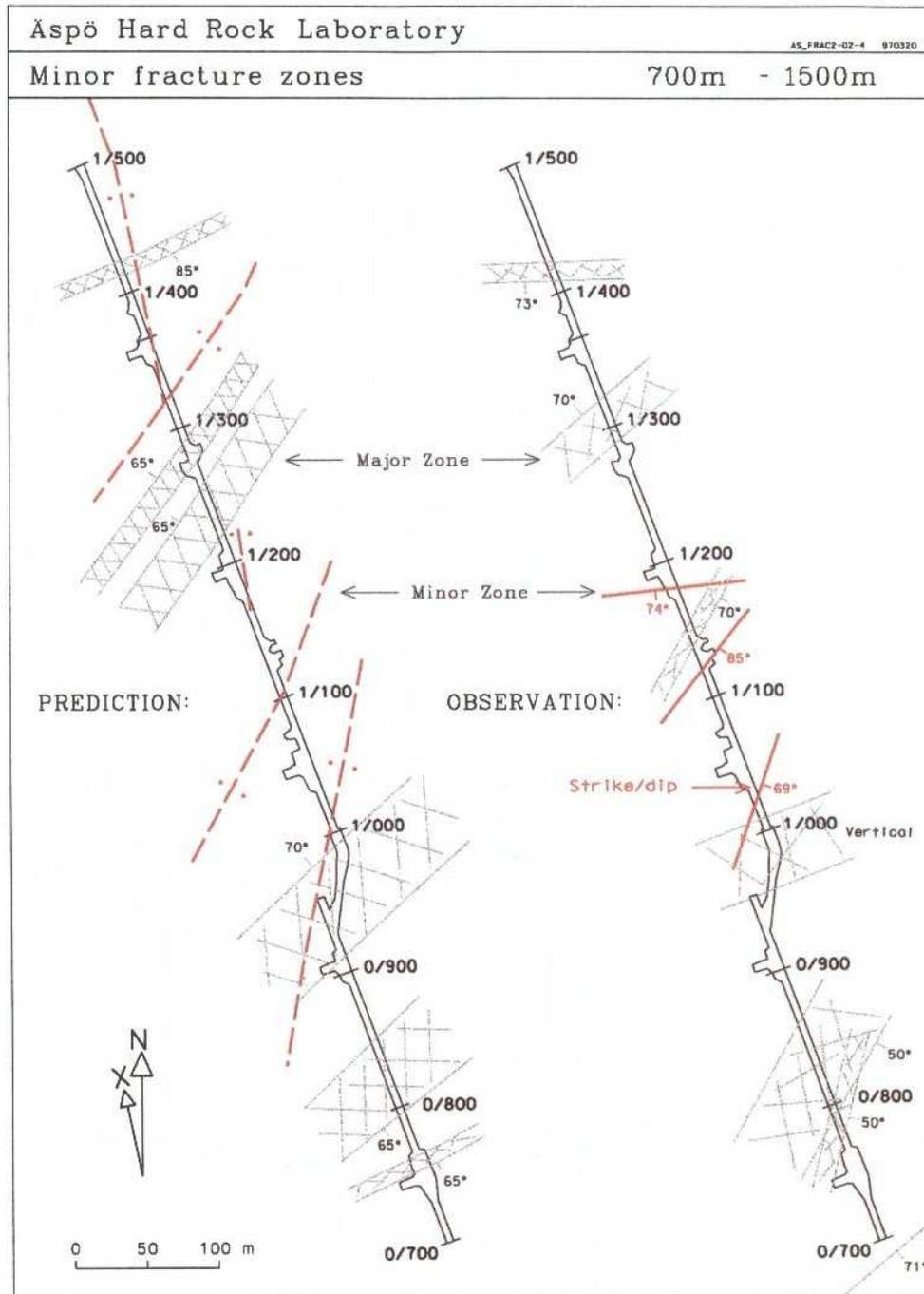
Figure 2-4. *Comparison between the minor fracture zone prediction (based on pre-investigation data) and outcome (based on tunnel data). Chainage 700-1500 m. Note, that features mapped as 'fractures' (less than 10 cm wide) are not included.*
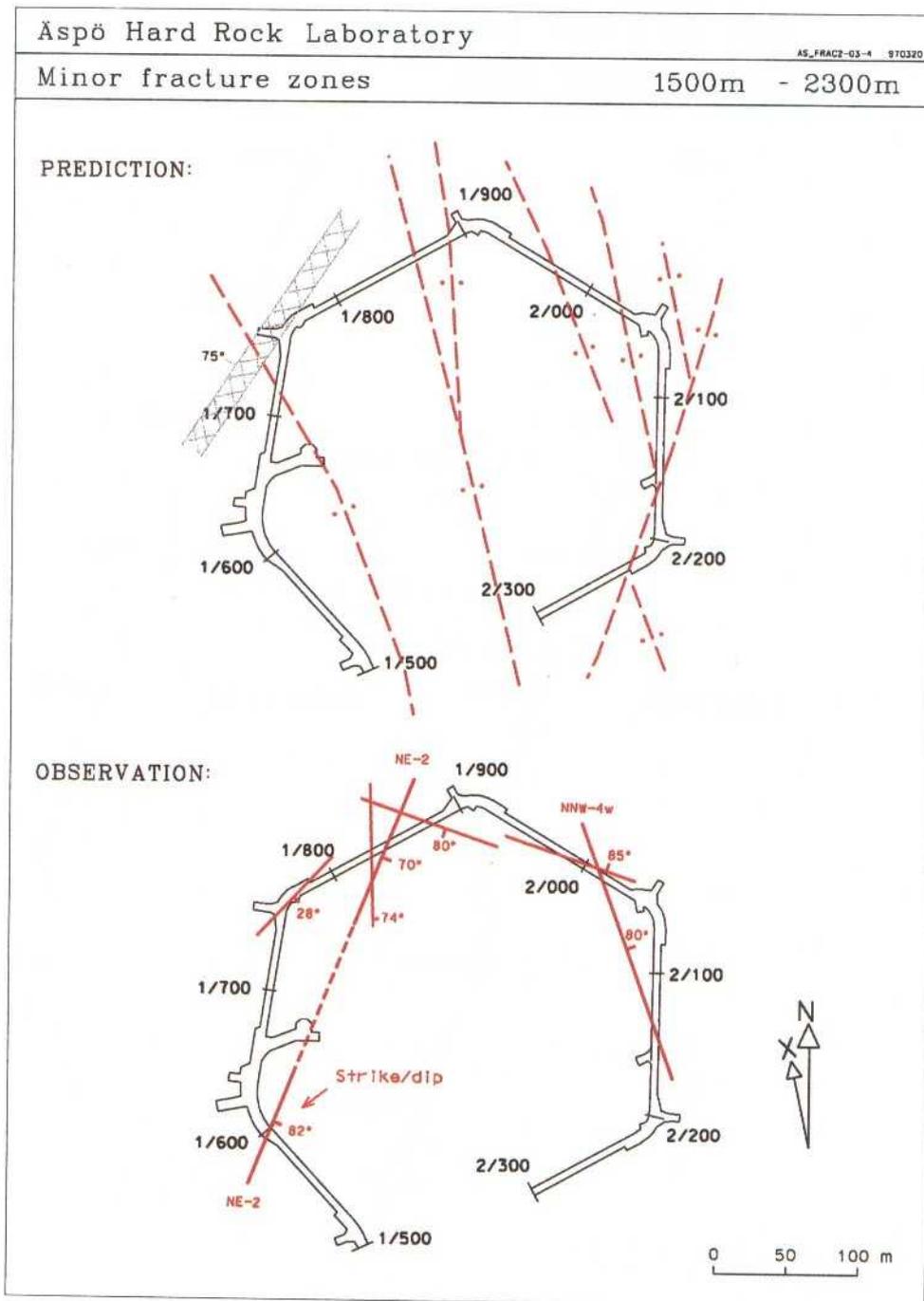
Figure 2-5. *Comparison between the minor fracture zone prediction (based on pre-investigation data) and outcome (based on tunnel data). Chainage 1500-2300 m. Note, that features mapped as 'fractures' (less than 10 cm wide) are not included.*
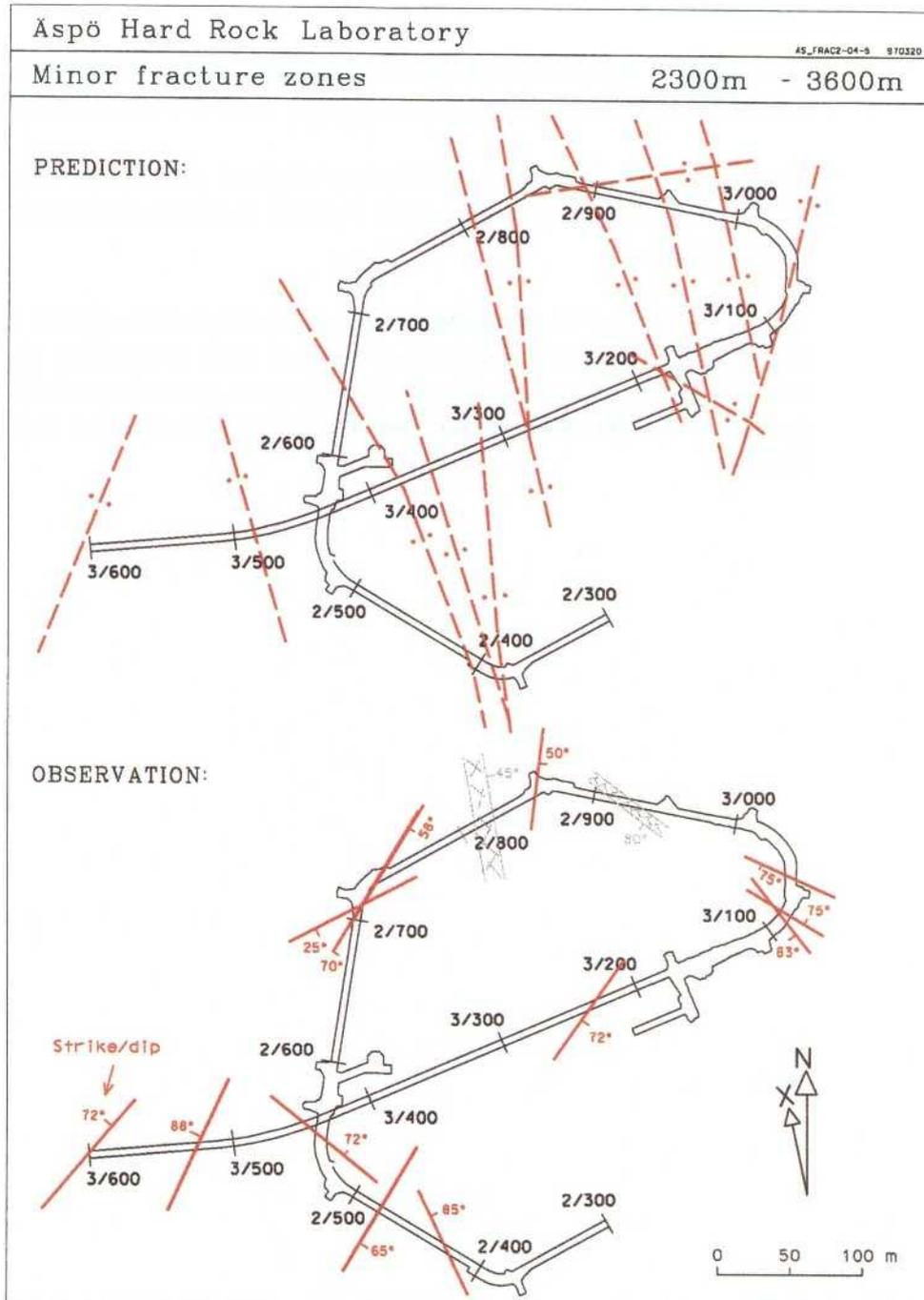
Figure 2-6. *Comparison between the minor fracture zone prediction (based on pre-investigation data) and outcome (based on tunnel data). Chainage 2300-3600 m. Note, that features mapped as 'fractures' (less than 10 cm wide) are not included.*

The mean frequency of minor fracture zones and single open fractures was predicted on the (50-m) block scale. It was not possible to predict the exact position of a separate minor fracture at depth.

The orientation of the main fracture sets and the dominating fracture minerals were also predicted on the block scale.

Comparisons between prediction and outcome for six 50-m blocks along the tunnel (P50-01 and P50-06) are presented in *Table 2-1 and Figures 2-7 to 2-9.*

Hermanson /1996/ constructed fracture network models for these six 50-m blocks based on tunnel mapping data. Fracture models and fracture orientations are illustrated.

The main fracture set orientation, fracture minerals and fracture spacing and lengths were predicted on the (5-m) detailed scale comprising the four main rock types Äspö diorite, Småland (Ävrö) granite, greenstone and fine-grained granite. A comparison between the prediction and outcome is presented in *Table 2-2.*

Table 2-1. **Structural models on the (50-m) block scale. Comparison between the prediction and outcome for six 50-m blocks. (P50-01--P50-06).**

Subject	PREDICTION						OUTCOME					
	P50-01	P50-02	P50-03	P50-04	P50-05	P50-06	P50-01	P50-02	P50-03	P50-04	P50-05	P50-06
Single open fractures*	2($\pm$1)**	2($\pm$1)	3($\pm$1)	2($\pm$1)	2($\pm$1)	3($\pm$1)	3	2	3	1	1	3
Minor fracture zones	3($\pm$1)**	1($\pm$1)	2($\pm$1)	3($\pm$1)	3($\pm$1)	3($\pm$1)	1	0	1	1	1	1
Fracture minerals	No prediction			Cl+++ Ca++	Cl+++ Ca++	Cl+++ Ca++				Ca=47% Chl=34%	Cl=44% Ca=34%	Cl=54%
+++ Dominating												
++ Frequent												
+ Less frequent				FeOH++ Ep+ Others+	FeOH++ Ep+ Others+	FeOH++ Ep+ Others+				Ep=11% FeOH=4% Others+	Ep=5% FeOH=8% Others+	Ep=2% FeOH=9% Others+

*   Persistent, several-metre-long fractures, mostly steep and estimated to be significant hydraulic conductors.

**   The confidence level (60% for single open fractures and minor fracture zones) is based mainly on expert judgement.

Cl = chlorite, Ca = calcite, Ep = epidote, FeOh = Fe-oxihydroxide

Predictions are normally based on one cored borehole in or close to the actual block.

1:35

Table 2-2. Structural models on the (5-m) detailed scale. Comparison between prediction and outcome for four (5-m) blocks involving small scale fracturing.

Subject	PREDICTION				OUTCOME			
	Småland (Ävrö) granite	Äspö diorite	Green-stone	Fine-grained granite	Småland (Ävrö) granite	Äspö diorite	Green-stone	Fine-grained granite
Fracture length (>0.5 m)	1.2(±0.3)	1.2(±0.3)	1.2(±0.3)	0.8(±0.1)	1.6	2.1	1.9	0.7
Fracture spacing (>0.5 m)	1.0(±0.3)	1.0(±0.3)	1.0(±0.3)	0.5(±0.1)	0.6	0.5	1.5	0.5
Main fracture orientation Equal area projection (lower hemisphere)	(stereonet diagram)	(stereonet diagram)	(stereonet diagram)	(stereonet diagram)	(stereonet diagram)	(stereonet diagram)	(stereonet diagram)	(stereonet diagram)
Fracture minerals	1. Cl,Ep,Ca,FeOH 2. Cl,Ca,FeOH 3. Cl,Ep,Ca 4. Cl,Ep,Ca	1. Cl,Ep,Ca,FeOH 2. Cl,Ca,FeOH 3. Cl,Ep,Ca 4. Cl,Ep,Ca	1. Cl,Ep,Ca,FeOH 2. Cl,Ca,FeOH 3. Cl,Ep,Ca 4. Cl,Ep,Ca	1. Cl,Ep,Ca,FeOH 2. Cl,Ca,FeOH 3. Cl,Ep,Ca 4. Cl,Ep,Ca	a. Cl,Ca,FeOH,Ep b. Cl,Ca,FeOH	a. Cl,Ca,FeOH b. Cl,Ep,Ca c. Cl,Ep,Ca	a. Cl,Ca b. Ca,Cl c. Ca,Cl,Cy,Ep d. Cl,Ca,Cy	a. Cl,FeOH,Ca b. Cl,Ep,Ca,FeOH

Cl = chlorite, Ca = calcite, Ep = epidote, FeOH = Fe-oxihydroxide, Cy = clay

The confidence level (60% for fracture length and spacing) is based mainly on expert judgement.
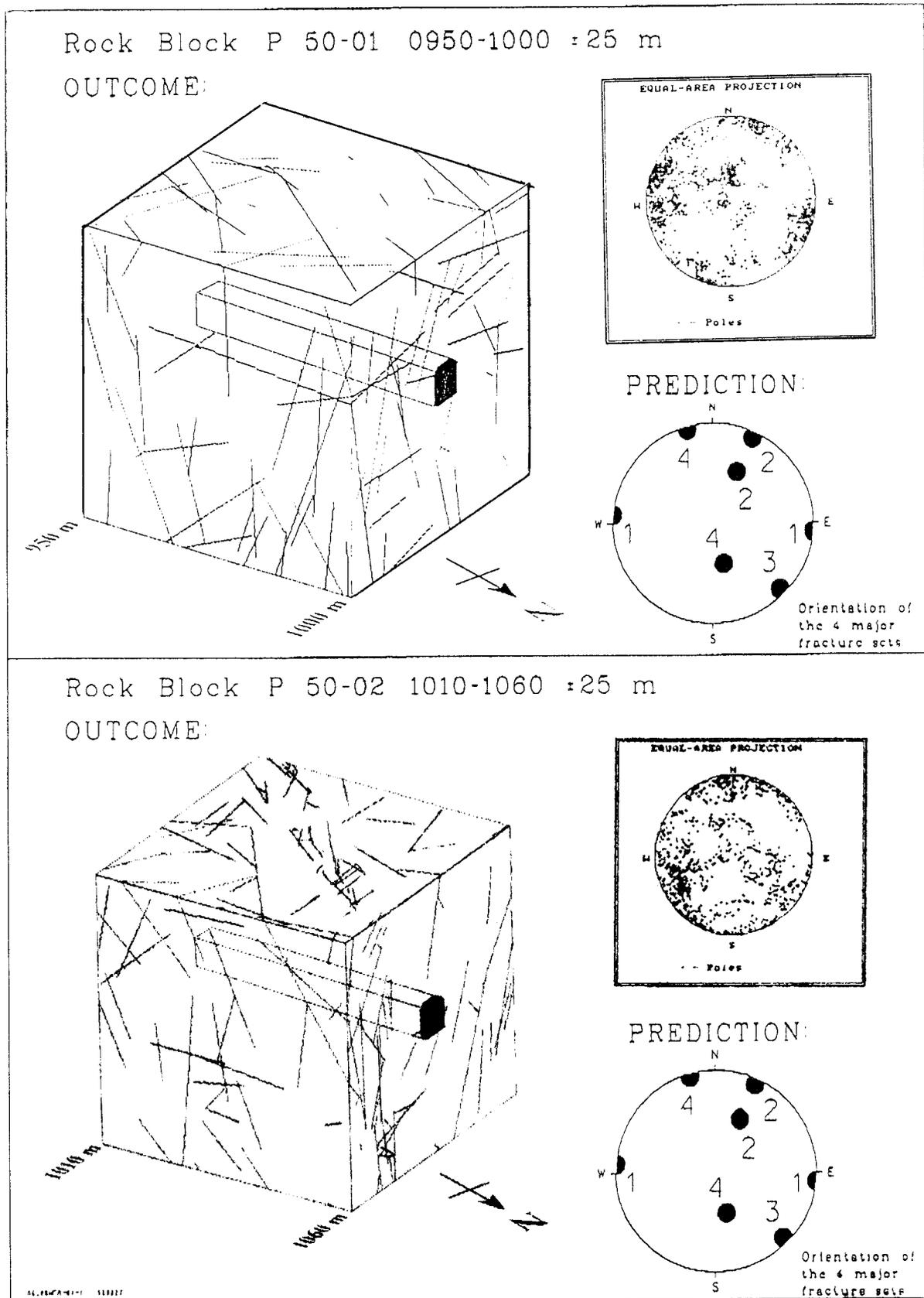
Figure 2-7. Structural models on the (50-m) block scale. Small scale fracturing. Fracture network model made for rock blocks P50-01 and P50-02 based on tunnel data.

Rock Block   P 50-03 1170-1220 ±25 m

OUTCOME:

PREDICTION:

Orientation of
the 4 major
fracture sets
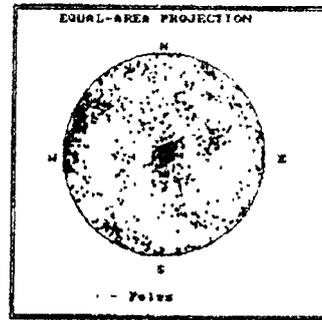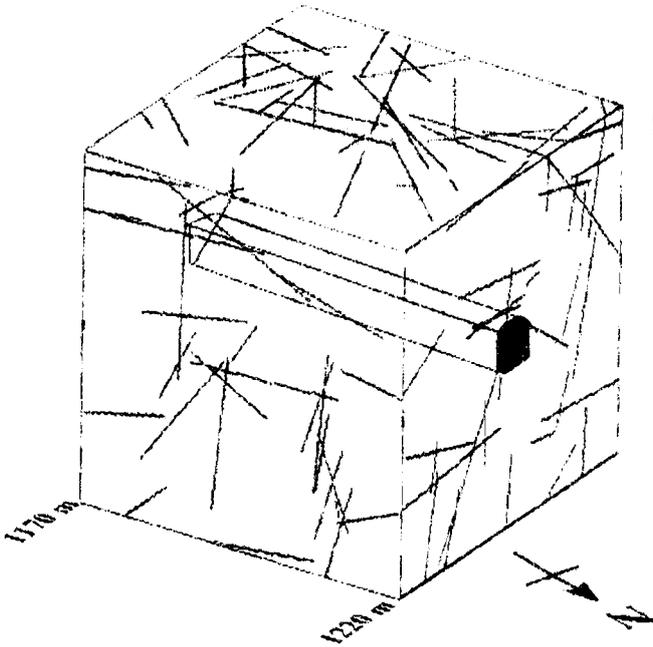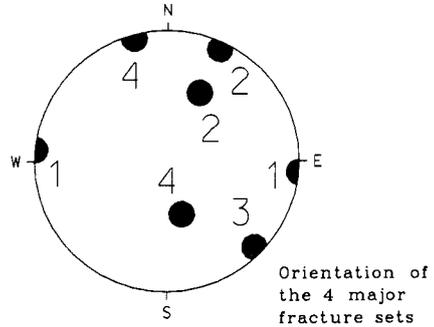
Rock Block   P 50-04 1570-1620 ±25 m

OUTCOME:

PREDICTION:

Orientation of
the 4 major
fracture sets
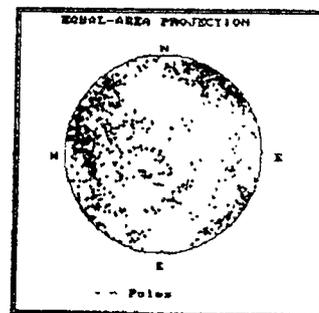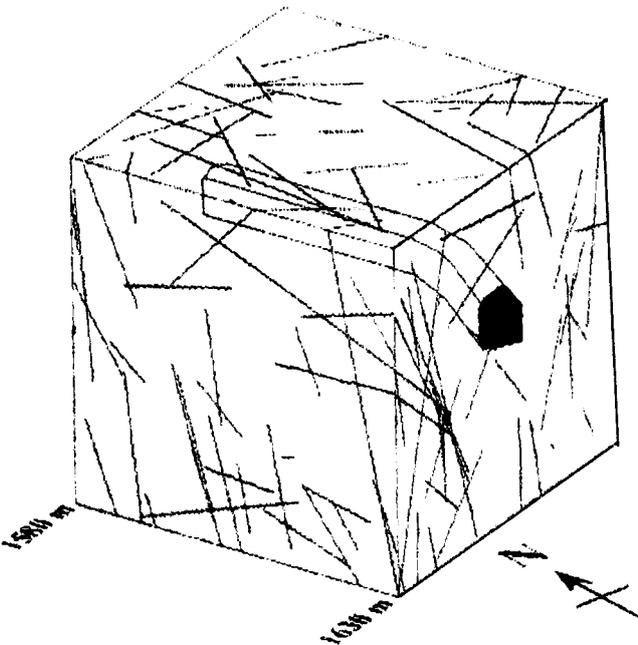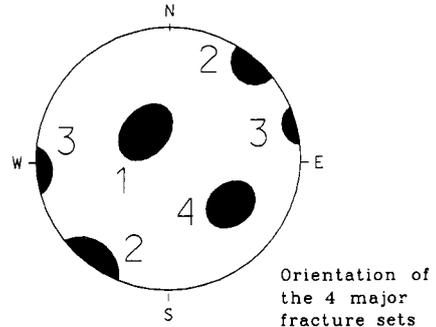
Figure 2-8.   Structural models on the (50-m) block scale. Small scale fracturing. Fracture network model for rock blocks P50-03 and P50-04 based on tunnel data.

Rock Block P 50-05 2422-2472 ±25 m
OUTCOME:

PREDICTION:

Orientation of
the 4 major
fracture sets

Rock Block P 50-06 2752-2802 ±25 m
OUTCOME:

PREDICTION:

Orientation of
the 3 major
fracture sets

RS_COMFR-03-1 960327
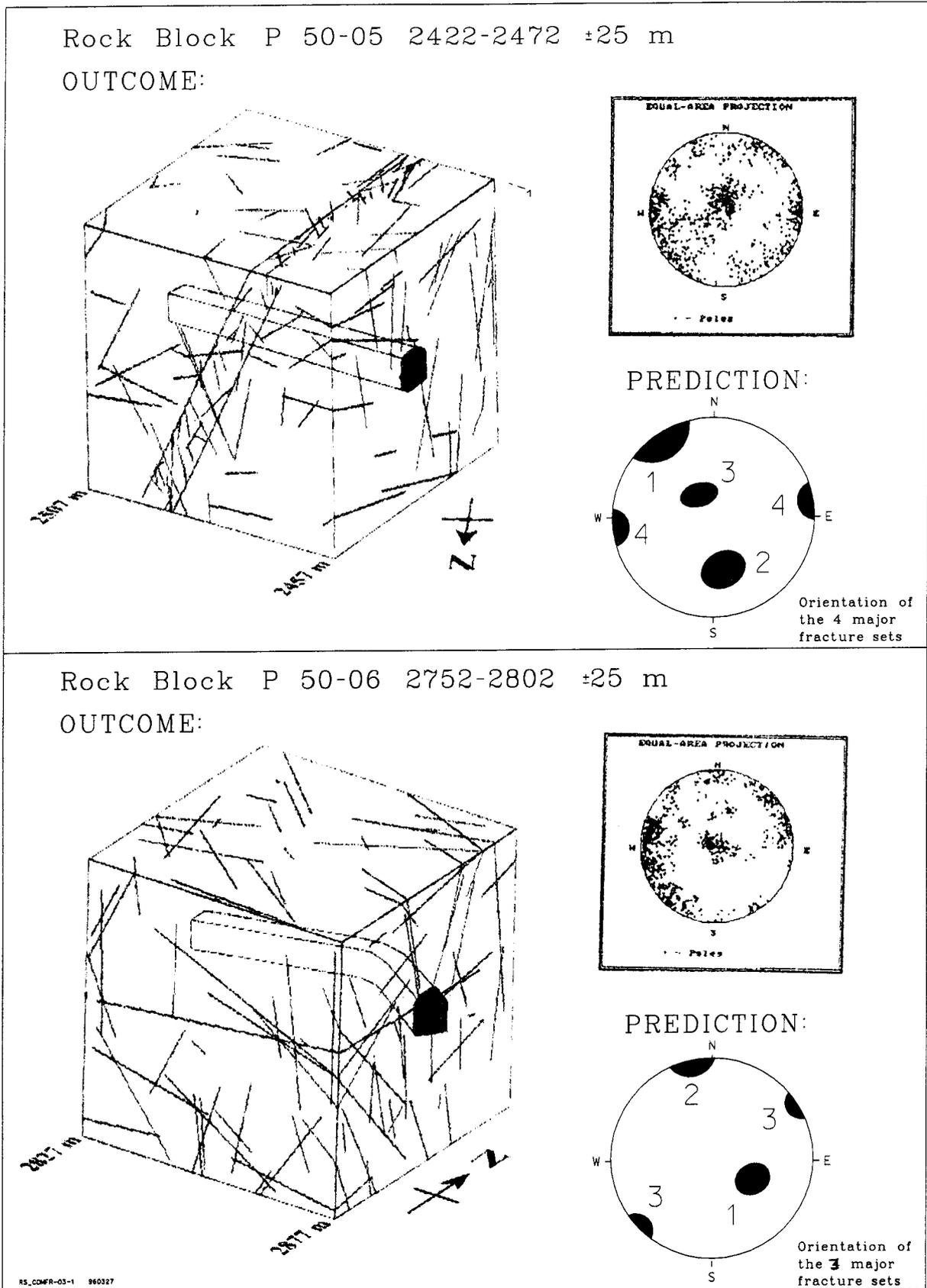
Figure 2-9. *Structural models on the (50-m) block scale. Small scale fracturing. Fracture network model for rock blocks P50-05 and P50-06 based on tunnel data.*

2.4 SCRUTINY AND EVALUATION

A number of minor, mostly steeply dipping, fracture zones were predicted to intersect the tunnel volume trending NNW-NNE. On the 500-m site scale, however, no exact position of a particular zone was predicted - only the frequency and main orientation of the fracture zones.

The different zones in the 'NNW' system were predicted to be 'possible-probable' and their predicted position in the tunnel very approximate. The widths were expected to be 1-3 m /Figure 2-3/. The characters of the zones were not predicted due to lack of relevant data.

Only structures that display indicators, such as slickensides, mylonitic fabrics or faults were mapped in the tunnel as minor fracture zones.

Most of them are generally not wider than 1 m. Most consists of a single or up to a handful of faults that generally contain gouge. The host rock is generally mylonitized shear faults. The nature of fracturing in sheets of fine-grained granite make such structures difficult to differentiate from fracture zones. However, fracture zones are here defined as broken volumes of rock that also display kinematic/tectonic indicators which discriminate most sheets of fine-grained granite.

The predicted water-bearing zone NNW-4W is an example of a minor fracture zone which is indicated in the tunnel by intersections, at 2018 m /Figure 2-10a/, 2116 m /Figure 2-10b/ and 2920 m. Some 5-10 cm wide open fractures in this metre-wide section of cataclastic granite are filled with grout.

Except for NNW-4W it is not possible to find persistent 'minor fracture zones' in the tunnel according to the definition given in the prediction based on surface indications. One reason for this may be the tendency of most fracture zones to be narrower at depth than what could be expected from surface indications in the form of fractured and weathered rock /Figure 2-11/.

Combined results from tunnel mapping and drilling show the characteristic pattern of the 'NNW-system'. They mostly occur in a complex pattern of steeply dipping fractures (fracture swarms) and some decimetre-wide 'fracture zones' trending WNW to NE. Many of the narrow fracture zones are connected to veins or dikes of fine-grained granite. It seems possible to correlate a number of a few decimetre-wide fracture zone indications in the tunnel to observations in boreholes crossing the central part of the spiral and forming a hydraulically active structure trending WNW-NNW /Figure 2-11/. The character of many of these structures as a 'fracture zone' is not very evident. They should rather be described as a 10-30 m wide swarm of mostly subvertical conductive fractures trending WNW-N where the WNW trending fractures are normally the most frequent and hydraulically important.

Figure 2-10a. *Fracture zone NNW-4W. Intersection the tunnel at 2018 m. The yellow fracture filling is coloured grouting material /Photo K Annertz/.*

Figure 2-10b. *Fracture zone NNW-4W. Intersection the tunnel at 2116 m. White fracture filling is calcite, grey is grouting material /Photo K Annertz/.*
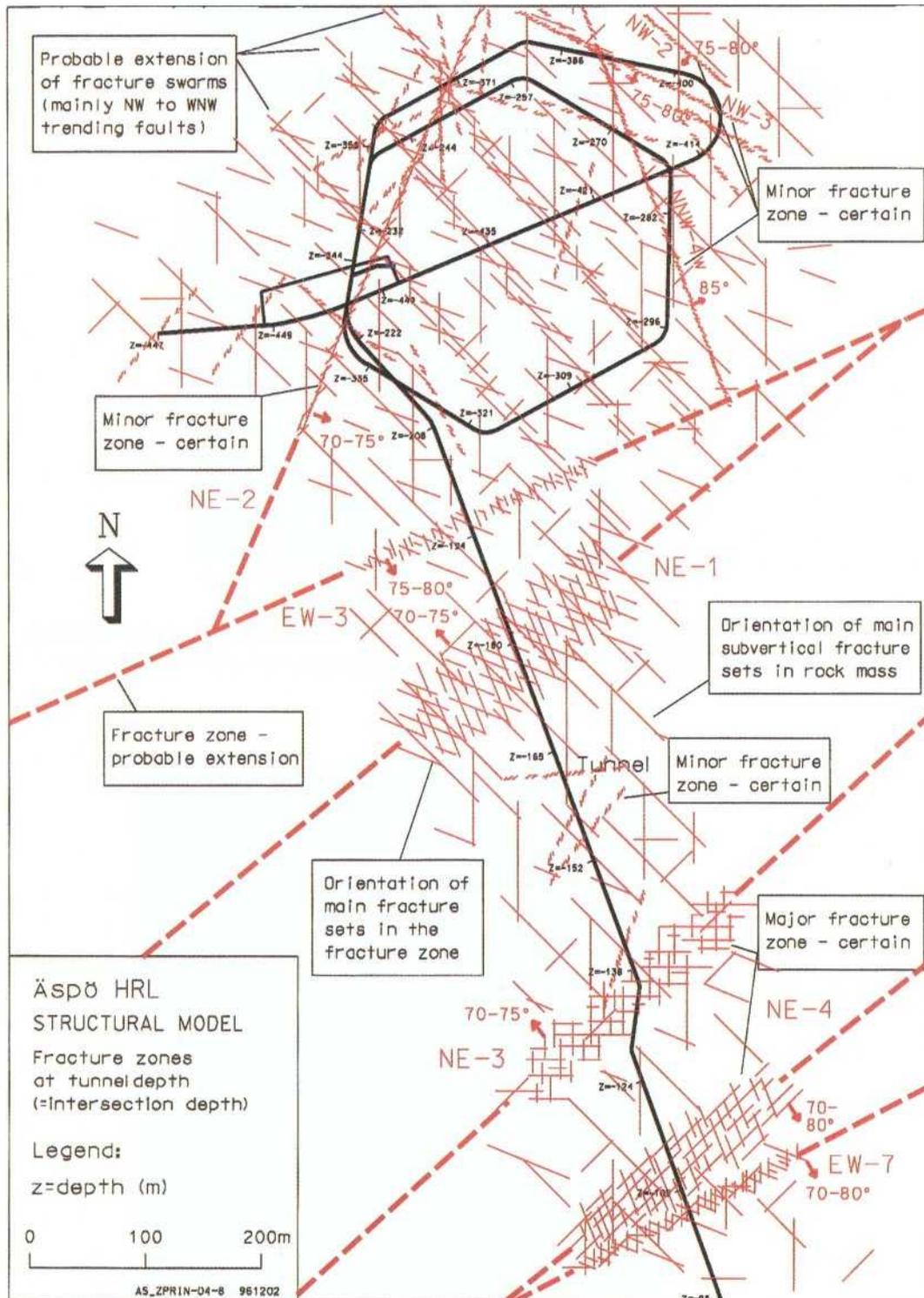
Figure 2-11. *Structural model of the rock mass surrounding the Äspö tunnel. The model represents the positions and estimated extents of fracture zones (swarms) at tunnel level. The orientation of the main subvertical fracture sets in major fracture zones and the intact rock mass are based on tunnel mapping data. 'Fracture swarms' comprise concentrations of subparallel, often water-bearing faults.*

During the course of the investigations for the SELECT Project, minor fracture zones NW-2 and NW-3 were identified /Winberg et al, 1996/.

On the 50-m scale minor fracture zones are penetrated by the tunnel in rock blocks 50-01 and 50-02. In rock block 50-01 – where the prediction/outcome discrepancy is most evident – three minor fracture zones were predicted, based on core borehole KBH02. In the tunnel the increased fracturing is found to occur more or less continuously over an approximately 40-m long section.

In rock block P50-04 three minor fracture zones were predicted, based on the cored boreholes. In the rock block only one minor fracture zone was found.

Three(±1) minor fracture zones were predicted for each of the blocks P50-05 and P50-06 but only one zone was mapped in each block.

The discrepancy between the prediction and outcome regarding minor fracture zones shows that it is almost impossible to predict the exact position of a specific minor fracture zone based solely on surface data and information from a single borehole in or close to an actual rock block. The main orientation, however, of the 'NNW-system' and its water-bearing character was in fair accordance with the prediction.

Small scale fracturing in the rock mass

Predictions, in the 50-m blocks, of small scale fracturing were based on surface fracture mapping and analysis of fracturing in cored boreholes.

As there was no core orientation in borehole KBH02 the prediction of the main fracture set orientation in P50-01 to P50-03 was based solely on data from surface mapping. The best agreement with predictions seems to be for the approximately N-S and E-W fracture set orientations, which could be explained by the dominating character of these fracture sets in the whole area.

The prediction of the main fracture set for the rock blocks P50-04 to P50-06 was based mainly on data from TV orientation in core borehole KAS05. The best agreement with predictions seems to be for the approximately N-S and NW-SE fracture set orientations /Table 2-2/.

Hermanson /1996/ visualized fracture data for the six 50-m blocks based on tunnel fracture data. Fracture lengths, orientations and terminations were used for calculating fracture intensity and the orientation of main fracture sets in a fracture network model.

As regards predictions of small scale fracturing on the 5-m scale for typical examples of the four main rock types, there is good agreement between the prediction and outcome regarding 'fracture minerals' and 'main fracture orientation' (especially concerning the two dominant fracture sets striking approximately E-W and N-S – less good as regards fracture spacing and fracture length /Table 2-2/.

As regards fracture frequency (fracture spacing) it is important to make some comments on the different fracture data recorded during the investigations.

During pre-investigation of the Äspö target area a large number of core boreholes were drilled. Most of them were subvertical but one (KBH02) is subhorizontal. Core mapping of these boreholes recorded 'natural' fractures defined as fractures that have parted the core. Fractures that did not part the core were recorded as 'sealed' fractures /Strähle, 1989/. 'Fractures' induced by drilling were recorded as 'breaks'.

Natural fractures are often weathered, slickensided and/or contain fracture fillings. It is important to note that many closed, sealed fractures in the rock mass were broken up during drilling and handling of the core. These fractures were mostly mapped as natural fractures, since they were hard to distinguish from 'real natural' fractures. This means that 'natural' fractures are over-represented in the core mapping data.

The amount of 'natural' fractures in the surface core boreholes is calculated to be in the order of 3.7 fractures/m (crushed zones, with more than 20 fractures/m, excluded) for the subvertical boreholes and 3.5 fractures/m in KBH02. If we exclude all sections in the core with a fracture frequency above 5 fractures/m (fracture zones, increased fracturing) we get 2.2 fractures/m as a mean value for all pre-investigation core boreholes.

To compare core mapping fracture data from surface boreholes and tunnel mapping data, all fractures longer than 1 m that intersect the tunnel axis were recorded.

For the upper part of the tunnel, down to a depth of approximately -400 m, the mean fracture frequency for a scan line parallel to the tunnel axis is estimated to be approximately 0.5 fractures/m - below the -400 m level 0.4 fractures/m.

The mean fracture frequency in the TBM tunnel is 0.3 fractures/m along the tunnel axis. It is interesting to note that the mean mapped fracture frequency in core borehole KA3191F - which was drilled as a investigation hole parallel to the TBM tunnel before excavation of the tunnel - is 1.5 fractures/m.

The mean fracture frequency in the hoist shaft is calculated to be approximately 0.3 fractures/m along a vertical scan line.

The amount of 'natural' fractures in a drill core is normally overestimated due to the fact that many sealed fractures are broken during drilling and handling of the core. These fractures are sealed and tight in the tunnel. Most of the fractures mapped in the tunnel as natural fractures are faults.

We also note a decrease in fracture frequency below a depth of approximately -400 m both in the tunnel and in boreholes drilled from surface. This is probably explained by an increasing homogeneity of the rock mass below -400 m.

In the very inhomogeneous rock mass in the upper part of the tunnel 9-10 rock boundaries/100 m borehole/tunnel were mapped (for boundaries between different rock types except veins less than 0.5 m wide). Below -400 m only four rock boundaries/100 m are documented in boreholes and tunnel, five in the TBM tunnel and seven rock boundaries in the hoist shaft.

By way of comparison, it may be mentioned that four rock boundaries/100 m are recorded as a mean for the 1700 m deep borehole KLX02 in the Laxemar area some kilometres west of Äspö. In KLX02 Äspö diorite is dominating and the frequency of dikes and veins of fine-grained granite is much less than in the Äspö area. The figure of 2.3 fractures/m in this borehole compared with 3.7 fractures/m in the HRL boreholes clearly indicates a correspondence between the fracture frequency and lithologic complexity of the rock mass.
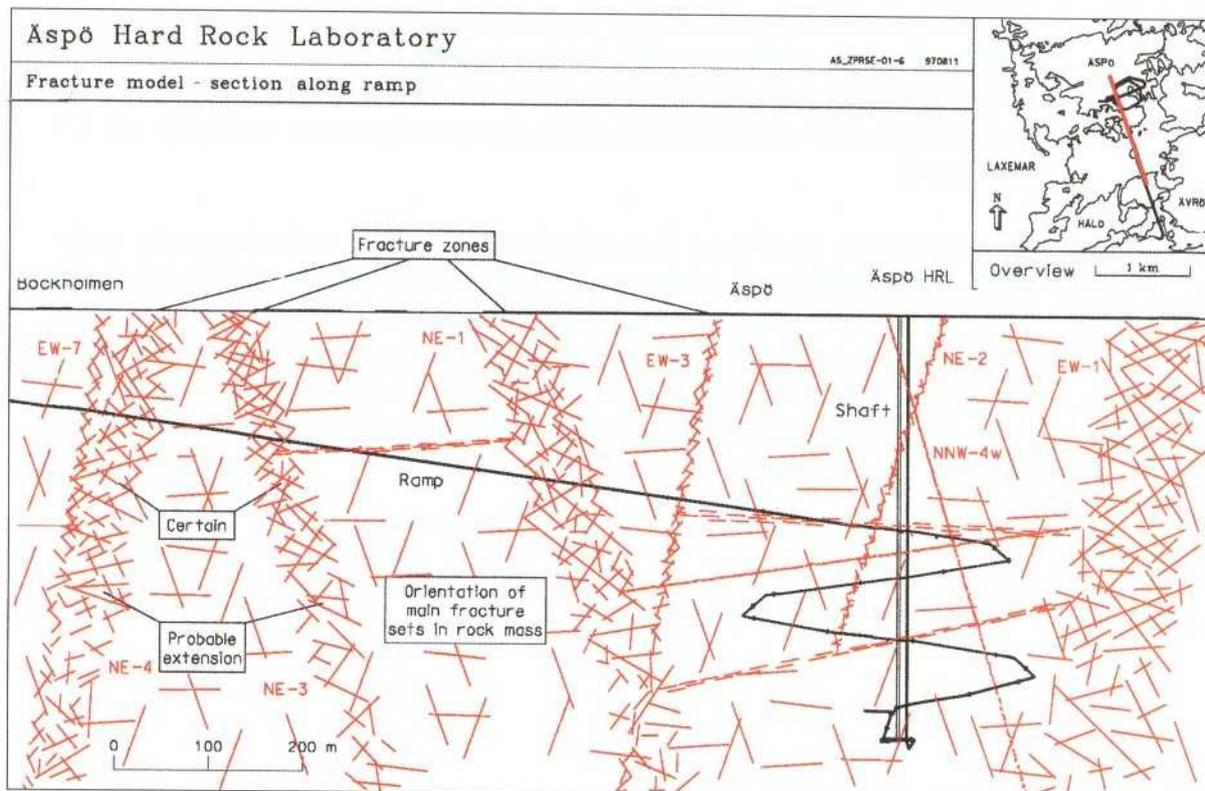
Figure 2-12. *Structural model - section along ramp.*

2.5 BRIEF ANALYSIS OF ACCURACY AND CONFIDENCE

This chapter contains a discussion of these geological variables in the block scale:

- Number of single open fractures
- Minor fracture zone widths

The *number of single open fractures* was predicted by a best estimate and a confidence level. For three out of six blocks, the best estimate corresponded to the outcome, and for six out of six, the outcome was within the 60% confidence limit.

As regards the number of minor fracture zones, the predictions overestimated the outcomes.

A minor fracture zone is penetrated by the tunnel and means 'fracture zone less than five metres wide'. For rock block 50-04 three minor fracture zones were predicted, based on the cored boreholes. In the rock block only one minor fracture zone was found. In the initial tunnel section 700-1475 m (P50-01, P50-02 and P50-03), the number of minor fracture zones was also overestimated, as it was in the previous tunnel section 1475-2265 m (P50-04).

The overestimation seems partly to include a systematic error.

The minor fracture zones all had predicted *widths* of 0.1 to 5 metres. Their median observed widths were 0.6 metres, ranging from 0.2 to 9.3 metres. The estimated width scale corresponded well to the observed widths. As regards the positioning of the minor fracture zones, the error increases weakly (p = 0.13) with depth.

The positioning error even for small depths (say 200 metres) is in the same order as the depth itself. This raises the question of whether all the zones are properly matched. Minor fracture zones can be localized on the surface to some extent by means of geological and geophysical mapping and hydraulic testing. Prediction of more exact position and extent at depth is almost impossible using the investigation and prediction methods and techniques employed on this project.

3   SUBJECT: LITHOLOGY

3.1   SCOPE AND CONCEPTS

The petrographical classification of the rocks, using modal analyses, is in accordance with the system worked out by *Streckeisen /1967/* and *IUGS /1973, 1980/*.

The rocks are divided into 4 rock groups, */Figure 3-1/*. The physical properties density and magnetic susceptibility were used to classify the main lithological units.

The density of crystalline rock is very closely related to its mineral composition. The influence of porosity on density, in crystalline rocks is less than one per cent.

The density of the rock is controlled by the amount of mafic minerals and the SiO_2 content. Rocks containing a large amount of mafic minerals and with a low SiO_2 content generally have a high density ($>3\ 000\ kg/m^3$) while rocks containing less mafic mineral and having a high SiO_2 content generally have a lower density ($2\ 600 - 2\ 700\ kg/m^3$).

The magnetic susceptibility in crystalline rocks is proportional to the content of magnetite by volume (less than 10 %) and to some degree by the content of paramagnetic minerals (iron in silicates).

Äspö Hard Rock Laboratory
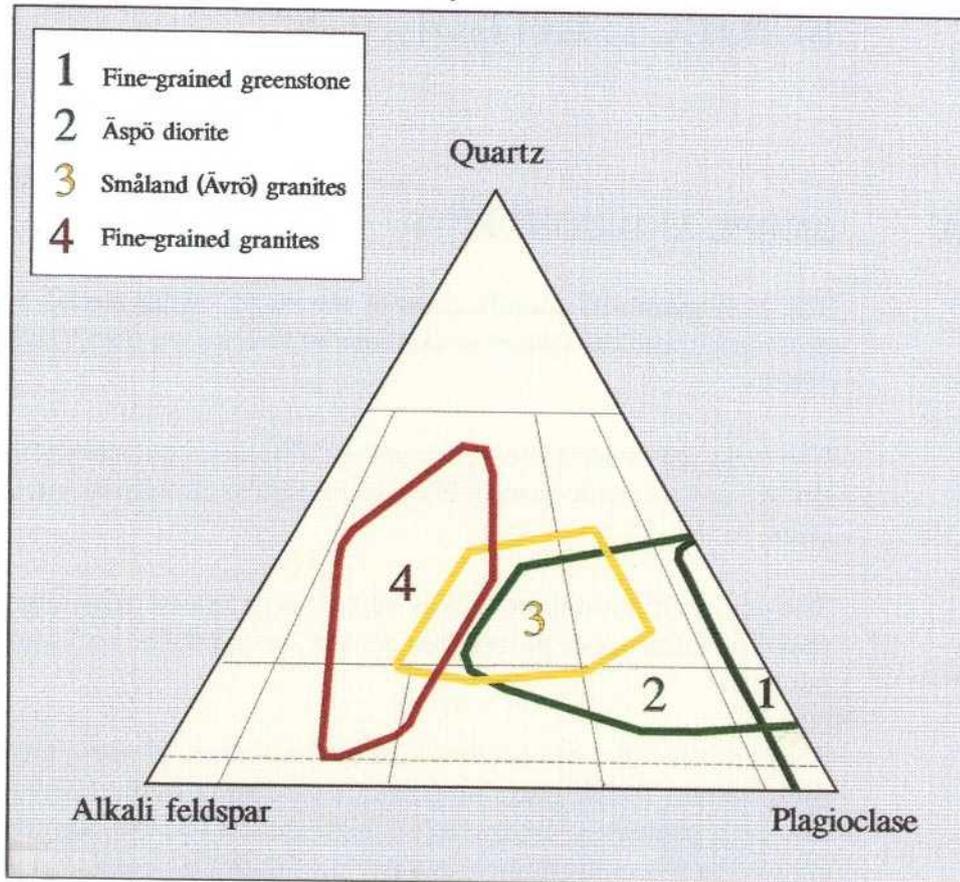
Figure 3-1. Modal classification according to IUGS /1973, 1980/ of 4 rock groups from the Äspö area.

Magnetite is the most frequent magnetic mineral in crystalline rocks and by using a special classification diagram the effect of magnetite on the density is easily removed. **Silicate density** is the density when the effect of the magnetite has been removed.
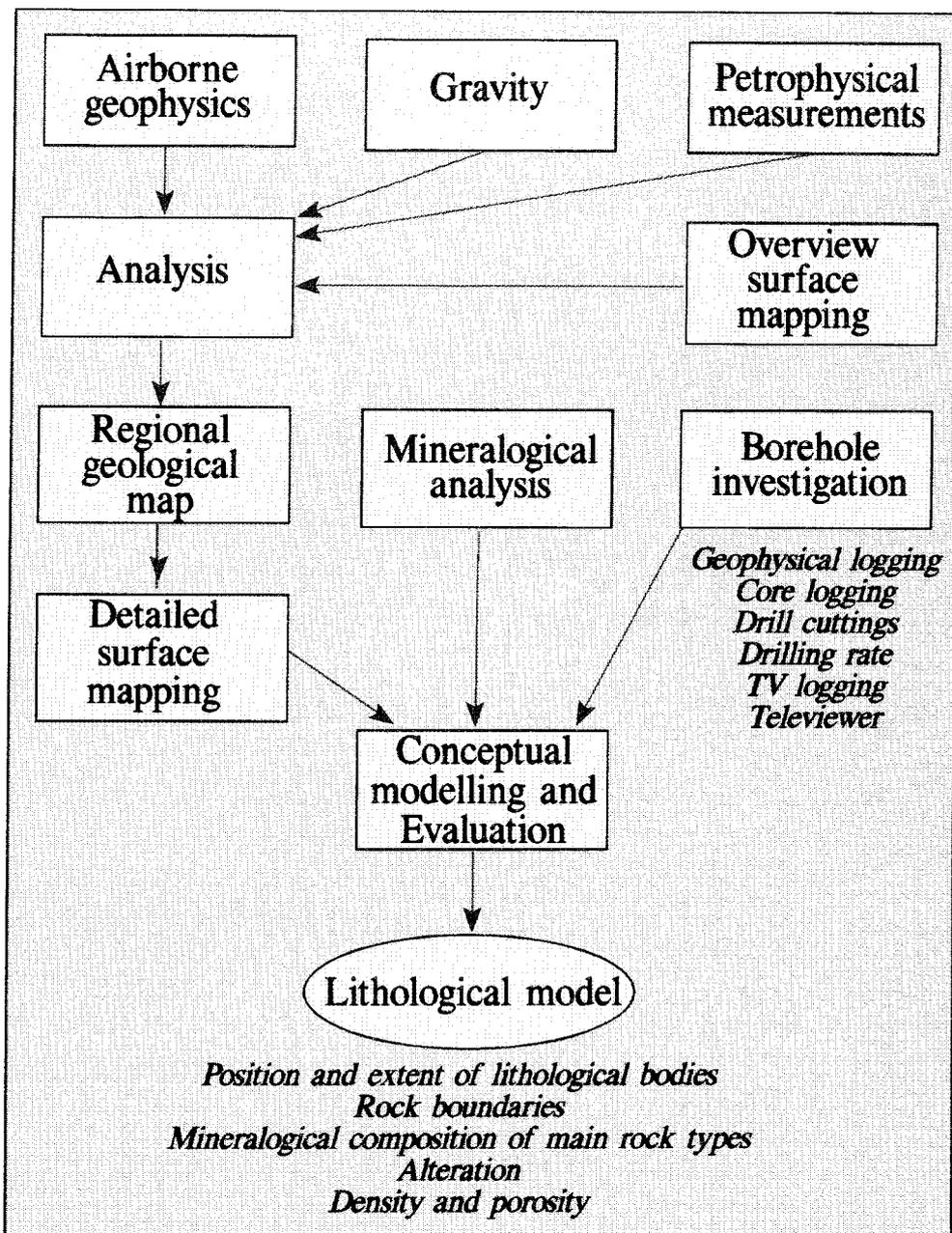
Figure 3-2. Pre-investigation methodology. Lithological characterization.

A classification limit between a more acid variety of the Småland (Ävrö) granite intrusion and a more basic variety called Äspö diorite was fixed at the silicate density of 2.65 - 2.70 g/cm^3.

The most basic rock variant observed in some boreholes in Äspö, with a silicate density above 2.75 g/cm^3, was assigned to the greenstone group (including diorites-gabbros).

Distribution of the main rock types and number of rock boundaries were estimated for 100 m slabs on the (500-m) site scale.

Rock composition and boundaries were estimated for six models on the (50-m) block scale.

Rock type characteristics were estimated for the four main rock types on the (5-m) detailed scale.

3.2 METHODOLOGY FOR TESTS OF CONCEPTS AND MODELS

The different methods used for lithological characterization are briefly presented below and summarized in *Figure 3-2*.

3.2.1 Prediction methodology

Surface methods

Airborne geophysics

Airborne magnetic, electromagnetic and radiometric investigations gave an initial general idea of the distribution of the major rock types on the regional scale - especially between granite and older rocks, basic intrusion and diapirs of younger granite /Nisca, 1987; Wikberg et al, 1991 and Almén et al, 1994/.

Petrophysical measurements

Petrophysical laboratory measurements of rock samples supplemented by an overview of surface mapping described below contributed to the evaluation of the aerophysical data for the regional map of the main rock extent. The measurements comprised determination of density, magnetic susceptibility and IP (induced polarization). In a later stage of the investigation density and porosity measurements were used to distinguish between Småland (Ävrö) granite and Äspö diorite /Nisca, 1988/.

Gravity measurements

Gravity data confirmed the extent in depth, especially of diapiric younger granites and bodies of basic rocks /Nylund, 1987/.

Overview of surface mapping

Data from an overview of surface mapping of road cuts, quarries and major outcrops combined with information from available geological maps made it possible to compile a brief description of the main rock units on a regional scale /Kornfält and Wikman, 1987; Wikberg et al, 1991 and Almén et al, 1994/.

Analysis

Integrated analysis of data from the methods described above resulted in an initial regional description of the main rock units.

Detailed surface mapping

Detailed surface mapping along cleaned trenches crossing the main direction of foliation provided very good information on the rock boundaries of small-scale structures, mylonites and petrographic variations of the main rock types /Kornfält and Wikman, 1988; Wikberg et al, 1991 and Almén et al, 1994/.

Borehole methods

Mapping of solid rocks on the surface contributed to a good understanding of the two-dimensional extent of the main rock types. In order to obtain a three-dimensional lithological model, borehole investigations were performed, comprising core mapping and geophysical logging.

Geological documentation of cored and percussion drill holes

The drill cores were mapped and gave information on rock types, rock boundaries, mylonites and fracturing. This information contributed to the three-dimensional modelling of the rock mass. Geophysical logging data were used as a complement to the core mapping.

During drilling of the percussion boreholes, the feed pressure and drilling rate were recorded continuously. The drilling rate was measured in a very simple manner. The time for every 20 cm of advance was determined, providing an adequate resolution for this purpose. Samples of the drill cuttings were examined with a binocular microscope for rock type classification /Stråhle, 1988/.

Geophysical logging

The complete geophysical logging programme carried out generally in the boreholes comprised the following logging methods:

- gamma-gamma (density),
- neutron (cored boreholes only),
- borehole deviation,
- caliper (cored boreholes only),
- sonic,
- natural gamma,
- single-point resistance,
- self potential (SP),
- magnetic susceptibility,
- normal resistivity (1.6 m),
- lateral resistivity (1.6 - 0.1),
- temperature,
- borehole fluid resistivity.

Geophysical borehole logging - especially the sonic log, natural gamma, magnetic susceptibility and gamma-gamma logs - are relevant for lithological characterization of the rock mass.

The rock type classification was mainly based on density (gamma-gamma) logging and thin section analyses of the cores /Sehlstedt and Stråhle, 1989/.

Mineralogical investigation of rock samples

Sampling of the main rock types was done on the surface and on drill cores. The rock type characterization is based on microscopical investigations and chemical analysis of rock samples. Modal analysis was used for classification of the main rock types /Kornfält and Wikman, 1987 and 1988, Eliasson, 1993/ investigated red-coloured alteration rims along fractures in granite from Äspö.

The U-Pb multiple zircon technique was used for radiometric age determinations of Äspö diorite and fine-grained granite /Wikman and Kornfält, 1995/.

3.2.2   Methodology for determining outcome

Geological documentation in the tunnel

The rock type distribution in the tunnel was assessed in connection with the general geological mapping performed after each new round had been excavated. Fine-grained granite and greenstone are generally rather easy to distinguish as are true Småland (Ävrö) granite and Äspö diorite. However, the transition forms between the latter rock types are very often impossible to identify macroscopically. In these cases drill core samples from the tunnel walls were analysed regarding silicate density and checked by means of microscopical modal analyses.

Core drilling

Core drilling - often related to some experiments concerning major fracture zones - provided supplementary information regarding rock distribution around the tunnel. Core mapping and different analysis of core samples were performed.

3.3   COMPARISON OF PREDICTED AND MEASURED ENTITIES

The prediction of the lithological model comprised the four main rock types - Småland (Ävrö) granite, Äspö diorite, fine-grained granite and greenstone. The percentages of the four rock types, predicted on the site scale, were based on a calculation of the average distribution of the different rock types in boreholes and distribution at the surface in the Hålö-Äspö area. The surface values are based on the average of rock mapping data along profiles trending N-S across the island of Äspö.

The lithological prediction on the (50-m) block scale was normally based on one cored borehole in or close to the actual block.

The blocks predicted on the detailed (5-m) scale should mainly be regarded as typical examples of the four most frequent rock types based on calculation of the average mineralogical composition and fracture pattern of these rock types in boreholes and outcrops in the target area. The positions of the predicted blocks are based on information from boreholes which penetrate the blocks or the rock volume close to the blocks.

The outcome is based on tunnel mapping data and borehole observations.

Lithological model on the site (500-m) scale

On the site scale the predictions were divided into four parts: 700-1475 m, 1475-2265 m, 2265-3064 m, 3064-3854 m. Due to a change in the planned tunnel layout it has only been possible to make a comparison between the prediction and outcome of tunnel section 700-2874 m. A comparison between rock composition and rock boundaries for this part of the tunnel is presented in *Figure 3-3*.

Lithological model on the (50-m) block scale

Comparison between the prediction and outcome concerning rock composition and mylonite (shear) for six 50-m blocks with fixed coordinates (±25 m) along the tunnel is presented in *Figures 3-4 to 3-9* and *Table 3-1*.

Rock type characteristics of four main rock types on the (5-m) detailed scale

The general purpose of the (5-m) detailed-scale models is to describe the rock on a scale of interest after the positioning of deposition holes and for the assessment of the near field rock, including the disturbed zone. However, as the deterministic description of the rock on this scale cannot be made until during the excavation of deposition tunnels, the aim of modelling rock blocks measuring 5x5x5 m in this project was to develop generic detailed models of different rock types in the Äspö bedrock.

The detailed scale modelling was always done parallel to the block-scale modelling. In all stages, generic 5-m blocks were made to describe what were considered typical 5-m blocks within the investigated volume */Figure 3-10/.* Each block described one of the four main rock types found in the investigated area, Småland (Ävrö) granite, Äspö diorite, fine-grained granite and greenstone */Figure 3-11/.*

Figure 3-3. Comparison between the prediction and outcome on the (500-m) site scale. Lithological model.

1:55

Rock Block P 50-01 0950-1000 ±25 m

PREDICTION:

Fine-grained granite

50m

0950m

1000 m

Increased fracturing (narrow fracture zones)

Småland granite $\rho < 2.70$

■ Hybridized-mylonitized - 5% (±5)$_{60\%}$[*]
■ Fine-grained granite -80% (÷5)$_{60\%}$
■ Småland (Ävrö) granite =15% (±5)$_{60\%}$

[*] Confidence level - 60%

OUTCOME:

0980   1005   1030 m

l
c
r

Tunnel Mapping Data

■ Pegmatite   - 2%
■ Fine-grained granite   = 59%
■ Småland (Ävrö) granite - 16%
■ Äspö diorite   - 23%

Figure 3-4. *Comparison between the prediction and outcome on the (50-m) block scale. Lithological model. P50-01.*
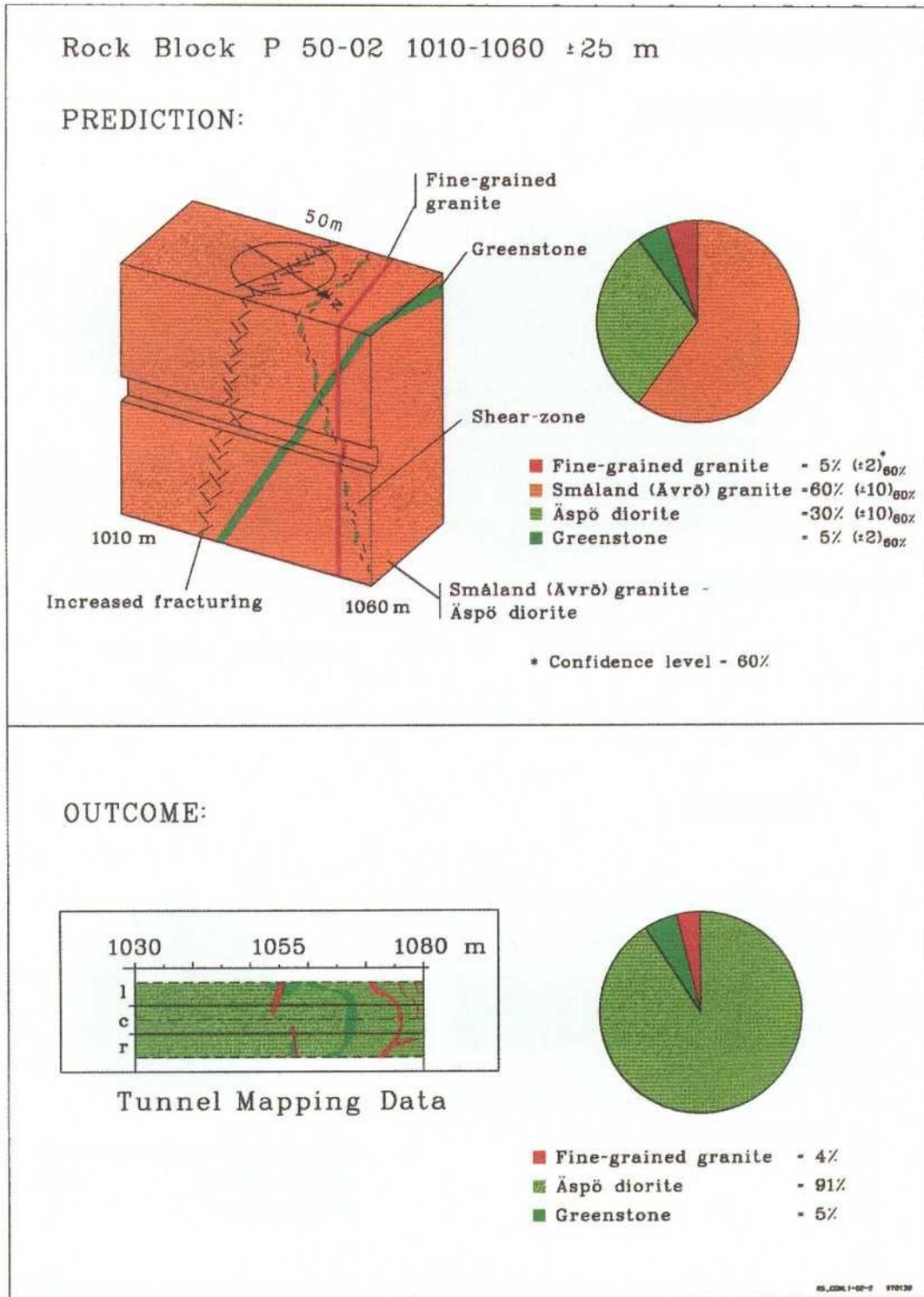
Figure 3-5. *Comparison between the prediction and outcome on the (50-m) block scale. Lithological model. P50-02.*
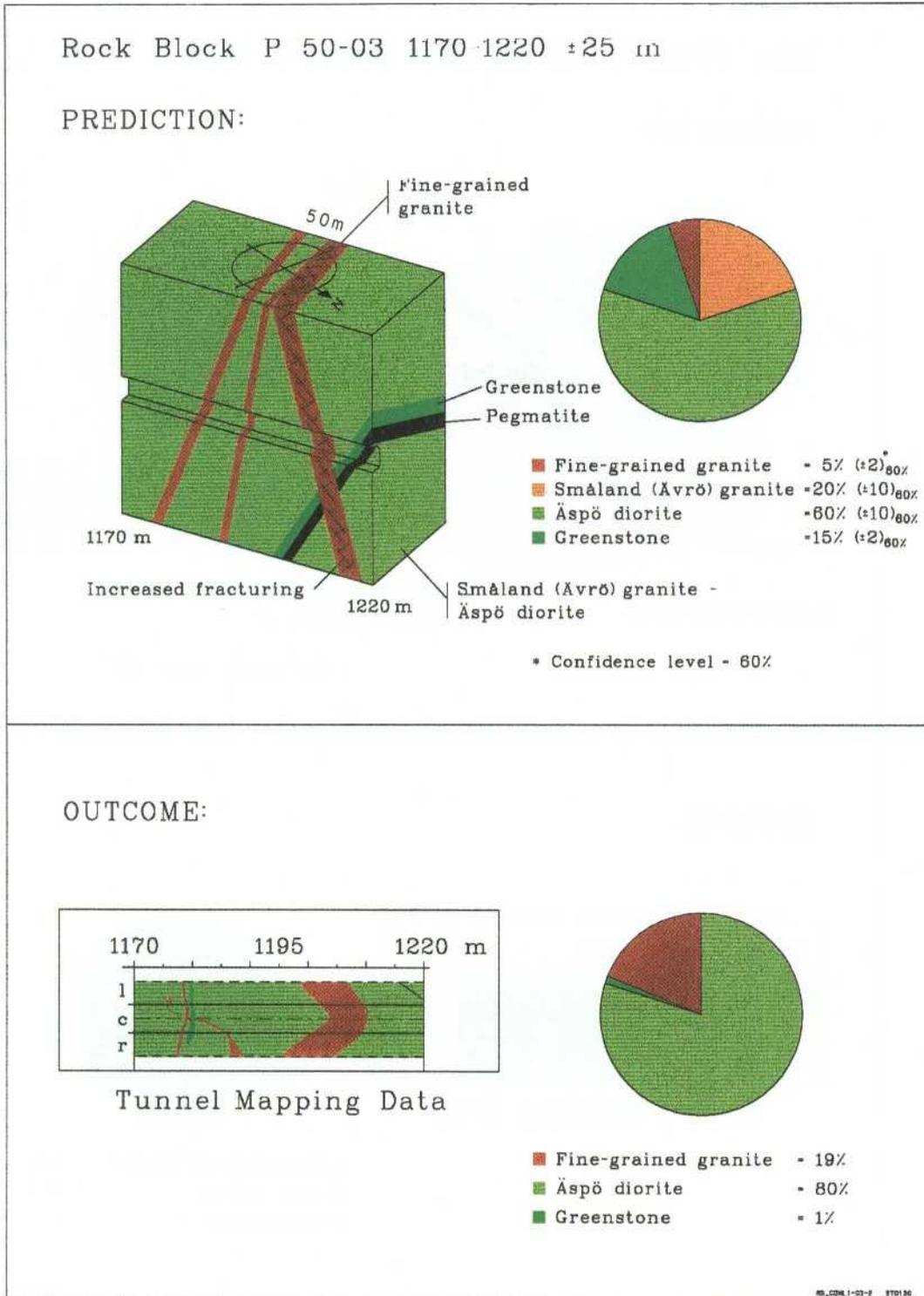
Figure 3-6. *Comparison between the prediction and outcome on the (50-m) block scale. Lithological model. P50-03.*

Rock Block P 50·04 1570-1620 ±25 m

PREDICTION:

■ Fine-grained granite	-10% (±3)$_{60\%}$*
■ Småland (Avrö) granite	-15% (±5)$_{60\%}$
▨ Äspö diorite	-25% (±5)$_{60\%}$
■ Greenstone	-50% (±10)$_{60\%}$

* Confidence level - 60%

OUTCOME:

Tunnel Mapping Data

■ Fine-grained granite	- 12%
■ Pegmatite	- 1%
▨ Äspö diorite	- 32%
■ Greenstone	- 55%
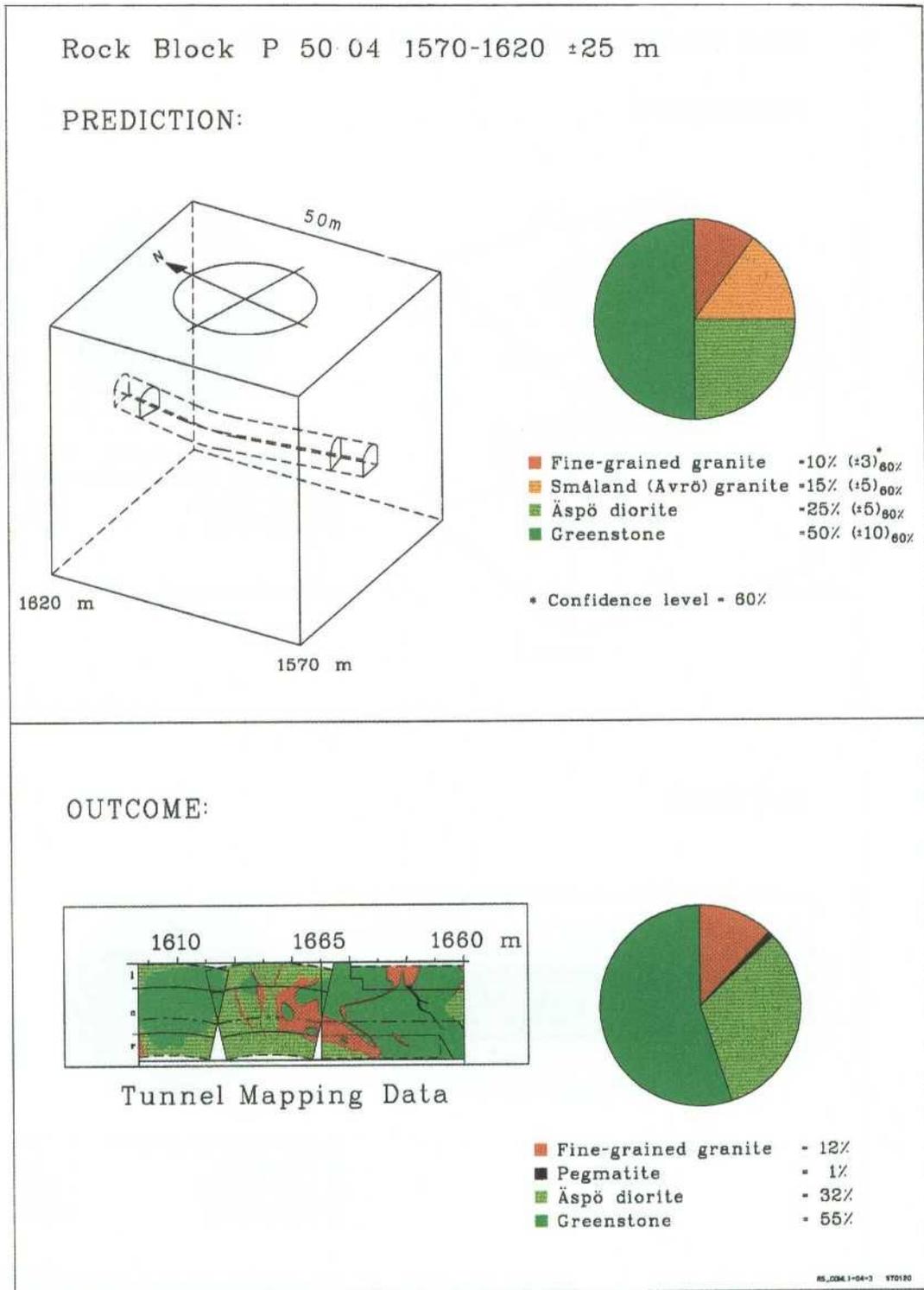
Figure 3-7. *Comparison between the prediction and outcome on the (50-m) block scale. Lithological model. P50-04.*
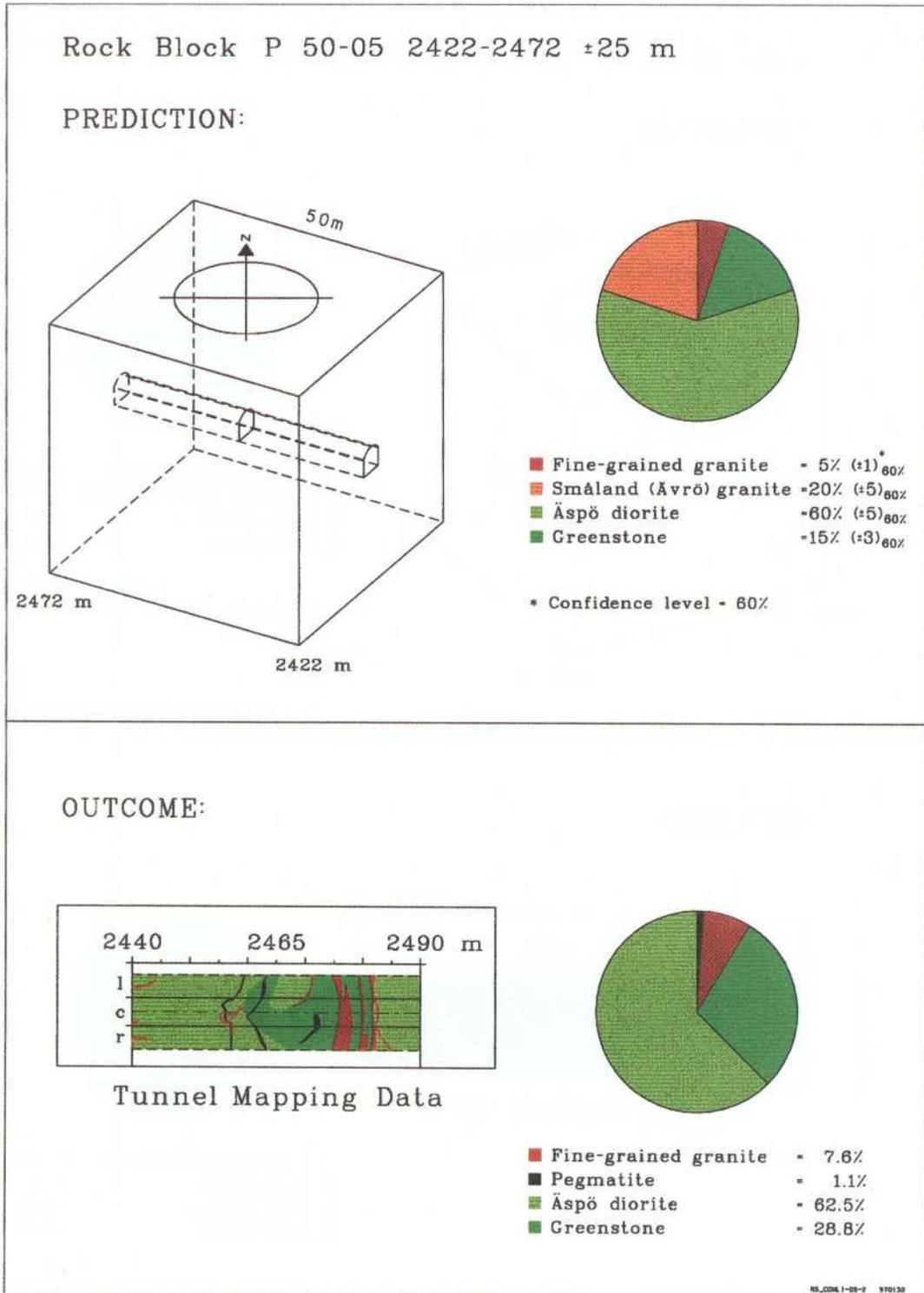
Figure 3-8. *Comparison between the prediction and outcome on the (50-m) block scale. Lithological model. P50-05.*

Rock Block P 50-06 2752-2802 ±25 m

PREDICTION:

- ■ Fine-grained granite -15% (±3)$_{60\%}$*
- ■ Småland (Ävrö) granite -25% (±10)$_{60\%}$
- ■ Äspö diorite -50% (±10)$_{60\%}$
- ■ Greenstone -10% (±3)$_{60\%}$

* Confidence level - 60%

OUTCOME:

Tunnel Mapping Data

- ■ Småland (Ävrö) granite - 81.9%
- ■ Äspö diorite - 17.7%
- ■ Greenstone - 0.4%
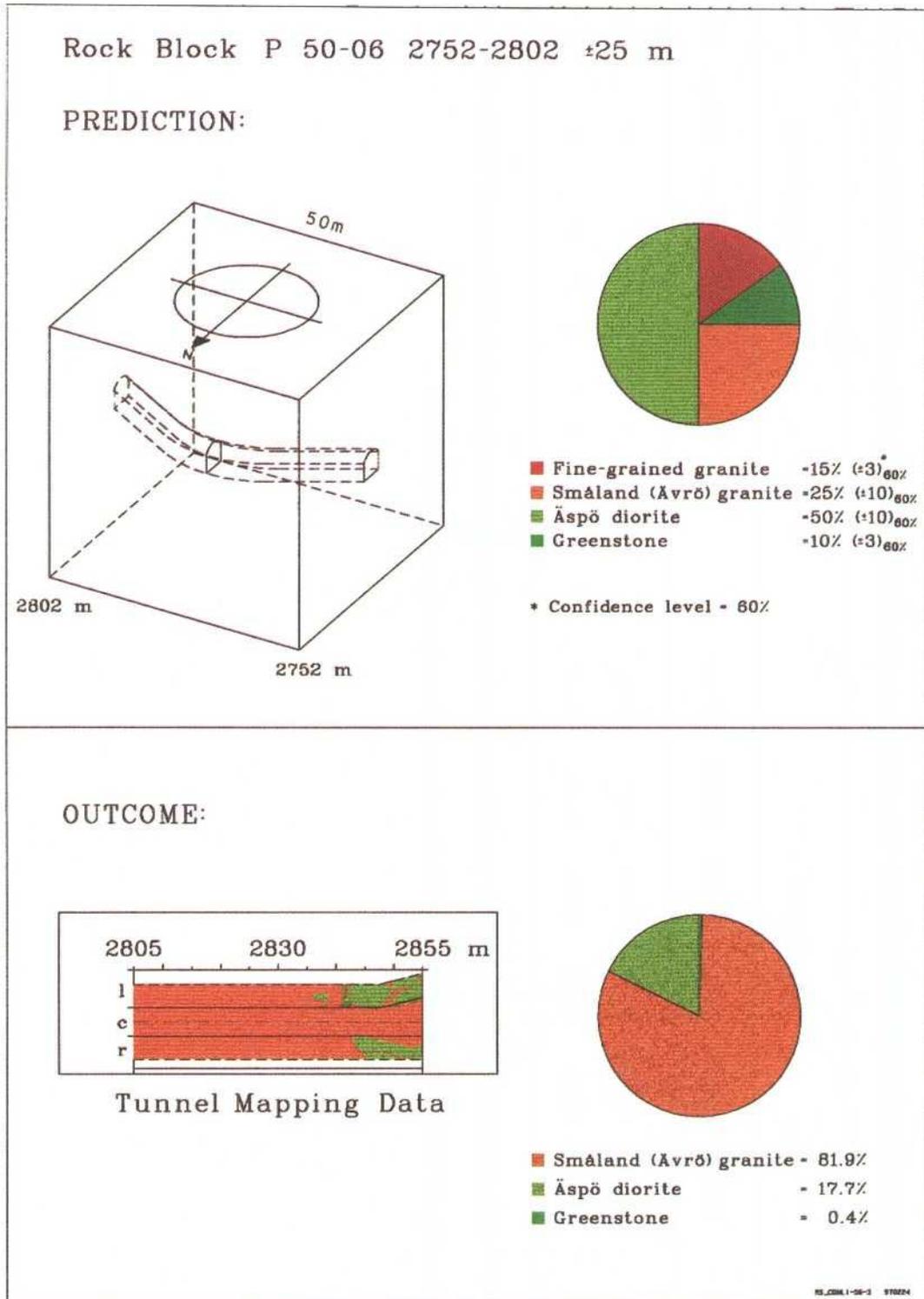
Figure 3-9. Comparison between the prediction and outcome on the (50-m) block scale. Lithological model. P50-06.

Table 3-1. Lithological models on the (50-m) block scale. Comparison between the prediction and outcome for six 50-m blocks. (P50-01--P50-06).

Subject	PREDICTION						OUTCOME					
	P50-01	P50-02	P50-03	P50-04	P50-05	P50-06	P50-01	P50-02	P50-03	P50-04	P50-05	P50-06
Rock boundaries*	7(±2)	4(±2)	8(±2)	6(±1)	8(±2)	6(±2)	3	6	6	6	10	2
Mylonite (shear)	3(±1)	3(±1)	2(±1)	5(±1)	7(±2)	3(±1)	0	0	0	1	3	0

*   Veins less than approximately 0.5 m and the normally very diffuse contacts between the rock variants Småland (Ävrö) granite and Äspö diorite are excluded.

The confidence level (75% for rock boundaries and 60% for mylonite) is based mainly on expert judgement.

Figure 3-10. *Illustration of conceptual modelling on the block and detailed scales.*
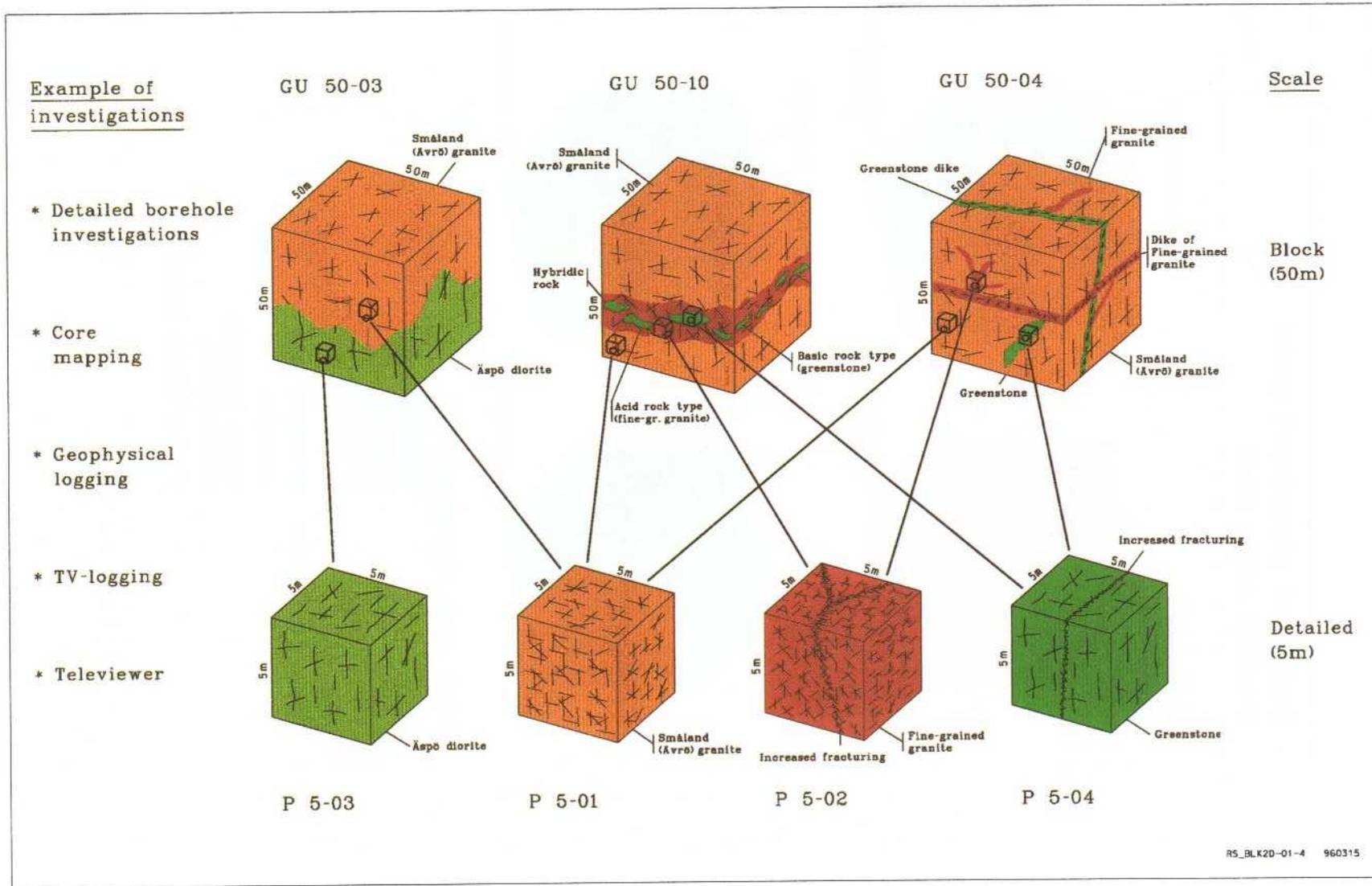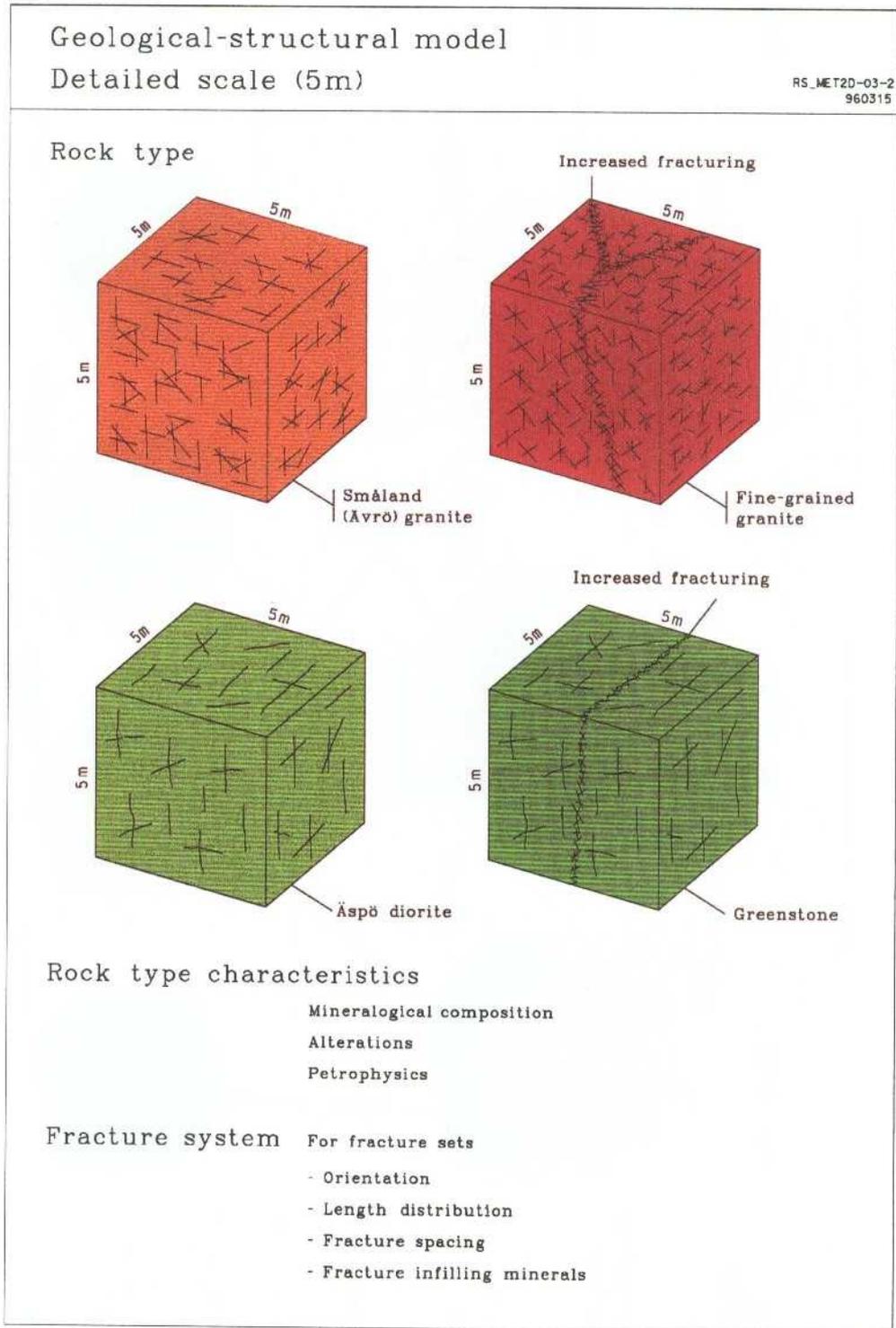
Figure 3-11 *Overview of the subject rock type characteristics of the lithological models (for the four main rock types), addressed on the detailed scale.*

The comparison between the prediction and outcome for the four main rock types is presented in *Table 3-2*.

3.4 SCRUTINY AND EVALUATION

3.4.1 Lithology and rock boundaries on the (500-1000 m) site scale

Distribution of the main rock types

The prediction and outcome are presented for tunnel section 700 m - 2874 m. The prediction of the distribution of the main rock types was based on a calculation of the average distribution of the different rock types in boreholes and the distribution at the surface in the Hålö-Äspö area. The surface values are based on the average rock mapping data along profiles trending N-S across the island of Äspö.

Data from both surface mapping and drill cores were corrected with respect to a mean estimated orientation of fine-grained granite and greenstone which often occur as dikes in the Småland (Ävrö) granite/Äspö diorite. Fine-grained granite dikes were estimated to trend N50°E with an almost vertical dip. The greenstone lenses were estimated to trend N75°E with an almost vertical dip. In some cases – mainly in the vertical boreholes – a sub-horizontal dip of the greenstone lenses was noticed and used in the calculation.

By way of comparison, data from surface rock mapping and the spiral volume in four different depth sections, 0-100 m, 100-200 m, 200-300 m and 300-400 m, are presented in *Figure 3-3*.

Äspö diorite and Småland (Ävrö) granite are the dominating rocks. These two rock types make up approximately 80 % of the investigated tunnel area. The predicted amount of 75-76 (±5) % for the three different levels should be compared with 78-83 % found by mapping in the tunnel.

The fine-grained granite which was predicted to make up 14 (±3) % was found to comprise 14-19 % in the tunnel.

Greenstone generally occurs as very small irregular veins, thin lenses and sheets, to form old inclusions in the granite-dioritic rock mass but occasionally also as massifs some ten metres wide. Greenstone was predicted to make up 8-14 (±3) % of the rock mass but was found in the tunnel to amount to only 2.5-8 %. The relative amount of greenstone was overestimated mainly due to the very frequent occurrence of this rock type in the form of sub-horizontal irregular sheets at the surface.

Table 3-2. Lithological models on the (5-m) detailed scale. Comparison between the prediction and outcome for four (5-m) blocks. The generic 5-m blocks were made in order to describe what is considered to be typical 5-m blocks within the investigated rock volume. Each block describes one of the four main rock types Småland (Ävrö) granite, Äspö diorite, greenstone and fine-grained granite.

Subject	PREDICTION				OUTCOME			
	Småland (Ävrö) granite	Äspö diorite	Green-stone	Fine-grained granite	Småland (Ävrö) granite	Äspö diorite	Green-stone	Fine-grained granite
Mineral components (%)								
Quartz	20(±3)	15(±5)	5(±3)	30(±5)	26	12	4	27
Alkali-feldspar	25(±5)	15(±5)	-	40(±5)	26	17	-	36
Plagioclase	40(±5)	40(±5)	50(±5)	23(±5)	37	47	7	20
Biotite/Muscovite	10(±3)	20(±5)	20(±5)	7(±2)**	5	12	33	17
Amphibole	-	-	20(±5)	-	-	-	54	-
Epidote/pyroxene	-	-	5(±3)	-	-	-	2	-
Minor minerals	5(±2)	10(±3)	-	-	6	12	-	-
Total	100	100	100	100	100	100	100	100
Alteration (IUGS-classification)	1-2	1-2	1-2	1-2	2	2	2	1
Density (g/cm³)	2.62(±0.03)	2.70(±0.05)	2.80(±0.05)	2.56(±0.02)	2.64	2.75	2.96	2.67
Porosity (%)*	0.24(±0.02)	0.32(±0.02)	0.16(±0.02)	0.30(±0.01)	0.29	0.42	0.17	0.26

*   Total porosity of matrix.
**   Biotite, epidote and minor minerals.
***   'Greenstone' includes different basic rocks (dacite-gabbro) with different densities.
The confidence level (60% for mineral components and 90% for density/porosity) is based mainly on expert judgement.

Rock boundaries

The prediction of 9-12 (±3) rock boundaries per hundred metres of tunnel section should be compared with the 8-12 boundaries mapped in the tunnel. Consequently it is possible to predict the average number of rock boundaries in a tunnel section between rock types such as fine-grained granite and greenstone, which appear in the form of dikes and bodies with distinct contacts with the wall-rock. The gradual transition boundaries between minor units of Småland (Ävrö) granite and Äspö diorite were not included in the prediction.

The geophysical borehole surveys were intended to aid definition of the location and character of the lithological units and their contacts. The sonic log and magnetic susceptibility and gamma-gamma logs seem to be very relevant for lithological characterization of an inhomogeneous rock mass like that in the Äspö area. There is a specially significant correlation between high gamma radiation and the fine-grained granites in the boreholes.

3.4.2   Lithology and rock boundaries on the (50 m) block scale

Distribution of the main rock types

The prediction and outcome are presented for six 50-m blocks with fixed co-ordinates (±25 m).

Rock Composition

The prediction of the rock types contribution in the three blocks P50-01 to P50-03 was mainly based on the inclined borehole KBH02 */Figures 3-4, 3-5 and 3-6/.* The change in the layout of the tunnel is one reason for the discrepancy between the prediction and outcome. As these rock blocks all represent very specific rock volumes, a rather small change in the tunnel layout from the predicted route may cause a big deviation in an inhomogeneous rock mass like that in the Äspö area.

The prediction of the rock types contributing to rock block P50-04 */Figure 3-7/* was mainly based on boreholes KAS05 and KAS13 and the prediction of the rock types contributing to rock blocks P50-05 and P50-06 on boreholes KAS05 and KAS12 */Figures 3-8* and *3-9/.* As the tunnel layout was changed during construction there are also differences in the predicted and outcome positions of rock blocks P50-05 and P50-06. The lateral deviations are 30 m and 35 m respectively and vertical ones 10 m and 15 m respectively.

As there is no distinct difference between the two rock types − Småland (Ävrö) granite and Äspö diorite − but rather a gradual transition which has to be based on density measurements and microscopical analysis − it seems to be more relevant to compare the total amount of these two rock types.

The greenstone, fine-grained granite and pegmatite are especially sensitive to the layout change as they normally occur as very local lenses, irregular veins and sheets in the rock mass.

Rock Boundaries

Rock boundaries were found by mapping the different rock types – more than 0.5 m wide – along the tunnel axis in the rock blocks.

The main reason for the big discrepancy regarding rock boundaries in rock block P50-01 is probably the predicted hybridized-mylonitized veins which did not occur in the tunnel, possibly due to the change in the layout of the tunnel */Table 3-1/*.

Mylonite

Mylonite was only observed by the ordinary mapping in rock blocks P50-04, 05 and 06. The reason for the discrepancy between prediction and outcome concerning the mylonites could be the fact that the mostly very thin mylonite veins in the drill cores – on which the predictions were based – are much easier to detect than by mapping in the tunnel */Table 3-1/*.

3.4.3 Rock Type Characteristics on the (5 m) detailed scale

Rock type characteristics for the (5-m) blocks representing the four main rock types were predicted.

The prediction of the mineralogical composition of the four main rock types */Figure 3-11/* was based on numerous microscopical analyses of core samples from the Äspö area. The petrophysical parameters density and porosity were based on geophysical logging data. There is an agreement between prediction and outcome regarding alteration and the major minerals – less good concerning biotite and minor minerals. The outcome data are normally based on 2-3 microscopical analyses per rock block and the density and porosity are based on 10-12 analyses */Table 3-2/*.

The mineralogical composition data should also be compared with the mean composition of the four relevant rock types in the whole Simpevarp area */Table 3-3/* according to *Wikman /1993/*.

Table 3-3. Main composition of main rock types in the whole Simpevarp area based on microscopical analyses.

Minerals	Småland (Ävrö) granite (n=41) %	Äspö diorite (n=87) %	Fine-grained granite (n=41) %	Greenstone (n=23) %
Quartz	25.8	14.0	30.6	3.5
K-feldspar	25.5	13.0	38.6	0.8
Plagioclase	37.1	44.7	20.8	35.4
Biotite	5.2	14.5	-	14.0
Epidote	-	-	-	6.0
Pyroxene/Amphibole	-	-	-	35.7
Minor minerals	6.4	13.8	10.0	4.6
Total	100	100	100	100

It is important to note that the designation 'greenstone' was used to cover all basic rocks such as fine-grained metavolcanics to the rocks of dioritic-gabbroid composition.

3.4.4 Assessment of the usefulness of investigation methods

The gravity and aero-magnetic methods were found to be very useful, especially for studies of a regional nature, i.e. for investigating the boundaries of the Götemar-Uthammar diapirs in three dimensions and the basic rocks of large extent. The densities and magnetic contents of these granitic rocks usually differ from those of the surrounding rocks, and they were therefore good targets for both of these methods. Based on these investigations it was possible to carry out an initial three-dimensional lithological-structural modelling on the regional scale.

The petrophysics, based on physical measurements in the laboratory of a large number of representative samples, is necessary for making a good interpretation of the geophysical data.

The sonic log and the magnetic susceptibility and gamma-gamma logs seem to be very relevant for the lithological characterization of a inhomogeneous rock mass such as the one in the Äspö area. There is in particular a significant correlation between high gamma radiation and the fine-grained granites in the boreholes.

A combination of the density (gamma-gamma) and magnetic susceptibility logs was preferred for the rock type classification.

Detailed geological mapping on the surface combined with drill core analysis is the best method of investigating rock composition, rock boundaries and mylonites on the block scale. The density borehole log gives the best

information concerning the difference between Småland granite and Äspö diorite. Microscopic examination of thin sections supplemented by chemical analysis is the best way of performing rock type characterization and classification.

3.5 BRIEF ANALYSIS OF ACCURACY AND CONFIDENCE

In this chapter, these geological variables in the block scale are discussed:

- Lithology
- Number of rock boundaries
- Number of mylonite zones
- Alteration
- Mineral composition
- Porosity

The prediction of *lithology* distribution on the site scale has an absolute error of 0-11 percentage units.

The best accuracy (lowest APE) was obtained for Äspö diorite, the most abundant rock type. The second best accuracy was obtained for Småland (Ävrö) granite, which also is the second most abundant rock type.

The accuracy (APE) is closely correlated to the observed portion of the rock type. This means that we may formulate a model to estimate the error already when the prediction is made.

The typical APE for the lithology on the site scale is about 15 percentage units as a median value for the rock types. It is smaller for the abundant ones and higher for the less frequent rock types. There is a clear relationship between the observed portion of the rock type and APE. This means that the error size can be estimated from the typical APE related to that predicted amount.

For rock type with portions more than 10%, the rough estimate of APE is:

$$APE = 33 - 0.6 \bullet P$$

APE = absolute percentage error (%)
P = prediction (%)
(n = 8)
(R^2 = 59%)

This means that for a rock type predicted at say 25% of the total, the APE is roughly 18%. This relationship may provide an estimate of the anticipated range for the observation.

The number of *rock boundaries* was both over- and underestimated. Four out of six predictions were within the estimated 75% confidence level.

The *number of mylonite zones* was overestimated. It seems like the error contains partly a systematic error, the error includes a constant of 2-3 more zones than are present.

Mylonite was not observed in the initial mapping in the rock blocks. The reason for the discrepancy between prediction and outcome concerning the mylonites could be the fact that the mostly very thin mylonite veins in the drill cores - on which the predictions were based - are much easier to detect than by mapping in the tunnel where normally only mylonites more than 10 cm wide are mapped. Thus, the occurrence of thin veins in cores led to overestimation in the tunnel due to different mapping scales. This was also the case in section 700-1475 m (P50-01, P50-02 and P50-03).

Regarding the lithological models on the detailed scale /see *Table 3-2/*, the absolute errors in predicting the *mineral composition* of the most common rock types are 5-10 percentage units. Especially, the greenstone composition was difficult to predict precisely. The accuracy is rather poor, the maximum error could well be over 10 percentage units for any rock type and any mineral components. Excluding greenstone, the absolute percentage error is typically in the order of 10 to 100%. The absolute percentage errors in predicting quartz are relatively lower than for that of biotite/muscovite.

The *alteration* (IUGS-classification) was predicted to be one to two, which complies with the outcome.

The *density* of the four rock types was underestimated. The best precision was obtained for Småland (Ävrö) granite. Two out of four densities were within the predicted range of confidence (90%). The absolute percentage errors were 1-5%.

The *porosity* was underestimated for three rock types out of four. Only greenstone porosity was within the range that was predicted width 90% confidence.

PART 2

MECHANICAL STABILITY

1 SUBJECT: ROCK QUALITY

1.1 SCOPE AND CONCEPTS

The purpose of the rock mass classification was to estimate rock qualities that will in different ways influence the rock excavation and support of the tunnel. The rock mass was therefore divided into five representative groups in which the rock mechanics characteristics were predicted to be different. Several different classification systems are used around the world.

For this classification the Geomechanics Rock Mass Rating (RMR) /Hoek, 1980/ system proposed by Bieniawski was applied. This system employs six parameters describing the rock mass and its use is appropriate when the classification is based on pre-investigation data. If any parameter is missing, it is possible to estimate the value of the missing character.

In the Geomechanics Rock Mass Rating System the rock mass is described by parameters for:

1   strength of rock material
2   RQD value
3   spacing of discontinuities
4   conditions of discontinuities, and
5   the flow of water into the underground development.

The sum of all the points allocated to the different parameters describes the rock mass in the form of a value called the RMR value (Rock Mass Rating). Finally the RMR value is adjusted for the joint orientation in relation to the tunnel geometry.

The RMR value varies between 0 and 100 and in general terms the different RMR values are often classified as follows:

RMR	Classification
100-81	Very good rock
80-61	Good rock
60-41	Fair rock
40-21	Poor rock
20-0	Very poor rock

1.2 METHODOLOGY FOR TESTS OF CONCEPTS AND MODELS

The different methods used for rock quality assessment in the pre-investigation are presented briefly below.

1.2.1 Prediction methodology

Study of terrain, topographical mapping and exposed bedrock

A visual inspection was made of the areas to obtain general information on the topography, major alignments and rock types present. Rock type properties, such as fracture frequency, degree of weathering, and preliminary mechanical characteristics were also observed /Figure 1-1/.

Seismic refraction

Seismic refraction profiles were used to obtain information on seismic velocities. Profiles were measured both on land and in sub-sea areas.

The seismic velocities provide on the large scale a brief indication on the existence of fracture zones. The fracture zones will to some extent be quantified as to width and general information will be gained on the rock quality in the zones.

Borehole investigations

For characterization of rock quality, core drilling and core mapping provide detailed information. Core drilling was performed in a number of holes. The holes were drilled with different orientations to obtain information on different fracture sets, e.g. steep and sub-horizontal fractures.

The cores were logged to provide further information on the distribution of different rock types and to determine their fracture frequencies (RQD), fracture distance and fracture surface properties (JRC, JCS and fracture fillings).

RQD =   Rock quality design is a classification system for drill-cores
JRC =   Joint roughness coefficient
JCS =   Joint compressive strength

Testing of mechanical characteristics and fracture surface properties

See /Chapter 3, Subject: Mechanical characteristics/.

1.2.2 Methodology for determining outcome

Documentation of the rock mass rating parameters was performed according to the field manual /Christiansson-Stenberg, 1991/ in conjunction with the general geological mapping carried out continuously with each round of blasting.

In the core holes geophysical logging was performed to identify fracture zones and geological anomalies in the rock mass.

Hydraulic tests performed in stages along the core holes pointed out the major hydraulic paths and the transmissive zone in the rock mass.
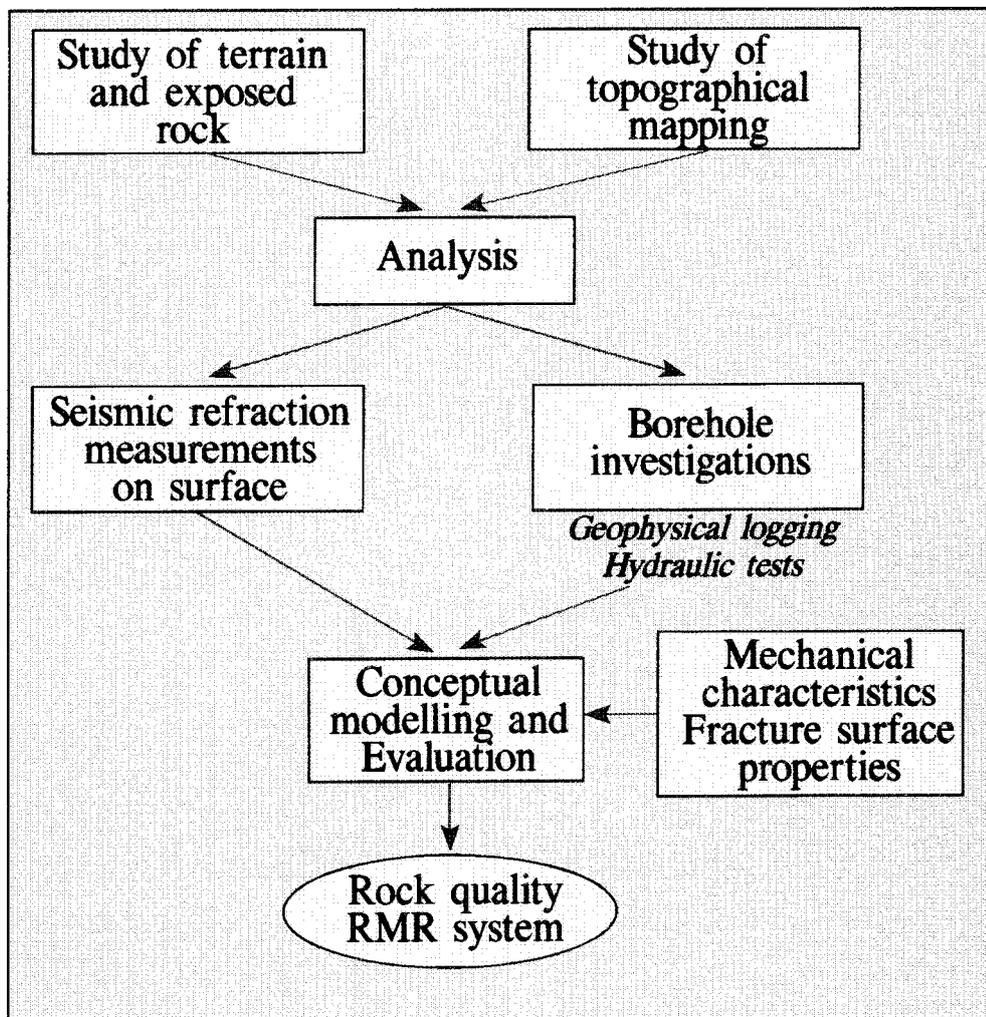
Figure 1-1. Flow chart of the rock quality investigations /Almén et al, 1994/.

1.3 COMPARISON OF PREDICTED AND MEASURED ENTITIES

The prediction of the rock quality was based mainly on rock surface mapping data and information obtained in conjunction with the coreholes. General experience obtained from other similar sites in Sweden was also applied and found valuable. The outcome is based on tunnel mapping data.

For the classification of the rock mass in the Äspö tunnel the RMR system was applied. The RMR system is usually divided into the five different groups which correspond to qualities from very good rock to very poor rock. To get a more accurate prediction for the Äspö tunnel the rock mass was divided into five groups, A-E, presented in *Table 1-1*. These were considered to better apply to the different stability conditions expected to be significant.

Rock quality model on the site (500-m) scale

On the site scale the predictions were made for four parts: 700-1475 m, 1475-2265 m, 2265-3064 m, 3064-3854 m. Due to a change in the planned tunnel layout it was only possible to make a comparison between the prediction and outcome of tunnel section 700-2874 m. A comparison between the rock quality and geological tunnel data for this part of the tunnel is presented in *Figure 1-2* by *Olsson-Stille in Stanfors et al /1992, 1993 and 1994/*.

A summary of the predicted and observed distribution of RMR values is presented in *Table 1-1*. The variations in observed RMR values along the tunnel are presented in *Figure 1-3*.

Table 1-1. Summary of predicted and observed RMR-values along the tunnel. (Section 700-2874 m).

Class	RMR-value	Predicted distribution	Outcome distribution
A	RMR >72	23 %	28 %
B	RMR 60-72	50 %	39 %
C	RMR 40-60	19 %	29 %
D*	RMR <40	3 %	4 %
E**	RMR <40	5 %	

*   Class D refers to zones less than 4 m wide
**   Class E refers to zones more than 4 m wide

RS_3XMEC-01-1 960321

0700-1475 m: 0/700 — 0/800 — 0/900 — 1/000 — 1/100 — 1/200 — 1/300 — 1/400 — 1/475

Fracture Zones: EW-7 · NE-4 · NE-3 · ∘∘ · ∘ · NE-1 · EW-3

Lithology

	PREDICTION					OUTCOME				
Rock Quality (RMR)	Class	A	B	C	D	E	Class	A	B	C	D	E
%	20	45	30	-	5	%	11	37	40	3	9

Rock Stress (Meas. position ⊙)	Vertical stress	Max horiz. stress	Min horiz. stress	Vertical stress	Max horiz. stress	Min horiz. stress
Magnitude [MPa]	$\sigma_v = Z(m)*0.0265$	$\sigma_{H,max} = 1.7\text{-}2.0*\sigma_v$	$\sigma_{H,min} = 1.1\text{-}1.5*\sigma_v$	$\sigma_{v,\,measured} = 1.1*\sigma_v$	$\sigma_{H,max} = 3.0*\sigma_v$	$\sigma_{H,min} = 1.9*\sigma_v$
Orientation		N30° W ±15°	N60° E ±15°		N73° W	N17° E

1475-2265 m: 1/475 1/500 — 1/600 — 1/700 — 1/800 — 1/900 — 2/000 — 2/100 — 2/200 2/265

Fracture Zones: NE-2 · ∘∘∘ · NE-2

Lithology

	PREDICTION					OUTCOME				
Rock Quality (RMR)	Class	A	B	C	D	E	Class	A	B	C	D	E
%	35	35	25	5	-	%	32	45	21	2	-

Rock Stress (Meas. position ⊙)	Vertical stress	Max horiz. stress	Min horiz. stress	Vertical stress	Max horiz. stress	Min horiz. stress
Magnitude [MPa]	$\sigma_v = Z(m)*0.0265$	$\sigma_{H,max} = 1.6\text{-}1.7*\sigma_v$	$\sigma_{H,min} = 0.8\text{-}0.9*\sigma_v$	$\sigma_{v,\,measured} = 1.2*\sigma_v$	$\sigma_{H,max} = 2.2*\sigma_v$	$\sigma_{H,min} = 1.2*\sigma_v$
Orientation		N25° W ±15°	N65° E ±10°		N58° W	N32° E

2265-2874 m: 2/265 2/300 — 2/400 — 2/500 — 2/600 — 2/700 — 2/800 — 2/874

Fracture Zones: (⊙ 2/198) · ∘

Lithology

Legend:
- ▮ Småland (Ävrö) granite
- ▮ Aspö diorite
- ▮ Greenstone
- ▮ Fine-grained granite
- ▮ Mylonite-hybridized

	PREDICTION					OUTCOME				
Rock Quality (RMR)	Class	A	B	C	D	E	Class	A	B	C	D	E
%	20	50	20	10	-	%	34	36	29	1	0

Rock Stress (Meas. position ⊙)	Vertical stress	Max horiz. stress	Min horiz. stress	Vertical stress	Max horiz. stress	Min horiz. stress
Magnitude [MPa]	$\sigma_v = Z(m)*0.0265$	$\sigma_{H,max} = 1.2\text{-}1.4*\sigma_v$	$\sigma_{H,min} = 0.6\text{-}0.8*\sigma_v$	$\sigma_{v,\,measured} = 1.1*\sigma_v$	$\sigma_{H,max} = 2.8*\sigma_v$	$\sigma_{H,min} = 1.1*\sigma_v$
Orientation		N30° W ±10°	N60° E ±10°		N46° W	N44° E

Figure 1-2. Comparison between prediction and outcome on the (500-m) site scale. Rock quality model.

2:5
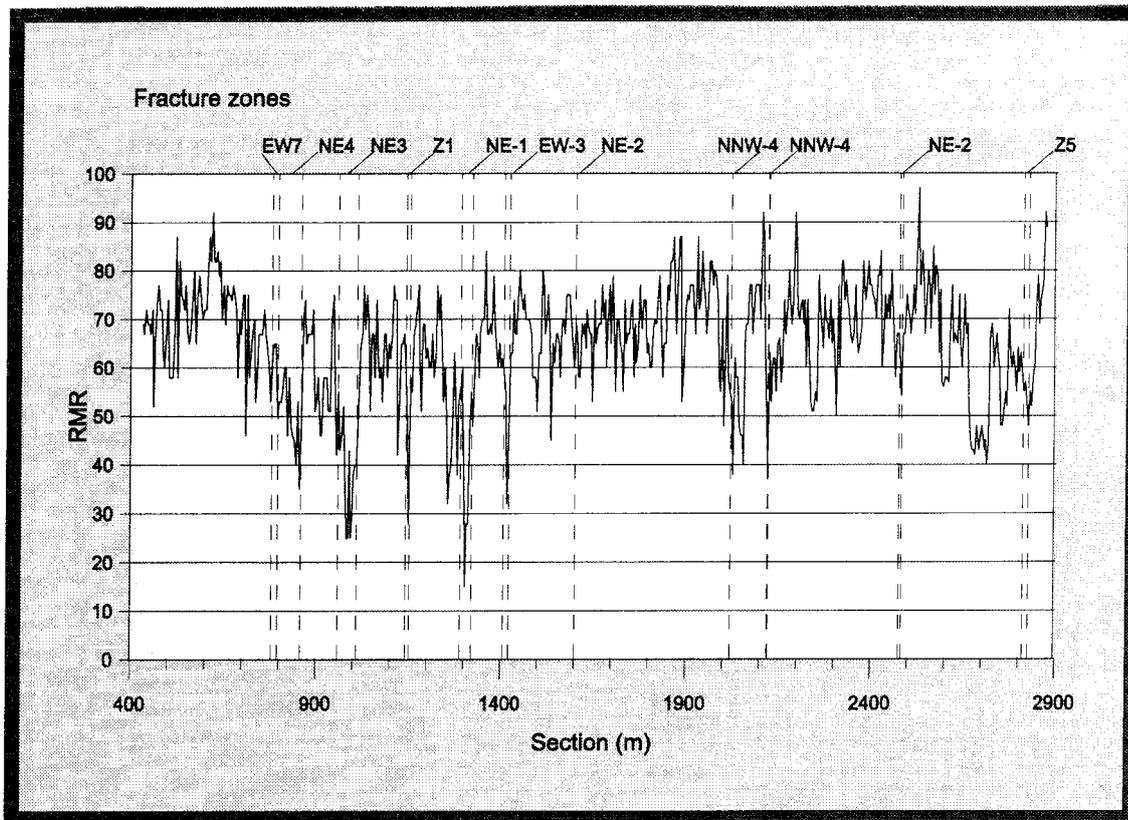
Figure 1-3. Observed RMR values along the tunnel /Stille-Olsson, 1996/.

Rock quality model on the (50-m) block scale

Comparisons between prediction and outcome concerning rock quality in six 50-m blocks with fixed coordinates (±25 m) along the tunnel are presented in *Figures 1-4 and 1-5.*

The predicted values and outcomes for the three 50-m blocks, P50-01 to P50-03, are presented in *Figure 1-4.*

In the prediction three minor fracture zones were forecast to intersect P50-01. In the tunnel increased fracturing was found along a 40-m long section of fine-grained granite. There is therefore also a big difference between the predicted distribution of rock quality and the outcome. It was estimated that 20 % of the rock would consist of rock of quality D or E while the outcome was almost 60 %.

There is a rather good correlation between predicted and documented rock quality in P50-02 and -03. In both blocks 100 % of the rock was documented as quality A, B or C. A domination of the observed rock classes was also predicted. It was, however, also predicted that Class D rock would represent 20 % in P50-02 and 10 % in P50-03. The discrepancy regarding Class D rock

Figure 1-4. Comparison between prediction and outcome on the (50-m) block scale. Rock quality models P50-01 to P50-03.

Äspö Hard Rock Laboratory

Predictions and Outcome of Models on the Block Scale (50 m)   Rock Quality - Rock stress

Rock Block P 50-01 0/950-1/000 ±25

Rock Quality (RMR)	Prediction					Outcome				
	Class	A	B	C	D	E	Class	A	B	C	D	E
	Class	A	B	C	D	E	Class	A	B	C	D	E
	%	5	35	40	10	10	%	8	17	17	-	58

Rock Stress Magnitude [MPa]	Vertical stress	Max hor. stress	Min hor. stress	Vertical stress	Max hor. stress	Min hor. stress
	$\sigma_v = 3.8$	$\sigma_{H,max} = 6.4$-7.6	$\sigma_{H,min} = 4.2$-5.7	$\sigma_{v, meas.} = 2.4$	$\sigma_{H,max} = 8.0$	$\sigma_{H,min} = 5.3$
Orientation		N30° W ±15	N60° E ±15		N53° W	N37° E

Rock Block P 50-02 1/010-1/060 ±25

Rock Quality (RMR)	Prediction					Outcome				
	Class	A	B	C	D	E	Class	A	B	C	D	E
	%	25	35	20	20	-	%	16	42	42	-	-

Rock Stress Magnitude [MPa]	Vertical stress	Max hor. stress	Min hor. stress	Vertical stress	Max hor. stress	Min hor. stress
	$\sigma_v = 3.8$	$\sigma_{H,max} = 6.4$-7.6	$\sigma_{H,min} = 4.2$-5.7	$\sigma_{v, meas.} = 4.5$	$\sigma_{H,max} = 14.9$	$\sigma_{H,min} = 7.2$
Orientation		N30° W ±15	N60° E ±15		N63° W	N27° E

Rock Block P 50-03 1/170-1/220 ±25

Rock Quality (RMR)	Prediction					Outcome				
	Class	A	B	C	D	E	Class	A	B	C	D	E
	%	30	40	20	10	-	%	8	50	42	-	-

Rock Stress Magnitude [MPa]	Vertical stress	Max hor. stress	Min hor. stress	Vertical stress	Max hor. stress	Min hor. stress
	$\sigma_v = 4.3$	$\sigma_{H,max} = 7.4$-8.7	$\sigma_{H,min} = 4.8$-6.5	$\sigma_{v, meas.} = 9.3$	$\sigma_{H,max} = 13.1$	$\sigma_{H,min} = 10.7$
Orientation		N30° W ±15	N60° E ±15		N76° W	N14° E

Äspö Hard Rock Laboratory											RS_MEC50-02-1 960321
Predictions and Outcome of Models on the Block Scale (50 m)										Rock Quality - Rock stress	

Rock Block P 50-04 1/570-1/620 ±25			Prediction						Outcome		
Rock Quality (RMR)	Class	A	B	C	D	E	Class	A	B	C	D	E
	%	-	20	50	20	10	%	23	69	8	-	-
Rock Stress	Vertical stress	Max hor. stress		Min hor. stress			Vertical stress	Max hor. stress		Min hor. stress		
Magnitude [MPa]	σ_v=5.9	$\sigma_{H,max}$=8.9-11.3		$\sigma_{H,min}$=4.1-5.9			$\sigma_{v,meas.}$=7.2	$\sigma_{H,max}$=13.3		$\sigma_{H,min}$=6.8		
Orientation		N25° W ±15		N65° E ±15				N56° W		N34° E		

Rock Block P 50-05 2/422-2/472 ± 25			Prediction						Outcome		
Rock Quality (RMR)	Class	A	B	C	D	E	Class	A	B	C	D	E
	%	20	50	20	10	-	%	59	33	8	0	0
Rock Stress	Vertical stress	Max hor. stress		Min hor. stress			Vertical stress	Max hor. stress		Min hor. stress		
Magnitude [MPa]	σ_v= Z(m)*0.0265	$\sigma_{H,max}$=1.2-1.7*σ_v		$\sigma_{H,min}$=0.5-0.8*σ_v			No Data					
Orientation		N35° W ±15		N55° E ±15								

Rock Block P 50-06 2/752-2/802 ± 25			Prediction						Outcome		
Rock Quality (RMR)	Class	A	B	C	D	E	Class	A	B	C	D	E
	%	30	40	20	10	-	%	0	33	67	0	0
Rock Stress	Vertical stress	Max hor. stress		Min hor. stress			Vertical stress	Max hor. stress		Min hor. stress		
Magnitude [MPa]	σ_v= Z(m)*0.0265	$\sigma_{H,max}$=1.2-1.7*σ_v		$\sigma_{H,min}$=0.5-0.8*σ_v			No Data					
Orientation		N35° W ±15		N55° E ±15								

is explained by a better rock quality in fine-grained granite and greenstone than had been predicted.

The predicted values and outcome for P50-04 are presented in *Figure 1-5*.

P50-04 was forecast to comprise greenstone to a large extent. The outcome also proved that greenstone is the dominating rock type in the block. The greenstone is, however, often mixed with other rock types like diorite.

It was predicted that 90 % of the rock would be of Class C or poorer quality. The outcome, however, proved that only 8 % was of Class C while Class D and E were not found in the block.

The poor correlation between the prediction and outcome is explained by a generally better quality of greenstone than was expected, although the fracture density proved to be higher than predicted. As will be seen in *Chapter 5*, the greenstone proved to be somewhat more fractured than predicted.

The mixing with diorite also affected the observed quality of the greenstone and possibly increased its quality.

The predicted values outcome and absolute error (AE) for P50-05 and P50-06 are presented in *Figure 1-5* and *Tables 1-2 and 1-3*.

P50-05

In P50-05 the outcome exhibited higher rock qualities than predicted.

Table 1-2. RMR classification in blocks, prediction and outcome in P50-05.

RMR class	Prediction %	Outcome %	Difference %
Class A	20	59	39
Class B	50	33	17
Class C	20	8	12
Class D	10	0	10
Class E	0	0	0

As mentioned before, the Småland (Ävrö) granite and Äspö diorite have in general proved to be more competent than was predicted.

The deviation in Class D is related to a better rock quality of greenstone than predicted. Greenstone was also found in general to be more competent than anticipated. The limited extent of the greenstone and the mixing with adjacent rock types, here diorite, may have been favourable for the rock quality.

P50-06

In P50-06 the outcome showed lower rock qualities than predicted.

Table 1-3. RMR classification in blocks, prediction and outcome in P50-06.

RMR class	Prediction %	Outcome %	Difference %
Class A	30	0	30
Class B	40	33	13
Class C	20	67	47
Class D	10	0	10
Class E	0	0	0

The RMR values in P50-06 were reduced locally by rather unfavourable water conditions and joint orientations. These local conditions were not expected and are very difficult, or even impossible, to predict on the 50-m scale. The conditions observed are considered to be within the natural variations in the rock mass. However, here both water conditions and joint orientations did coincide to reduce the rock quality according to the RMR classification.

1.4   SCRUTINY AND EVALUATION

In summary, the predicted RMR values for the tunnel show acceptable correlation with the observations made in the tunnel.

The portion of poor rock will have a considerable influence on cost and time factors for the tunnelling work. It is therefore desirable that the prediction of poor rock show a reasonably good correspondence with the outcome. For the Äspö tunnel poor rock (with an RMR value below 40) was predicted to 8 % while the outcome was 4 % /Table 1-1/. When establishing a prediction of rock quality a rock classification system is commonly applied to core samples. General experience shows that the prediction will be somewhat conservative, i.e. lower RMR values will be predicted than will actually be found in the tunnel.

Experience from the Äspö tunnel shows that the rock quality correlates with the rock type. Fine-grained granite, which is often fractured shows both significantly lower mean RMR values and larger variations. The differences between greenstone, Småland (Ävrö) granite and Äspö diorite are smaller and show smaller variations.

The prediction on the site scale proved to show good correlation with the outcome. On the block scale the correspondence is lower and even a small deviation from the predicted rock type will influence the rock quality.

2 SUBJECT: ROCK STRESS

2.1 SCOPE AND CONCEPTS

Rock stress conditions are an important factor for the mechanical stability in an underground opening. Rock stress conditions also affect hydraulic paths in the area. Changes in rock stress conditions may also release future movements in existing fracture zones.

A lot of experience in the measurement of stress orientations and magnitudes has been gained from other projects. If it can be confirmed that the rock stress conditions at a new site conform to general behaviour, then experience from other sites can be applied. General behaviour is taken to mean, for example, that a factor can be found between the depth and the magnitude of the rock stress.

Since the rock stress conditions in Sweden are often favourable for underground construction work, one of the main objectives of determining rock stress conditions is to verify that the present stress levels are within the normal range in relation to experience from other Swedish underground construction works.

For the site-scale and block-scale the rock stresses were estimated as the average rock stress condition to be anticipated within a rock volume of site or block size. For the detailed scale the rock stress conditions were estimated for individual readings in core holes within the rock mass.

On the block scale, it is important to ascertain variations in rock stress conditions. Variations in rock stresses on the block scale will determine the potential rock burst and stability problems due to low stresses, for example, and provide data for quantitative stability modelling of underground facilities.

Variations in rock stresses on the detailed scale will provide information on local variations in different stability aspects. However, there is still a lot of research to be carried out on the local variations of rock stresses on the detailed scale.

2.2 METHODOLOGY FOR TESTS OF CONCEPTS AND MODELS

The methods used for rock stress measurements are presented briefly below.

2.2.1 Prediction methodology

During the site investigation phase, stress measurements were made in surface boreholes KAS02, KAS03 and KAS05 /Figure 2-1/, /Stille-Olsson, 1990/. KAS02 and KAS05 were drilled almost vertical, within and below the rock volume later enveloped by the ramp loops. KAS03 is also nearly vertical, but located some 500 m to the north-west of the ramp area. The surface borehole measurements employed both hydraulic fracturing and overcoring techniques. Hydraulic fracturing was used in holes KAS02 and KAS03, and provided a total of 41 point measurements, distributed over depths down to about 950 m. In brief, hydraulic fracturing is a two-dimensional method that provides information on stress conditions in the plane perpendicular to the borehole (i.e. in this case horizontal stress components).

In KAS05, an early version of the three-dimensional deep-hole overcoring method developed by Vattenfall was used. A total of 7 tests were reported from the overcoring work. Three points were located at a depth of 195 metres and the remaining four at about 355 metres.
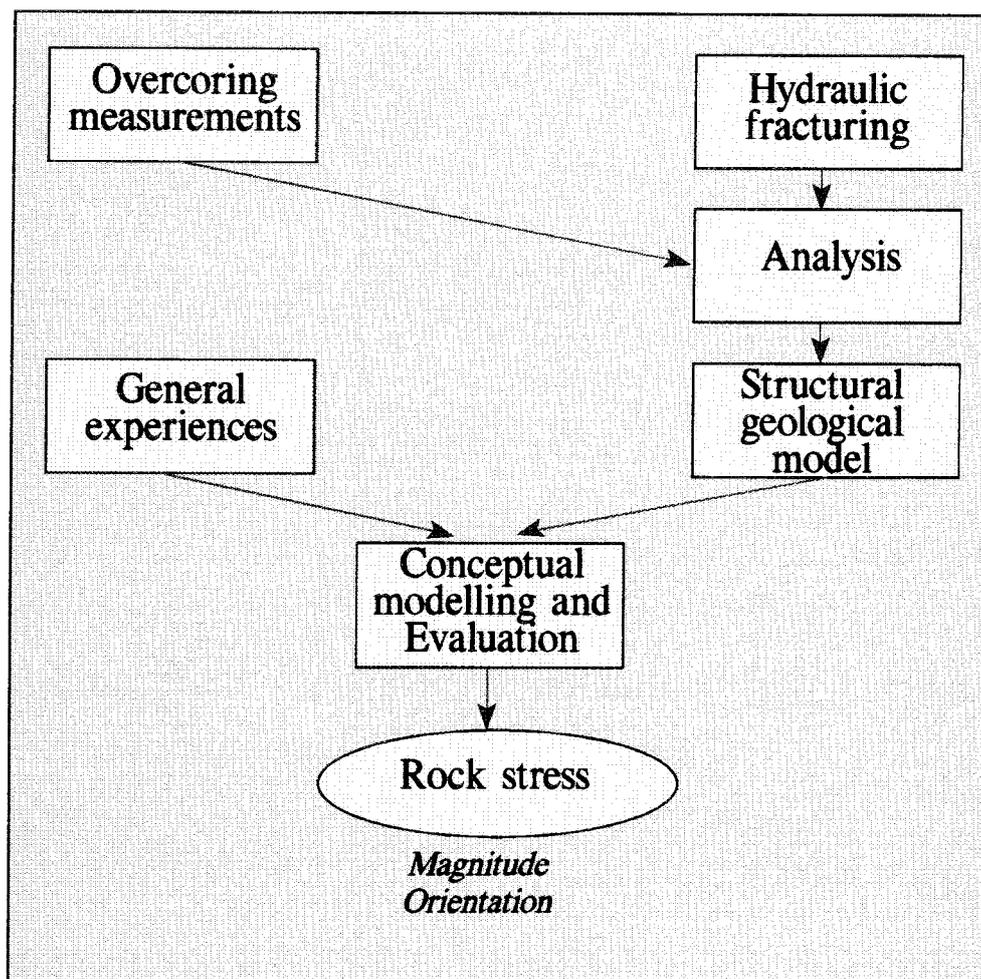
Figure 2-1. Flow chart of the rock stress investigations.

2.2.2 Methodology for determining outcome

Concurrent with the excavation of the access ramp, overcoring measurements were made in a series of 12 to 18 metre long, near-horizontal boreholes drilled from suitable locations along the ramp. The main objective was to evaluate predictions made prior to excavation. An additional objective was to provide background data required to establish stress conditions on a site scale.

Starting at a depth of 143 m, measurements were made in a total of 11 boreholes, representing 8 locations along the ramp, the deepest being at 408 metres. Two measurement locations are located in the first, straight part of the ramp. The remainder are distributed along the spiral part /Leijon, 1995/.

The procedure at each measurement location was basically to:

1   drill a sub-horizontal hole (in some cases more than one hole) 5 to 20 metres out from the drift to avoid unacceptable influence due to the presence of the excavation itself.

2   conduct repeated three-dimensional overcoring tests along the hole.

Four to seven successful tests were chosen at each location, to provide some grasp on data consistency and allow meaningful averaging procedures. All ramp overcoring work was done by the same crew, using the same instrumentation (the CSIRO Hollow inclusion) and, to the extent possible, consistent experimental routines.

2.3   COMPARISON OF PREDICTED AND MEASURED ENTITIES

Based on the rock stress measurements made in deep surface boreholes a prediction was established for the magnitude and orientation of maximum and minimum horizontal stresses. The magnitude of the vertical stress was also estimated. The predicted stresses were expressed as a factor of the theoretical vertical stress, also called K_0, to eliminate any depth dependency.

For the prediction of the documented rock stresses the mean value of K_0 and orientation for the three boreholes drilled from ground level were calculated and used as a characteristic value for the 500-m site scale.

For the evaluation the mean values of measurements made from the tunnel were used.

Comparisons between rock stress predictions and outcomes are presented by Olsson-Stille in Stanfors et al /1992, 1993 and 1994/ on the site scale in Figure 1-2 (Subject: Rock quality).

For the interpretation of the measured rock stresses in the 50-m blocks in the tunnel the mean value of the three readings in every borehole was used as the characteristic value for each 50-m block. The stress magnitudes and orientations were presented in the prediction as ranges. The ranges for the magnitudes were based on the results of the measurements in the pre-investigation phase, while the orientations were expressed as a value plus or minus 15°, i.e. as a range of 30° (see *Figure 1-4* and *Figure 1-5 (Subject: Rock quality))*.

The predicted rock stress magnitude and orientation in P50-01 correspond rather well to the measured values. The measured horizontal stresses are 5 % outside the predicted range and 8 degrees outside the predicted orientation range. The observed vertical stress is 37 % lower than the predicted value.

The discrepancy between the prediction and outcome for the horizontal stresses in P50-01 is judged to be of the same order as the accuracy of the measurements.

There is a big difference between the predicted and measured rock stress levels in P50-02. Measured stresses are up to twice as big as the predicted stresses. The biggest difference was found for the maximum horizontal stress, where the observed value is 95 % higher than the prediction.

For the interpretation of the measured rock stresses in P50-04 the mean value of the three measured boreholes was used. The outcome gives a higher stress level than was predicted. Measured values for horizontal and vertical stresses are approximately 20 % higher than predicted. The discrepancy is believed to be of the same order as the accuracy of the measurements and will not have any practical influence on the stability conditions.

No rock stress measurements were made in rock blocks P50-05 and P50-06.

2.4 SCRUTINY AND EVALUATION

The rock stress situation around a tunnel is important for the general stability condition and will have an influence on the demand for rock support. It is important to identify both the rock stress orientation and magnitude before a final layout and design of larger underground openings are made.

One prerequisite for creating a stable roof is that the relationship between the maximum horizontal stress and the theoretical vertical stress, K_o, be greater than 1. The magnitude of the rock stresses is also important for prediction of potential rock burst.

The relationship between the maximum horizontal stress and the theoretical vertical stress, K_o, was estimated prior to the excavation to be in the range of 1.7. According to the measurements made this value was estimated to be typical for the section between 300 m and 500 m below the surface */Stille-Olsson, 1990/*.

In the tunnel wall rock stress measurements were made in 11 different boreholes. The measurements verify a dominating NW-SE orientation, which corresponds to the prediction.

The measurements made in the tunnel wall showed a considerably higher stress level than was anticipated. The estimated mean value of K_0 for all boreholes is 2.9, with the average for individual boreholes ranging between 1.7 and 4.0. Single measurements in the individual boreholes varied between 1.5 and 4.0. The values of K_0 at different depths are presented in *Figure 2-2*.

Figure 2-3 shows the maximum horizontal stress component measured att different depths for both the prediction and outcome.

Figure 2-4 shows the relationship between the highest horizontal stress and the lowest horizontal stress for the same measurements as in the figure above.
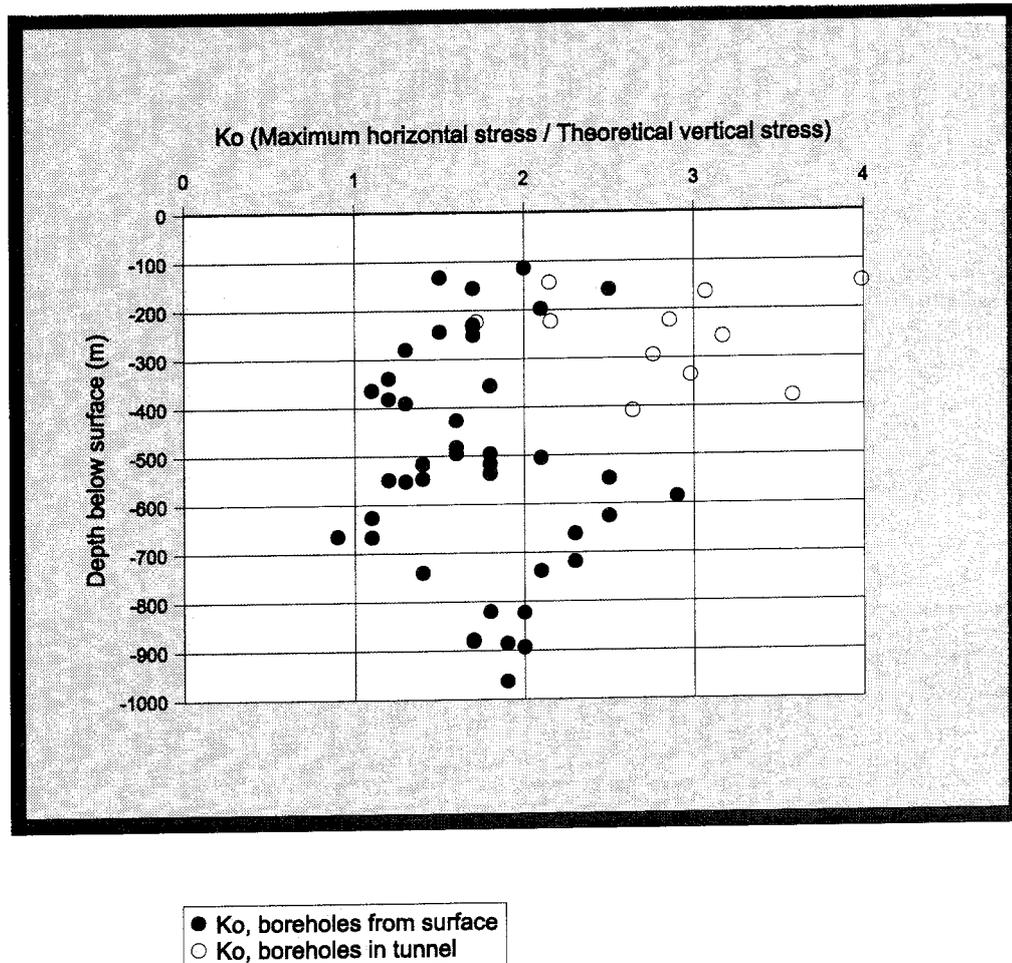
Figure 2-2. Values of K_0 at different depths /Stille-Olsson, 1996/.
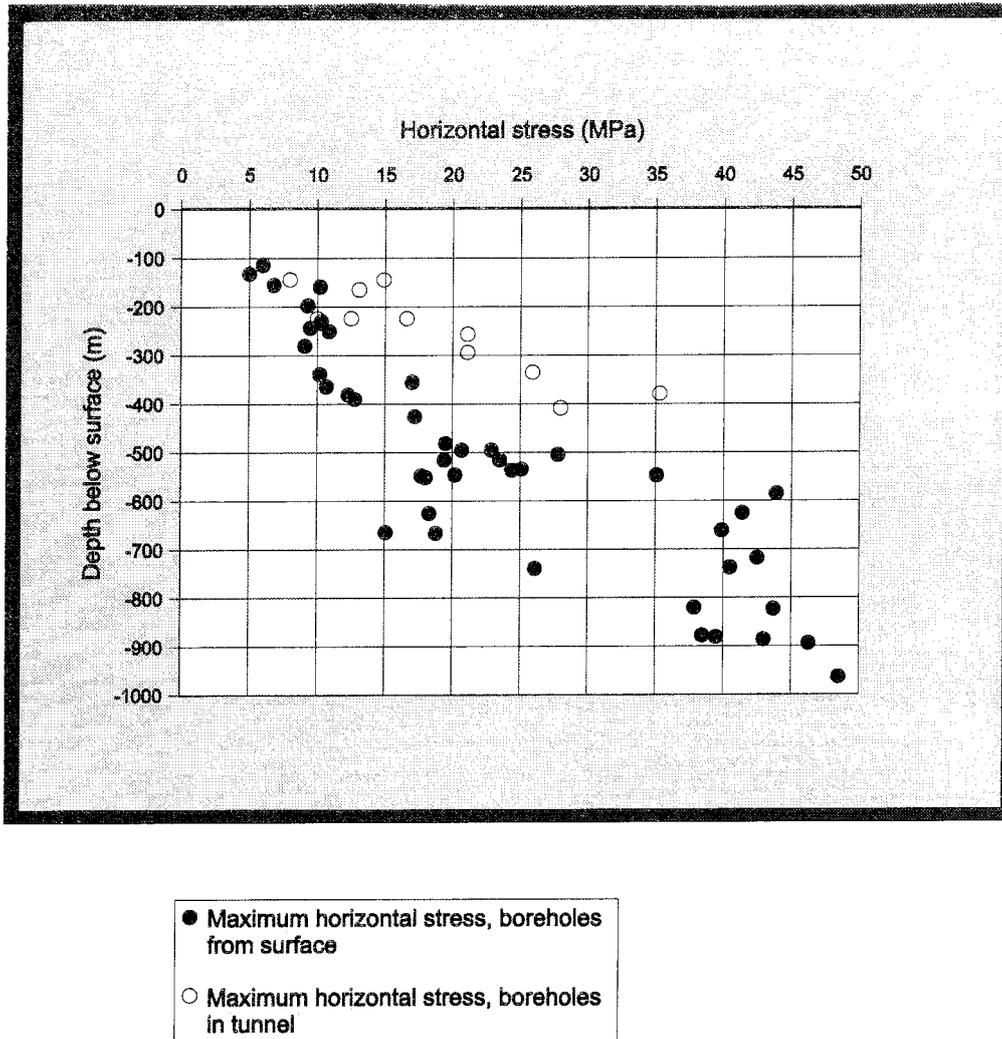
Figure 2-3. Measured maximum horizontal stress /Stille-Olsson, 1996/.

The difference between rock stress measurements made from the surface and in the tunnel wall can not be explained by geometrical factors, such as the fact that the measurements in the tunnel were made to close to the tunnel.

Some differences are possibly due to natural variations in the rock mass.

It is, however, likely that a large portion of the differences is due to the two different methods used to make the measurements, i.e. overcoring and hydraulic fracturing. A brief survey of all measurements shows that the hydraulic fracturing provides significantly lower stress levels. In the pre-investigation phase the majority of the measurements were made by hydraulic fracturing while overcoring was used for all measurements made in the tunnel.

A comprehensive analysis of the rock stress conditions at Äspö is needed to give a clear explanation of the significant difference between the rock stress magnitude measured from the surface and from the tunnel. It is recommended that such a study be made.
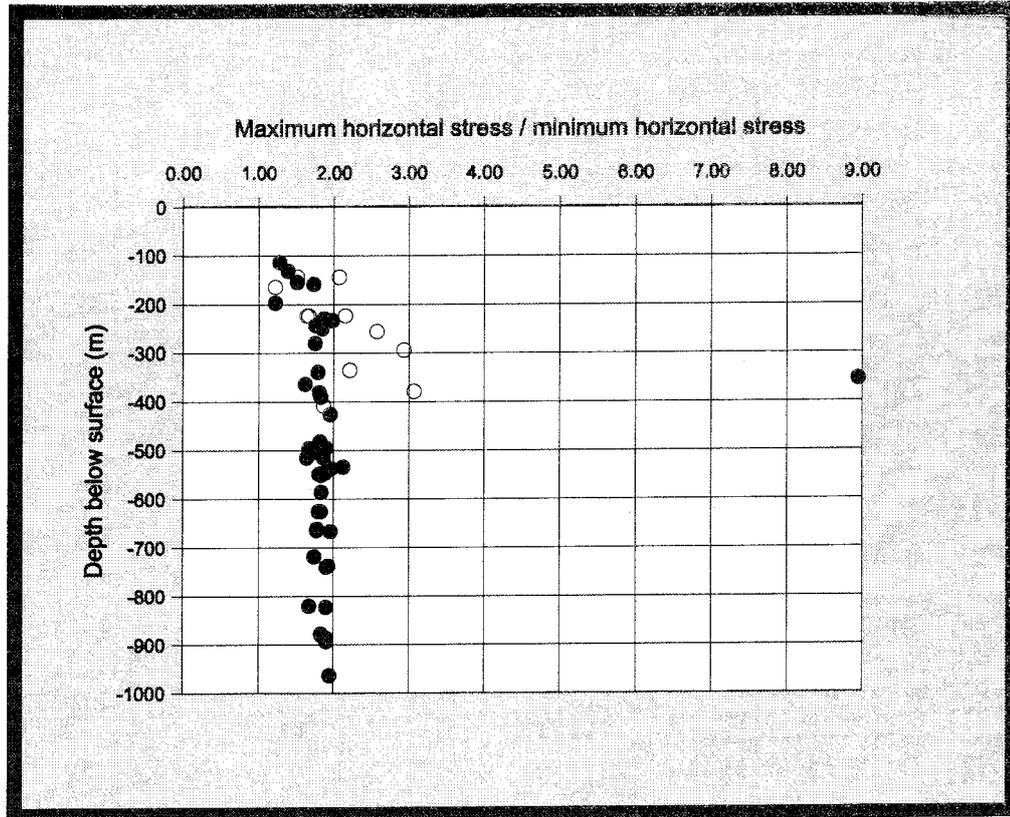
Figure 2-4. Ratio between the highest and lowest horizontal stress /Stille-Olsson, 1996/.

3   SUBJECT: MECHANICAL CHARACTERISTICS. FRACTURE SURFACE PROPERTIES

3.1   SCOPE AND CONCEPTS

To analyse stability conditions on the block and detailed scale, the mechanical characteristics of the rock must be investigated. The mechanical characteristics predicted prior to the excavation were rock strength, elastic moduli, Poisson's ratio and brittleness ratio /Stille et al, 1989/.

In rock conditions dominated by hard rock, investigations to determine mechanical characteristics should be concentrated to defining a range or approximate values of the parameters of interest.

The fracture surface properties predicted prior to the excavation were joint roughness coefficient (JRC) and joint compressive strength (JCS) /Stille et al, 1989/. These values constitute important information for quantification of stability conditions in different rock types.

3.2   METHODOLOGY FOR TESTS OF CONCEPTS AND MODELS

The different methods used for mechanical characteristics definition and investigation of fracture surface properties are briefly presented below.

3.2.1   Prediction methodology

Unconfined compressive test

The mechanical characteristics were defined by uniaxial compressive tests on core samples. The cores used for the testing were all taken from one single borehole, KAS02. The specimens were prepared before testing was performed. The compressive tests were carried out in a press with very high stiffness. The high stiffness was necessary to detect deformations during failure, which determined the brittleness ratio /Brown, 1981/ (see /Figure 3-1 and 3-2/).

Empirical references

The mechanical behaviour of Scandinavian rock types is in general fairly well known. Comprehensive documentation has been accumulated over the years and a considerable body of experience is available.

With general information on the conceptual geological model and what rock types are present an initial prediction of mechanical behaviour can be made based on experience from other projects.
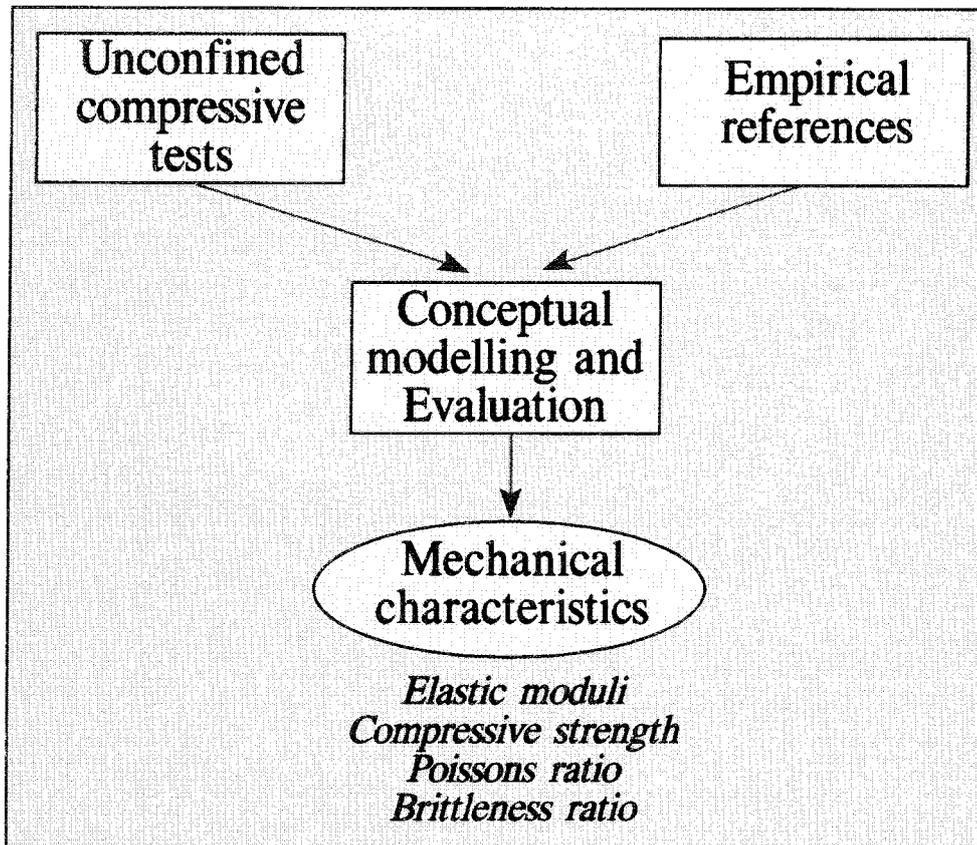
Figure 3-1. Flow chart of the mechanical characteristics programme.

Laboratory testing – shear testing

The joint roughness coefficient was determined by laboratory shear testing. Existing joints were sheared after being grouted into a steel cylinder. Shearing was performed several times with different normal loads (see *Figure 3-2*).

Graphical references

The JRC values were also determined by comparing fractures with graphical references in well established textbooks */Brown, 1981/.*

Empirical characterization

To determine the joint compressive strength, empirical relations between JCS values and JRC values were used /Brown, 1981/. The JCS values were determined by applying the empirical relations to the JRC values established by the shear testing performed and graphical determination.
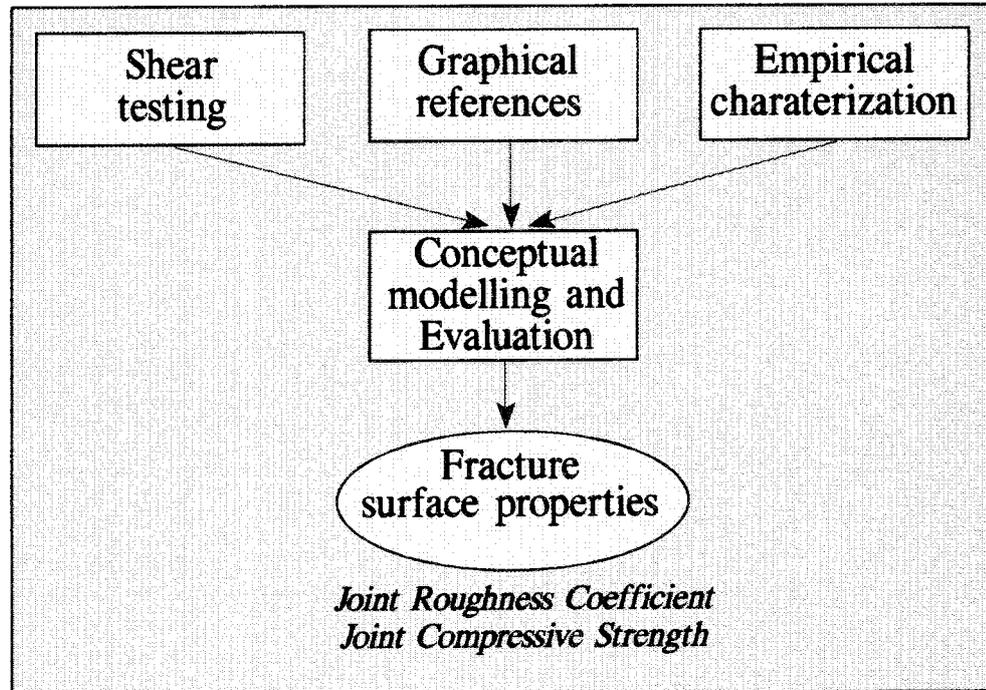
Figure 3-2. Flow chart for the fracture surface investigations.

3.2.2   Methodology for determining outcome

During the excavation period cores were drilled and selected from the tunnel for laboratory testing. Similar testing had been carried out during the prediction phase. A total of ten tests was generally made for each parameter and rock type. For fine-grained granite only nine tests were performed. The cores for each rock type were selected from 2-8 different boreholes, mainly located in the first 1500 metres of the tunnel. The testing of joint surface parameters has not, however, been done and is not further discussed here.

The reason for this is that the testing and evaluation performed in the prediction phase were found too limited to be representative of the fracture surface properties. A complete study and analysis of fracture surface properties must comprise a larger amount of fractures, representing different rock types and also all present fracture sets. This was not considered during the pre-investigations phase when the predictions were established.

3.3 COMPARISON OF PREDICTED AND MEASURED ENTITIES

3.3.1 Mechanical characteristics

The predictions of mechanical characteristics were based on laboratory testing of samples from the deep core boreholes /Stille and Olsson, 1989/. Between four and six samples were tested for each of the rock types present.

The prediction and outcome of mechanical characteristics are presented in Table 3-1.

Rock strength and elastic moduli

The estimated rock strengths correspond rather well to the outcome for Äspö diorite and fine-grained granite. The discrepancy for Småland (Ävrö) granite is to some extent exaggerated by the sub-division selected for the prediction. In the prediction the measured mean value of the rock strength was 189 MPa compared with the outcome of 255 MPa. A mean value of 189 MPa is just below the interval 100-200 MPa which was used in the prediction. 90% of the rock was therefore predicted to be within the interval 100-200 MPa. The outcome proved that the rock strength in general was greater than 200 MPa with a mean value of 255 MPa. This means that most observed values were outside the interval 100-200 MPa. If the sub-division had been made with a interval of 150-250 MPa, the correlation between the prediction and the outcome would have been much better.

The estimated elastic moduli correspond rather well to the outcome except in the case of greenstone. The discrepancy for Äspö diorite is exaggerated by the sub-division of values. In the prediction the measured mean value was 60 GPa compared with an outcome of 73 GPa.

The predicted rock strength and elastic moduli for greenstone proved to be underestimated compared with the outcome. It seems likely that the fact that the predictions were based on solely four tested samples influenced the rather poor correlation between prediction and outcome. It also seems that the mechanical characteristics of greenstone vary significantly between different samples.

Poisson's ratio

The predicted values of Poisson's ratio correspond to the outcome rather well.

Table 3-1. Laboratory testing of mechanical parameters. From /Stille, Olsson, 1996/.

Unconfined compressive strength (MPa)	Greenstone (Mpa)	Fine-grained granite (Mpa)	Äspö diorite (Mpa)	Småland (Ävrö) granite (Mpa)
Prediction				
-mean	119	236	184	189
-range	103-168	152-336	164-217	147-260
No. of tests	4	4	4	4
Outcome				
-mean	207	258	171	255
-range	121-274	103-329	103-210	197-275
No. of tests	10	9	10	10
Young's modulus (GPa)	**(GPa)**	**(GPa)**	**(GPa)**	**(GPa)**
Prediction				
-mean	53	65	60	62
-range	32-74	59-70	54-65	62-63
No. of tests	4	4	4	4
Outcome				
-mean	78	77	73	74
-range	71-96	72-80	65-80	63-79
No. of tests	10	9	10	10
Poisson´s ratio	**(-)**	**(-)**	**(-)**	**(-)**
Prediction				
-mean	0.25	0.22	0.23	0.24
-range	0.24-0.26	0.20-0.22	0.20-0.25	0.24
No. of tests	4	4	4	4
Outcome				
-mean	0.24	0.23	0.24	0.23
-range	0.18-0.31	0.21-0.25	0.22-0.29	0.20-0.26
No. of tests	10	9	10	10
Brittleness				
Prediction				
-	more brittle	less brittle	brittle	brittle
No. of tests	4	4	4	4
Outcome				
-	brittle	more brittle	more brittle	more brittle
No. of tests	10	9	10	10

Brittleness

Brittleness is difficult to measure and the methods for test evaluation of the testing have not been fully developed. To determine the brittleness a press with very high stiffness were used for testing the compressive strength. By registering and analysing the deformations during the failure, the brittleness ratio can be determined for a sample. The degree of brittleness was described for each sample as brittle, or not brittle. The interest in brittleness is related to the possibility of predicting rock burst. Brittleness is one of a number of factors that will determine the risk for rock burst.

It was predicted that all rock types would show some brittleness. The lowest intensity was predicted for fine-grained granite while the highest intensity was predicted for greenstone.

The outcome proved that all rock types exhibited a brittle behaviour which corresponds well to the prediction.

However, the intensity of the brittleness did not correspond to the prediction. Greenstone exhibited a lower degree of brittleness than all the other rock types. Fine-grained granite, Äspö diorite and Småland (Ävrö) granite all exhibited the same degree of brittleness.

3.3.2 Fracture properties

Fracture surface property prediction was based on laboratory tests on a few samples and on the general geological descriptions and roughness measurements of fractures and their fillings in respective rock types /*Stille and Olsson, 1989/*. The laboratory testing comprised shear tests on six steep and six gently dipping fractures.

The fracture frequency and fracture density predictions were based on information from several core holes, surface mapping and general experience of the rock types present.

The fracture property prediction and outcome are presented in *Figures 3-3* to *3-6*.

Figure 3-3. *Predictions and outcomes of models of mechanical characteristics. Rock block P5-01.*

Äspö Hard Rock Laboratory

Models on the Detailed Scale (5m) in Rock Block P 50-01 — Mechanical Stability

Småland (Avrö) Granite
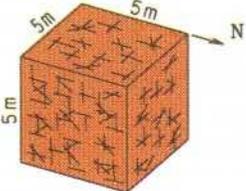
P 5-01

	Predictions					Outcome				
Rock Strength [MPa]	>200 25%	100-200 75%	<100 -			>200 90%	100-200 10%	<100 -		
Elastic Moduli [GPa]	>60 90%	50-60 10%	<50 -			>60 100%	50-60 -	<50 -		
Poisson's Ratio	>0.25 10%	0.20-0.25 90%	<0.20 -			>0.25 10%	0.20-0.25 90%	<0.20 -		
Brittleness	Wu/Wk > 1 25%		Wu/Wk < 1 75%			Wu/Wk > 1 10%		Wu/Wk < 1 90%		
Joint Roughness Coefficient (JRC)	>14 60%	14-6 30%	< 6 10%			>14 -	14-6 33%	< 6 67%		
Joint Wall Compression Strength (JCS) [MPa]	>75 60%	75-40 30%	<40 10%			Not measured				
Fracture Frequency [m]	1-3 20%	0.3-1 60%	<0.3 20%			>2 14%	0.6-2.0 32%	0.2-0.6 36%	<0.2 18%	
Fracture Density (RQD)	90-100 40%	75-90 40%	50-75 20%			90-100 9%	75-90 27%	50-75 27%	25-50 27%	< 25 9%

Rock Stress	Vertic.stress	Max hor. stress	Min hor. stress	Vertic.stress	Max hor. stress	Min hor. stress
Magnitude [MPa]	$\sigma_v = Z(m)*0.0265$	1.1-2.1* σ_v 100% 1.3-1.8* σ_v 70%	0.6-1.6* σ_v 100% 0.7-1.1* σ_v 70%	0.5-2.2* σ_v	2.0-4.0* σ_v 100% 2.1-3.9* σ_v 70%	1.3-2.7* σ_v 100% 1.4-2.1* σ_v 70%
Orientation		N12° W-N68° W 100% N25° W-N55° W 70%	N22° E-N78° E 100% N35° E-N65° E 70%		N38° W-N126° W 100% N48° W-N113° W 70%	N36° W-N52° W 100% N23° W-N42° W 70%

960321

Äspö Hard Rock Laboratory

| Models on the Detailed Scale (5m) in Rock Block P 50-03 | Mechanical Stability |
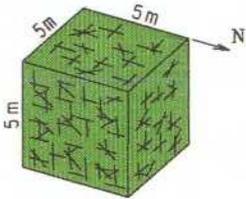
Äspö Diorite   5m   5m   N   5 m   P 5-02

	Predictions			Outcome				
Rock Strength [MPa]	>200 -	100-200 100%	<100 -	>200 10%	100-200 90%	<100 -		
Elastic Moduli [GPa]	>60 50%	50-60 50%	<50 -	>60 100%	50-60 -	<50 -		
Poisson's Ratio	>0.25 10%	0.20-0.25 80%	<0.20 10%	>0.25 20%	0.20-0.25 80%	<0.20 -		
Brittleness	Wu/Wk > 1 25%	Wu/Wk < 1 75%		Wu/Wk > 1 22%	Wu/Wk < 1 78%			
Joint Roughness Coefficient (JRC)	>14 60%	14-6 30%	<6 10%	>14 -	14-6 82%	<6 18%		
Joint Wall Compression Strength (JCS) [MPa]	>75 60%	75-40 30%	<40 10%	>150 70%	75-150 30%	<75 -		
Fracture Frequency [m]	1-3 20%	0.3-1 50%	<0.3 30%	>2 22%	0.6-2.0 28%	0.2-0.6 22%	<0.2 28%	
Fracture Density (RQD)	90-100 40%	75-90 40%	50-75 20%	90-100 33%	75-90 28%	50-75 17%	25-50 11%	<25 11%

Rock Stress	Vertic.stress	Max hor. stress	Min hor. stress	Vertic.stress	Max hor. stress	Min hor. stress
Magnitude [MPa]	$\sigma_v = Z(m)*0.0265$	1.1-2.1* σ_v 100% 1.3-1.8* σ_v 70%	0.6-1.6* σ_v 100% 0.7-1.1* σ_v 70%	0.5-2.2* σ_v	2.0-4.0* σ_v 100% 2.1-3.9* σ_v 70%	1.3-2.7* σ_v 100% 1.4-2.1* σ_v 70%
Orientation		N12°W-N68°W 100% N25°W-N55°W 70%	N22°E-N78°E 100% N35°E-N65°E 70%		N38°W-N126°W 100% N48°W-N113°W 70%	N36°W-N52°W 100% N23°W-N42°W 70%

930303

Figure 3-4. Predictions and outcomes of models of mechanical characteristics. Rock block P5-02.

Figure 3-5. *Predictions and outcomes of models of mechanical characteristics. Rock block P5-03.*

Äspö Hard Rock Laboratory

| Models on the Detailed Scale (5m) in Rock Block P 50-04 | | | | | | Mechanical Stability |

Greenstone
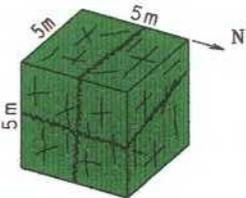
NOTE: Outcome is evaluated for all mapped tunnel fronts in section 1/597-1/684 where greenstone represents more than 50% of the present rock types

P 5-03

	Predictions			Outcome				
Rock Strength [MPa]	>200 –	100-200 75%	<100 25%	>200 60%	100-200 40%	<100 –		
Elastic Moduli [GPa]	>60 25%	50-60 50%	<50 25%	>60 100%	50-60 –	<50 –		
Poisson's Ratio	>0.25 10%	0.20-0.25 80%	<0.20 10%	>0.25 30%	0.20-0.25 60%	<0.20 10%		
Brittleness	Wu/Wk > 1 40%		Wu/Wk < 1 60%	Wu/Wk > 1 50%		Wu/Wk < 1 50%		
Joint Roughness Coefficient (JRC)	>14 30%	14-6 50%	< 6 20%	>14 6%	14-6 81%	< 6 13%		
Joint Wall Compression Strength (JCS) [MPa]	>75 30%	75-40 50%	<40 20%	>75 26%	75-40 14%	<40 –		
Fracture Frequency [m]	1-3 20%	0.3-1 60%	<0.3 20%	>2 –	0.6-2 31%	0.2-0.6 61%	0.05-0.2 8%	<0.05 –
Fracture Density (RQD)	90-100 % 20%	75-90 % 50%	50-75 % 30%	90-100 % –	75-90 % 53%	50-75 % 31%	25-50 % 8%	< 25 % 8%

Rock Stress	Vertic.stress	Max hor. stress	Min hor. stress	Vertic.stress	Max hor. stress	Min hor. stress
Magnitude [MPa]	$\sigma_v = Z*0.0265$	1.1-2.1* σ_v 100% 1.3-1.8* σ_v 70%	0.6-1.6* σ_v 100% 0.7-1.1* σ_v 70%	0.7-2.1* σ_v	1.5-3.3* σ_v 100% 1.8-2.9* σ_v 70%	0.5-2.4* σ_v 100% 0.9-1.8* σ_v 70%
Orientation		N12° W-N68° W 100% N25° W-N55° W 70%	N22° E-N78° E 100% N35° E-N65° E 70%		N40° W-N74° W 100% N47° W-N70° W 70%	N16° E-N50° E 100% N20° E-N48° E 70%

931101

Figure 3-6. *Predictions and outcomes of models of mechanical characteristics. Rock block P5-04.*

Äspö Hard Rock Laboratory

Models on the Detailed Scale (5m) in Rock Block P 50-01						Mechanical Stability
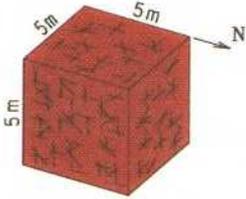
Fine-grained Granite   5m   5m   N   P 5-04

	Predictions			Outcome				
Rock Strength [MPa]	>200 50%	100-200 50%	<100 -	>200 78%	100-200 22%	<100 -		
Elastic Moduli [GPa]	>60 75%	50-60 25%	<50 -	>60 100%	50-60 -	<50 -		
Poisson's Ratio	>0.25 10%	0.20-0.25 80%	<0.20 10%	>0.25 -	0.20-0.25 100%	<0.20 -		
Brittleness	Wu/Wk >1 25%		Wu/Wk <1 75%	Wu/Wk >1 57%		Wu/Wk <1 43%		
Joint Roughness Coefficient (JRC)	>14 30%	14-6 50%	<6 20%	Not measured				
Joint Wall Compression Strength (JCS) [MPa]	>75 30%	75-40 50%	<40 20%	Not measured				
Fracture Frequency [m]	1-3 30%	0.3-1 50%	<0.3 20%	>2 -	0.6-2.0 -	0.2-0.6 17%	<0.2 83%	
Fracture Density (RQD)	90-100 30%	75-90 40%	50-75 30%	90-100 -	75-90 -	50-75 17%	25-50 33%	<25 50%

Rock Stress	Vertic.stress	Max hor. stress	Min hor. stress	Vertic.stress	Max hor. stress	Min hor. stress
Magnitude [MPa]	$\sigma_v = Z(m) \cdot 0.0265$	1.1-2.1* σ_v 100% 1.3-1.8* σ_v 70%	0.6-1.6* σ_v 100% 0.7-1.1* σ_v 70%	0.5-2.2* σ_v	2.0-4.0* σ_v 100% 2.1-3.9* σ_v 70%	1.3-2.7* σ_v 100% 1.4-2.1* σ_v 70%
Orientation		N12° W-N68° W 100% N25° W-N55° W 70%	N22° E-N78° E 100% N35° E-N65° E 70%		N38° W-N126° W 100% N48° W-N113° W 70%	N36° W-N52° W 100% N23° W-N42° W 70%

930302

3.4   SCRUTINY AND EVALUATION

3.4.1   Joint roughness coefficient and joint-wall compressive strength

The fracture surface properties were only documented in Äspö diorite (JRC and JCS), Småland (Ävrö) granite (JRC) and greenstone (JRC and JCS). The outcomes are quite different from the predictions. Fracture properties are important for the stability conditions. It has, however, proved to be very difficult to predict and measure these properties and establish reliable documentation.

The predictions were based on International Society of Rock Mechanics recommendations presented in 'Rock Characterization, Testing and Monitoring', /Brown, 1981/. Since the prediction was established further research work has indicated a size dependency in these factors and in general. A general down-grading has been found for the JRC and JCS. The result from Äspö must be further analysed and will provide input to improve recommendations for estimating fracture properties.

3.4.2   Fracture frequency and fracture density

The observed fracture frequencies show good agreement with the predictions for Äspö diorite and Småland (Ävrö) granite /Olsson-Stille in Stanfors et al 1992, 1993 and 1994/.

In the Äspö diorite 70 % of the fracture distances for the dominating fracture system were predicted to exceed 0.3 m while the outcome proved that 72 % exceeded 0.2 m. In the prediction 20 % were estimated to be between 1 and 3 m while the outcome showed that 22 % were more than 2 m.

The observed fracture density shows rather good agreement with the prediction for Äspö diorite. It was predicted that 80 % of the rock would have a RQD value higher than 75 while the outcome was 61 %. For Småland (Ävrö) granite a bigger difference was observed between prediction and outcome. It was predicted that 80 % of the rock would have a higher RQD than 75 while the outcome was 36 %.

It is difficult to explain the greater difference found in Småland (Ävrö) granite than in Äspö diorite. It seems that the quality of the Äspö diorite in general is slightly more competent than that of the Småland (Ävrö) granite. The mapping of rock quality proves that 53 % of the diorite and 45 % of the Småland (Ävrö) granite is of 'good' quality.

In the fine-grained granite the observations showed much lower RQD values and distances between fractures than was predicted. It was predicted that 70 % of the rock would have a RQD value higher than 75 while the outcome was 0 %. All the measured fracture distances are less than 0.6 m. It was predicted that approximately 50 % of the fracture distances would exceed 0.6 m. The

differences in the case of fine-grained granite are explained by the fact that fine-grained granite has mostly been found in fracture zones NE-3 and NE-1, where the rock is highly fractured.

The observed fracture frequency for greenstone shows rather good agreement with the prediction.

In the greenstone 80 % of the fracture distances for the dominating fracture systems were predicted to exceed 0.3 m while the outcome proved that 92 % exceeded 0.2 m. In the prediction 20 % were estimated to be between 1 and 3 m while the outcome showed that 31 % were between 0.6 and 2 m.

The observed fracture density shows some deviation from the prediction. In the prediction 20 % of the rock was estimated to have a higher RQD value than 90 and 70 % higher than 75. The outcome proved to be 0 % higher than 90 and 53 % higher than 75. In the tunnel 16 % of the greenstone was also found to have an RQD value lower than 50, which was not predicted at all.

It should be noted that different intervals have been used for the grouping of fracture frequency and fracture density for the prediction and for the evaluation. The reason for this is that different versions of the RMR system were applied for the prediction and evaluation. During the time between the prediction and evaluation a new version of the RMR system were introduced. Although it caused some difficulties for the comparison between prediction and outcome there was motivation to use the most recent version for the evaluation.

PART 3

REFERENCES

REFERENCES

REFERENCES - CHAPTER 1

Gustafson G, Liedholm M, Rhén I, Stanfors R, Wikberg P, 1991. Äspö Hard Rock Laboratory. Predictions prior to excavation and the process of their validation, SKB TR 91-23.

R&D-Programme 86, 1986, Parts I-III. Handling and final disposal of nuclear waste. Programme for research, development and other measures, SKB, Stockholm.

R&D-Programme 89, 1989, Parts I-II. Handling and final disposal of nuclear waste. Programme for research, development and other measures, SKB, Stockholm.

R&D-Programme 95, 1995, Parts I-II. Treatment and final disposal of nuclear waste. Programme for encapsulation, deep geological disposal and research, development and demonstration, SKB, Stockholm.

REFERENCES - PART 1
GEOLOGY

Almén K-E, Olsson P, Rhén I, Stanfors R, Wikberg P, 1994. Äspö Hard Rock Laboratory - Feasibility and usefulness of site investigation methods. Experiences from the pre-investigation phase. SKB TR 94-24.

Bäckblom G, 1989. Guide-Lines for use of nomenclature on fractures, fracture zones and other topics. SKB. HRL-96-18.

Carlsten S, 1989. Results from borehole radar measurements in KAS05, KAS06, KAS07 and KAS08 at Äspö. Interpretation of fracture zones by including radar measurements from KAS02 and KAS04. SKB PR 25-89-10.

Carlsten S, 1990. Borehole radar measurements at Äspö Boreholes KAS09, KAS10, KAS11, KAS12, KAS13 and KAS14. SKB PR 25-90-05.

Cosma C, Heikkinen P, Keskinen J, Kormonen R, 1990. VSP-survey including 3-D interpretation in Äspö, Sweden. Borehole KAS07. SKB PR 25-90-07.

Eliasson T, 1993. Mineralogy, geochemistry and petrophysics of red coloured granite adjacent to fractures. SKB TR 93-06.

Ericsson L-O, 1987. Fracture mapping on outcrops. SKB PR 25-87-05.

Ericsson L O, 1988. Fracture mapping study on Äspö island. Findings of directional data. SKB PR 25-88-10.

Fridh B, Stråhle A, 1989. Orientation of selected drillcore sections from the boreholes KAS05 and KAS06 Äspö, Sweden. A Televiewer investigation in small diameter boreholes. SKB PR 25-89-08.

Gustafson G, Liedholm M, Rhén I, Stanfors R, Wikberg P, 1991. Predictions prior to excavation and the process of their validation, SKB TR 91-23.

Hermansson J, 1995. Structural Geology of water bearing fractures. SKB PR 25-95-23.

Hermansson J, 1996. Visualization of fracture network using DFN approach in a number of rock blocks in the Äspö HRL. SKB PR HRL 96-08.

IUGS SUBCOMISSION ON THE SYSTEMATICS OF IGNEOUS ROCKS 1973. Classification and Nomenclature of Plutonic Rocks. Recommendations. N. Jb. Miner. Mh. 1973, H4, 149-164.

IUGS SUBCOMISSION ON THE SYSTEMATICS OF IGNEOUS ROCKS 1980. Classification and Nomenclature of Volcanic Rocks. Lamprophyres, Carbonatites and Melilitic Rocks. Geol. Rundschau 69, 194-207.

Kornfält K-A, Wikman H, 1987. Description to the map of solid Rocks around Simpevarp. SKB PR 25-87-02.

Kornfält K-A, Wikman H, 1988. The rocks of the Äspö island. Description to the detailed maps of solid rocks including maps of 3 uncovered trenches. SKB PR 25-88-12.

Munier R, 1989. Brittle tectonics on Äspö, SE Sweden. SKB PR 25-89-15.

Munier R, Hermansson J, 1992-1993. Updating of the geological-structural model. Measurements performed during construction of section 1475-2265 m. Compilation of Technical Notes. SKB PR 25-94-05.

Nisca D, 1987. Aeromagnetic Interpretation 6G Vimmerby, 6H Kråkelund NW. SW. SKB PR 25-87-23.

Nisca D, 1988. Geophysical laboratory measurements on core samples from KLX 01, Laxemar and KAS02, Äspö. SKB PR 25-88-06.

Nisca D, 1987. Aero-geophysical interpretation. SKB PR 25-87-04.

Nisca D, Triumf C-A, 1989. Detailed geomagnetic and geo-electric mapping of Äspö. SKB PR 25-89-01.

Niva B, Gabriel G, 1988. Borehole radar measurements at Äspö and Laxemar. Boreholes KAS02, KAS03, KAS04, KLX-01, HAS02, HAS03 and HAV07. SKB PR 25-88-03.

Nylund B, 1987. Regional gravity survey of the Simpevarp area. SKB PR 25-87-20.

Ploug C, Klitten K, 1989. Shallow reflection seismic profiles from Äspö, Sweden. SKB PR 25-89-02.

Rydström H, Gereben L, 1989. Seismic refraction survey on Äspö and Hålö. SKB PR 25-89-18.

Sehlstedt S, Triumf C-A, 1988. Interpretation of geophysical logging data from KAS02 - KAS04 and HAS08 - HAS12 at Äspö and KLX01 at Laxemar. SKB PR 25-88-15.

Sehlstedt S, Stråhle A, 1989. Geological core mapping and geophysical borehole logging in the boreholes KAS05 - KAS08 at Äspö. SKB PR 25-89-09.

Sehlstedt S, Stråhle A, Triumf C-A, 1990. Geological core mapping and geophysical borehole logging in the boreholes KBH02, KAS09, KAS11 - KAS 14 AND HAS18 - HAS20 at Äspö. SKB PR 25-90-06.

Stanfors R, Gustafson G, Munier R, Olsson P, Stille H, Wikberg P, 1992. Evaluation of Geological Predictions in the access Ramp, 0-700 m. SKB PR 25-92-02.

Stanfors R, Liedholm M, Munier R, Olsson P, Stille H, 1993. Geological-structural and rock mechanical evaluation of data from section 1475-2265 m. SKB PR 25-93-10.

Stenberg L, Sehlstedt S, 1989. Geophysical profile measurements on interpreted regional aeromagnetic lineaments in the Simpevarps area. SKB PR 25-89-13.

Streckeisen A L, 1967. Classification and Nomenclature of Igneous Rocks. N. Jb. Miner. Abh. 107, 144-240.

Stråhle A, 1989. Drillcore investigation in the Simpevarp area, Boreholes KAS02, KAS03. KAS04, and KLX01. SKB PR 25-88-07.

Sundin S, 1988. Seismic refraction investigation at Äspö. SKB PR 25-87-15.

Talbot C, Riad L, Munier R, 1988. The geological Structures and Tectonic history of Äspö SE Sweden. SKB PR 25-88-05.

Talbot C, Munier R, 1989. Faults and fracture zones in Äspö. SKB PR 25-89-11.

Tirén S, Beckholmen M, Isaksson H, 1987. Structural analysis of digital terrain models, Simpevarp area. South-eastern Sweden. Method study EBBA 11. SKB PR 25-87-21.

Wikberg P (ed), Gustafson G, Rhén I, Stanfors R, 1991. Äspö Hard Rock Laboratory. Evaluation and conceptual modelling based on the pre-investigations. SKB TR 91-22.

Wikman H, Erlström M et al, 1992-1993. Petrological classification, petrophysical measurement and XRD analyses of minerals. Measurements performed during construction of section 700-2265 m. Compilation of Technical Notes. SKB PR 25-94-07.

Wikman H, 1993. Mean values of the mineral composition of rocks occurring in the Simpevarp area, arranged in four groups. Appendix 5 in SKB PR 25-93-05.

Wikman H, Kornfält K-A, 1995. Updating of a lithological model of the bedrock of the Äspö area. SKB PR 25-95-04.

Winberg A, Andersson P, Hermanson J, Stenberg L, 1996. Results of the select project. Investigation programme for selection of experimental sites for the operational phase. SKB PR HRL-96-01.

REFERENCES - PART 2
MECHANICAL STABILITY

Brown E T, 1981 (ed). Rock characterization. Testing and Monitoring. ISRM suggested methods. Pergamon Press.

Christansson R, Stenberg L, 1991. Manual for field work in the tunnel. SKB PR 25-91-10.

Hoek E, Brown E T, 1980. Underground Excavations in Rock. Inst. of Mining and Metallurgy, London. **Leijon B, 1995.** Summary of Rock stress data from Äspö. SKB PR 25-95-15, 1989.

Stanfors R, Gustafson G, Munier R, Olsson P, Stille H, Wikberg P, 1992. Evaluation of geological predictions in the access ramp, 0-700 m. SKB PR 25-92-02.

Stanfors R, Liedholm M, Munier R, Olsson P, Stille H, 1993. Geological-structural evaluation of data from tunnel section 700-1475 m. SKB PR 25-93-05.

Stanfors R, Liedholm M, Munier R, Olsson P, Stille H, 1994. Geological-structural evaluation of data from tunnel section 1475-2265 m. SKB PR 25-93-10. **Stanfors R, Liedholm M, Munier R, Olsson P, Stille H, 1994.** Geological-structural evaluation of data from tunnel section 2265-2874 m. SKB PR 25-94-19.

Stille H, Olsson P, 1989. First evaluation of rock mechanics, SKB PR 25-89-07.

Stille H, Olsson P, 1990. Evaluation of rock mechanics. SKB PR 25-90-08.

Stille H, Olsson P, 1996. Summary of rock mechanics experience from the construction of the Äspö Hard Rock Laboratory. SKB PR HRL 96-07.

This report is based on the following text files:

003pa0rs.wpd:	Summary, Introduction
003pa1rs.wpd:	Part 1
003pa2rs.wpd:	Part 2
003pa3re.wpd	Part 3

List of SKB reports

Annual Reports

1977-78
TR 121
KBS Technical Reports 1 – 120
Summaries
Stockholm, May 1979

1979
TR 79-28
The KBS Annual Report 1979
KBS Technical Reports 79-01 – 79-27
Summaries
Stockholm, March 1980

1980
TR 80-26
The KBS Annual Report 1980
KBS Technical Reports 80-01 – 80-25
Summaries
Stockholm, March 1981

1981
TR 81-17
The KBS Annual Report 1981
KBS Technical Reports 81-01 – 81-16
Summaries
Stockholm, April 1982

1982
TR 82-28
The KBS Annual Report 1982
KBS Technical Reports 82-01 – 82-27
Summaries
Stockholm, July 1983

1983
TR 83-77
The KBS Annual Report 1983
KBS Technical Reports 83-01 – 83-76
Summaries
Stockholm, June 1984

1984
TR 85-01
Annual Research and Development Report 1984
Including Summaries of Technical Reports Issued
during 1984. (Technical Reports 84-01 – 84-19)
Stockholm, June 1985

1985
TR 85-20
Annual Research and Development Report 1985
Including Summaries of Technical Reports Issued
during 1985. (Technical Reports 85-01 – 85-19)
Stockholm, May 1986

1986
TR 86-31
SKB Annual Report 1986
Including Summaries of Technical Reports Issued
during 1986
Stockholm, May 1987

1987
TR 87-33
SKB Annual Report 1987
Including Summaries of Technical Reports Issued
during 1987
Stockholm, May 1988

1988
TR 88-32
SKB Annual Report 1988
Including Summaries of Technical Reports Issued
during 1988
Stockholm, May 1989

1989
TR 89-40
SKB Annual Report 1989
Including Summaries of Technical Reports Issued
during 1989
Stockholm, May 1990

1990
TR 90-46
SKB Annual Report 1990
Including Summaries of Technical Reports Issued
during 1990
Stockholm, May 1991

1991
TR 91-64
SKB Annual Report 1991
Including Summaries of Technical Reports Issued
during 1991
Stockholm, April 1992

1992
TR 92-46
SKB Annual Report 1992
Including Summaries of Technical Reports Issued
during 1992
Stockholm, May 1993

1993
TR 93-34
SKB Annual Report 1993
Including Summaries of Technical Reports Issued
during 1993
Stockholm, May 1994

1994
TR 94-33
SKB Annual Report 1994
Including Summaries of Technical Reports Issued
during 1994
Stockholm, May 1995

1995
TR 95-37
SKB Annual Report 1995
Including Summaries of Technical Reports Issued
during 1995
Stockholm, May 1996

1996
TR 96-25
SKB Annual Report 1996
Including Summaries of Technical Reports Issued
during 1996
Stockholm, May 1997

List of SKB Technical Reports 1997

TR 97-01
**Retention mechanisms and the flow
wetted surface – implications for safety
analysis**
Mark Elert
Kemakta Konsult AB
February 1997

TR 97-02
**Äspö HRL – Geoscientific evaluation
1997/1. Overview of site characterization
1986–1995**
Roy Stanfors[1], Mikael Erlström[2],
Ingemar Markström[3]
[1] RS Consulting, Lund
[2] SGU, Lund
[3] Sydkraft Konsult, Malmö
March 1997

TR 97-03
**Äspö HRL – Geoscientific evaluation
1997/2. Results from pre-investigations
and detailed site characterization.
Summary report**
Ingvar Rhén (ed.)[1], Göran Bäckblom (ed.)[2],
Gunnar Gustafson[3], Roy Stanfors[4], Peter Wikberg[2]
[1] VBB Viak, Göteborg
[2] SKB, Stockholm
[3] VBB Viak/CTH, Göteborg
[4] RS Consulting, Lund
May 1997